

**Development of a surgical technique for partial  
cortico-hippocampectomy and standardized histologic  
evaluation of the hippocampal cytoarchitecture in  
normal cats**

Inaugural Dissertation

submitted to the Faculty of Veterinary Medicine

in partial fulfilment of the requirements

for the PhD-Degree

of the Faculties of Veterinary Medicine and Medicine

of the Justus Liebig University Giessen

by

Zilli, Jessica

of

San Daniele del Friuli (Italy)

Giessen 2022

From the Department of Veterinary Clinical Sciences, Small Animal Clinic  
Neurosurgery, Neuroradiology and Clinical Neurology

Dean: Prof. Dr. Stefan Arnhold

of the Faculty of Veterinary Medicine of the Justus Liebig University Giessen

First Supervisor: Prof. Dr. Carsten Staszky

Second Reviewer: Prof. Dr. Andrea Tipold

Chair: Prof. Dr. Christine Wrenzycki

Vice-chair and Second Supervisor: Prof. Dr. Anne Schänzer

Date of Doctoral Defence: 9<sup>th</sup> November 2022

# 1 Table of contents

1	Table of contents.....	3
2	Introduction.....	5
3	Literature review.....	6
3.1	Morphology of the temporal lobe.....	6
3.1.1	Macromorphology of the hippocampal formation.....	6
3.1.2	Cytoarchitectonic of the hippocampus proper.....	8
3.1.3	Longitudinal divisions of the hippocampus (cornu ammonis fields).....	10
3.1.4	Cytoarchitectonics of the dentate gyrus (dentate fascia).....	12
3.1.5	Septo-temporal axis of the hippocampus.....	13
3.2	Epilepsy in cats and dogs.....	14
3.2.1	Diagnostic investigations in patients with seizures.....	16
3.2.2	Medical therapy of seizures in cats.....	18
3.2.3	Antiepileptic drug resistance.....	19
3.3	Temporal lobe epilepsy (TLE) in cats.....	21
3.3.1	Temporal lobe pathologies underlying TLE in cats.....	22
3.4	Epilepsy surgery.....	28
3.4.1	Surgical techniques in human medicine.....	28
3.4.2	Post-operative complications after epilepsy surgery.....	33
3.4.3	Outcome in human patients.....	33
3.5	Epilepsy surgery in cats and dogs.....	36
3.5.1	Morphological differences between human and feline temporal lobe structures	38
3.6	Histopathology of hippocampal sclerosis.....	39
3.6.1	Hippocampal cellular densities.....	40
4	Study 1.....	42
4.1	Aims and objectives of the study.....	42
4.2	Materials and methods.....	43
4.3	Results.....	48
4.4	Discussion.....	57
5	Study 2.....	63
5.1	Aims and objectives of the study.....	63
5.2	Materials and methods.....	64

5.3	Results .....	70
5.4	Discussion .....	78
6	Conclusions.....	84
7	Summary .....	85
8	Zusammenfassung.....	86
9	List of Abbreviations .....	87
10	List of figures .....	89
11	List of tables .....	91
12	References .....	93
13	Appendix .....	120
14	List of publications.....	124
15	Declaration/Erklärung .....	125
16	Acknowledgements .....	126
17	Curriculum Vitae.....	127

## 2 Introduction

Epilepsy is a complex brain disease associated with an abnormal activity in neuronal networks, which causes seizures with motor, autonomic and/or behavioural features (Berendt et al., 2015). In a significant number of cases an underlying cause cannot be identified.

In these cases, genetic defects leading to imbalances between excitation and inhibition of electrical activity are suspected (Berendt et al., 2015). In some breeds, like Tervuren Belgian Shepherd and Lagotto Romagnolo, the genetic mutation has been further characterised (Jokinen et al. 2007; Seppala et al., 2011; Seppala et al., 2012; Stassen et al., 2013). A genetic basis has been also suspected in numerous other dog breeds (Berendt et al., 2008,2009; Casal et al., 2006; Famula and Oberbauer, 2000; Gullov et al., 2011; Hulsmeyer et al., 2010; Jaggy et al., 1998; Jokinen et al., 2007; Licht et al., 2007; Oberbauer et al., 2010; Petterson et al., 2003, 2005) and in cats as well. As the genetic defect is not known yet in most breeds or individuals, the authors refer to these forms as idiopathic epilepsy (IE) or epilepsy of unknown cause (EUC) (Berendt et al., 2015; Wahle et al., 2014). The prevalence of EUC in cats was considered to lie between 25-54% in the epileptic cats' population (Pakozdy et al., 2010; Wahle et al., 2014) (EUC) but recently it has been demonstrated that a subpopulation of these may be affected by hippocampal necrosis/sclerosis or limbic encephalitis (Brini et al., 2004; Fatzer et al., 2000; Fors et al., 2015; Pakozdy et al., 2013a; Pakozdy et al., 2014; Schmied et al., 2008; Wagner et al., 2014), and thus belong to the structural epilepsy category. Increasing evidence suggests that hippocampal sclerosis (HS) causes resistance to antiepileptic drugs (AED) which is why new treatment strategies are urgently needed in veterinary medicine.

The surgical treatment in cats with temporal seizures has been attempted in only one case report (Hasegawa et al., 2021) so far and for this reason the objective of this study is to lay the foundation of temporal epilepsy surgery also in Veterinary Medicine. Moreover, to help in reaching a standardized, systematic classification and diagnosis process in feline HS cases, this prospective cadaveric study aimed at evaluating normal reference values on cellular densities and the cytoarchitecture for normal feline hippocampus.

## 3 Literature review

### 3.1 Morphology of the temporal lobe

The temporal lobe is composed of two parts belonging to the telencephalon, the temporal isocortex (neocortex) and the mesial temporal structures, which consist of allocortex.

This extends from the suprasylvian sulcus (rostral, middle and caudal part) dorsally, to the lateral rhinal sulcus ventrally. At the level of the caudal fossa, from the lateral rhinal sulcus starts a deep but short sulcus directed dorso-caudally, named “*fissura pseudosylvia*”. The sylvian territory is built of two long, parallel gyri, which curve as a semicircle around the previously mentioned fissure, dorsally to it. Directly on its sides are located the rostral and the caudal sylvian gyrus, united by the intersylvian gyrus dorsally. These are separated from the ectosylvian gyri (rostral, middle and caudal in continuity) by the rostral ectosylvian sulcus and the caudal ectosylvian sulcus respectively (Barone and Bortolami, 2006b).

#### 3.1.1 Macromorphology of the hippocampal formation

The complex terminology of the hippocampus and its adjacent structures can be a challenge to understand, complicated by the differences between human and animal morphology and the different nomenclature used by various investigators. The term hippocampus was coined by an ancient anatomist (Stephan, 1975). Watching into the lateral ventricle of the human brain from above, he described a ridge of grey matter tissue, elevating from the ventricular floor that resembled a sea horse lying upside down in the temporal horn (Figure 1A). This impression can be explained by the unique shape of the human hippocampus, which considerably differs from that in animals. The “*uncus*” (from Latin hook) resembled the head of a sea horse and is the rostral part of the hippocampus, which bends where it merges with the parahippocampal gyrus. The thick head of the human hippocampus was described as the belly of a sea horse and the digitations at the surface of the hippocampus were seen as the trunk rings of the animal (Stephan, 1975). The body of the human hippocampus swiftly tapers to the tail that winds around the thalamus, such as the animals would hold on to a water plant (Stephan, 1975).



**Figure 1. The human hippocampus was originally named after a sea horse due to its structural similarities with this animal (A). Indeed, hippocampus means in greek “sea horse”. On the other hand, in mammals, the hippocampus shows a rather linear and uniform morphology; indeed, no clear divisions are present between its three sections (head, body and tail). In animals, the two hippocampi are characterised by a typical elongated, dorso-caudally curved shape, on each side of the thalamus and resemble a pair of horns on the head of a ram, which is why it was also called Ammon’s horn (B), from the Egyptian god Ammon, who was always represented with an Aries head (Barone and Bortolami, 2006a).**

The three-dimensional morphology of the human hippocampus differs from other mammals (Nickel, 2004). Domestic animals neither have an uncus, nor digitations on the body of the hippocampus, and lack a clearly distinct dorsal tapering into a tail. The hippocampus has a rather uniform shape in its dorso-ventral course (Nickel, 2004). The two hippocampi lie on each side of the thalamus and resemble a pair of horns on the head of a ram, which is why they were also called Ammon’s horns after the name of the Egyptian god of the air and fertility (Ram's horn; Figure 1B). As in a ram, the two horns approach in the midline where the hippocampal commissure connects the left and right hippocampus. Alongside the medial surface of the hippocampus lies a separate structure, which is the dentate gyrus (DG). The term DG also originates from the observation of the human brain, in which the surface of the DG has multiple indentations resembling a row of teeth (from Latin “*dentatus*”: toothed), which led to the name of this structure. This characteristic indentation is also not seen in domestic animals (Nickel, 2004). Within the parahippocampal gyrus, the allocortex of the hippocampus and the isocortex of the evolutionary modern part of the brain surface gradually merge by progressive alterations of the cytoarchitectonic composition of the hippocampus, which runs first into the subiculum, pre-, and parasubiculum, and then into the entorhinal cortex (Figure 2). The

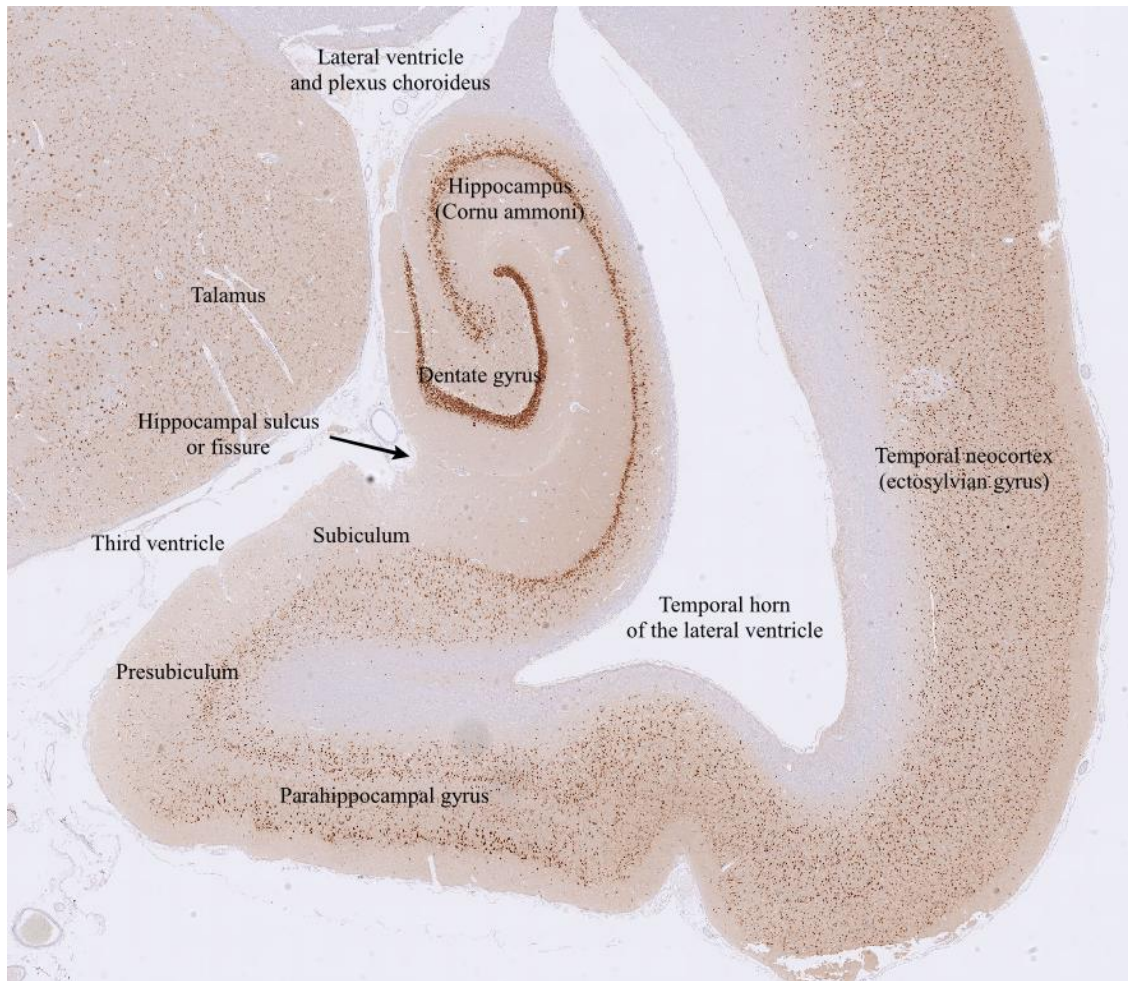


**Figure 2. Mesial temporal lobe and surrounding structures.**

hippocampus (proper), the DG, the subiculum and the entorhinal cortex are referred to as the hippocampal formation (Schultz and Engelhardt, 2014).

### **3.1.2 Cytoarchitectonic of the hippocampus proper**

In contrast to the six-layered isocortex of the forebrain, the architecture of the hippocampus and DG is relatively simple. Both contain only one neuronal layer. The principal neuron type in the hippocampus is the pyramidal cell, whereas in the DG, it is the granule cell (GC). Pyramidal neurons of the hippocampus have a large triangular cell body and two distinct dendritic “trees”, emerging from the base, and from the apex of the soma (Barone and Bortolami, 2006a). The position of the cell bodies and the arrangement of their dendrites create the characteristic lamination of the hippocampus in sectional images. In the Nissl staining (which highlights the cell bodies) the layer where the perikarya of cellular elements accumulate forms the stratum pyramidalis (pyramidal



layer) (Figure 3). The layer underneath the pyramidal cell layer is called the oriens layer (“*stratum oriens*”; in this context, from Latin “*oriēns*”: originating), which contains unmyelinated basal dendrites of the pyramidal cells and scattered cell bodies of inhibitory basket cells. The underlying layer that borders the ventricular surface of the hippocampus is the alveus (from Latin “*alveus*”: riverbed or channel) (Figure 3). It is composed by the myelinated axons of the pyramidal cells.

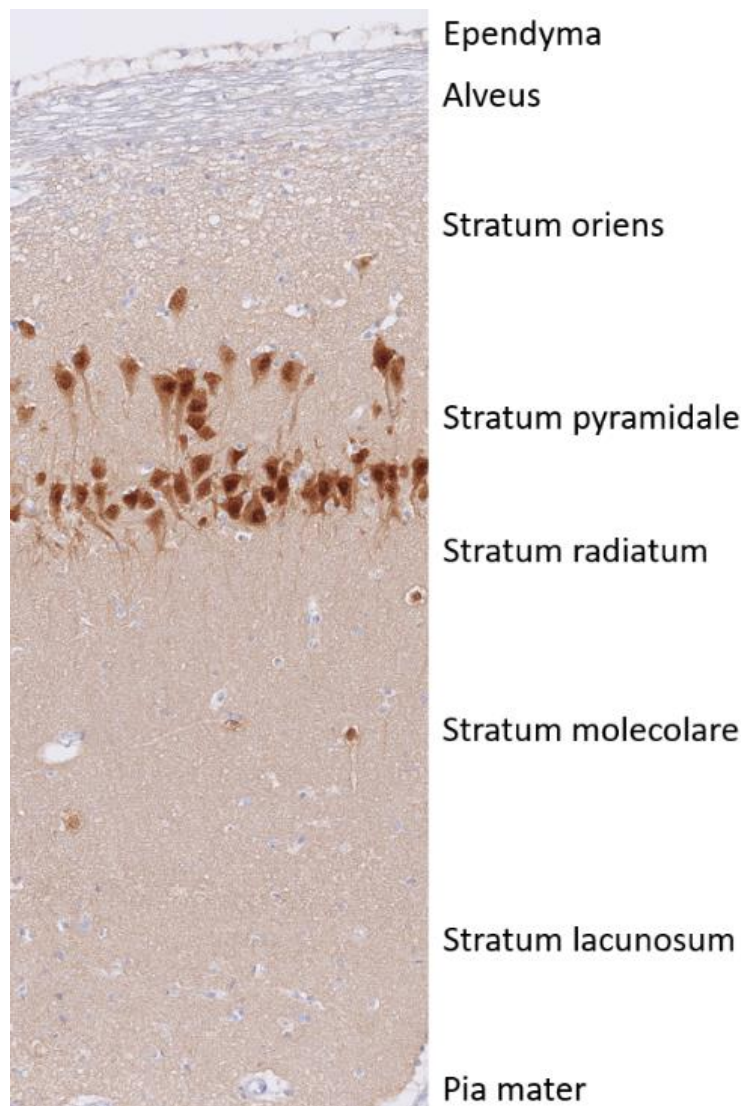


**Figure 3. Schema of the ammon’s horn layers’ structure (NeuN stained CA2 area from a feline hippocampus).**

The area above the pyramidal layer adjoining the hippocampal sulcus is the molecular layer containing mostly the unmyelinated apical dendrites of the pyramidal cells (Figure 3). It looks homogenous in Nissl-stained slides (Ramon y Cajal, 1893). Staining techniques that highlight Zinc in dendritic synaptic connections allow the identification of three sublayers characterized by different connectivity. Directly above the pyramidal

cell bodies the straight apical dendrites of the pyramidal cells can be seen in almost parallel orientation. This layer is called the radiant layer (“*stratum radiatum*”) as the arrangement of the fibres in this layer reminded Cajal of sunrays (Craigie and Gibson, 1968; Ramon y Cajal, 1911) (Figure 3). The radiant layer receives septal and commissural fibres as well as Schaffer collaterals. The next sublayer is the “*stratum lacunosum*” that contains incoming fibres from the entorhinal cortex (perforant path). The last layer is the actual molecular layer (“*stratum moleculare*”), which houses the arborizing apical dendrites of the pyramidal cells (Figure 3). The last two layers are often grouped together as the stratum lacunosum-moleculare.

### **3.1.3 Longitudinal divisions of the hippocampus (cornu ammonis fields)**

The layers of the hippocampus slightly differ in their arrangement in dependence of their position between the DG and the subiculum. In the proximal aspect of the hippocampus, the anatomist Santiago Ramon y Cajal identified another narrow zone just above the pyramidal cell layer and underneath the radiant layer. Due to the paucity of cells and fibres in this layer it does not stain as intense as other layers and appears translucent in Nissl-stained slides, which is why it was denominated “*stratum lucidum*” (from Latin the bright layer). This layer contains unmyelinated axons originating from the GCs of the DG. These axons form characteristic dense synaptic connections (boutons) with the dendrites of the pyramidal cells, which produce thin branches named “thorny excrescences” (from Latin “*excrescēntia*”: abnormal growths (Amaral, 1978, Chicurel and Harris, 1992). These excrescences give the dendrites an appearance that reminded Cajal of a moss-covered tree (Ramon y Cajal, 1911). He introduced the name “mossy fibres” for axons that connect with the excrescences of the pyramidal cells. The presence or absence of the pyramidal cells with excrescences was the basis for the earliest classification of the subfields in the longitudinal extension of the hippocampus as “*regio superior*” and “*regio inferior*” in rats (Ramon y Cajal, 1893). The two early subdivisions evidenced by Cajal were later further divided into four subfields based on pyramidal cell morphology. The term cornu ammonis was adopted in abbreviated form as CA (“*Cornu Ammonis*”) in naming the four subfields CA1-CA4 (Figure 4). In rats, pyramidal cell bodies in CA1 are smaller than in the other subfields and tend to stain less intensely in Nissl preparations (Dam, 1979; Lorente de Nó, 1934). In CA3, which contains the mossy

fibres, the cell bodies are larger, take up more stain, and are quite densely packed to a narrow band of cells (Stephan, 1975; Braak, 1980). CA2 is a sort of boundary zone sharing features of CA1 and CA3 (Bartesaghi and Gessi, 2004). It does not contain mossy fibres, but in this area pyramidal somata are as large as in CA3. The CA2 field has been a matter of some controversy. Its boundaries to CA1 and CA3 are clear in rodent and human hippocampi, but its presence could not be proven with certainty in other mammalian species (Amaral et al., 1984; Blackstad, 1956; Schwerdtfeger, 1984).

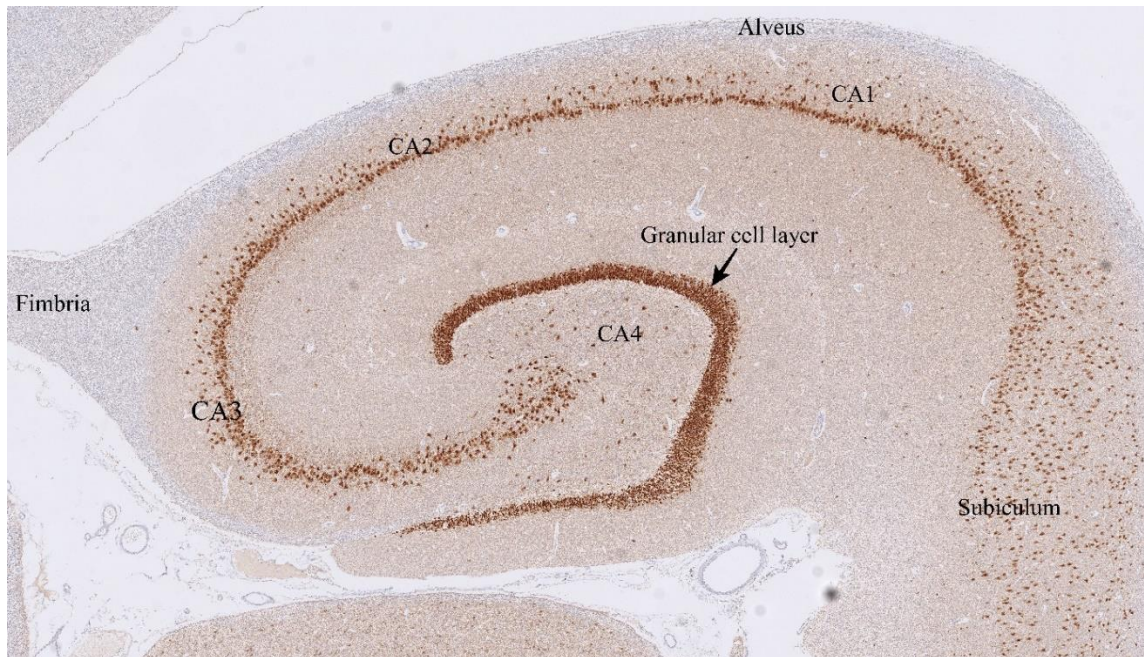


**Figure 4. Hippocampal subdivisions.**

CA4 is easy to visualize. It's a loose segment of cells arranged around the end of CA3 and linked up with the granular cell layer of the DG. Unlike other pyramidal cells, the somata of CA4 do not form a recognizable layer. They are scattered among intertwined mossy fibres in the hilar region underneath the granule cell layer (GCL) (Amaral et al., 1990). The cells in CA4 do not have the characteristic pyramidal cell morphology but are rather multipolar or fusiform neurons or have a polymorph morphology ("modified pyramids") (Stephan, 1975; Lorente de Nó, 1934). Due to the unclear developmental origin and clear classification of these cells, the term CA4 has been abandoned from the modern anatomical terminology and was replaced by the term "*endfolium*" (from Latin terminal leaf) of CA3 (Bartsch, 2012). The cells of the end folium are enclosed within the granular cell layer of the DG. This area between the two blades of the GCL is described as the hilus of the DG (from Latin "*hilum*": small depression or indentation). Although

different structures, the terms hilus and end folium are commonly used as synonymous. The dendrites of CA4 are also covered by abundant thorny excrescences where they form synapses with the axons coming from the GCL of the DG.

### **3.1.4 Cytoarchitectonics of the dentate gyrus (dentate fascia)**

The structure of the “*gyrus dentatus*” is simpler than the hippocampus. Three layers are visible in Nissl stains. The main cellular layer contains somata of very small granular neurons (stratum granulosum; from Latin “*granulum*”: grain) (Figure 4). It is a densely packed layer, whose shape is position- and also markedly species-specific. In dorsal slices of the rat hippocampus, it presents as a more or less compressed “C” in the ventral (temporal) part of the hippocampal formation and as a “V” or a “U” in the dorsal (septal) part (Amaral et al., 2007). The limb of the granular cell layer, which is localised between CA3 and CA1 and capping CA4, is referred to as the supra-pyramidal layer or supra-pyramidal “blade”. The transition point adjacent to the end folium is the crest of the layer, merging into the infra-pyramidal blade sitting below the CA3 field. The GCs have a round to elliptical cell body, which is also smaller than the soma of the pyramidal cells and give rise to axons forming only one cone-shaped tree of spiny apical dendrites (Amaral, 1978). The stratum that contains these dendrites is relatively cell free. This layer is called molecular layer just as in the hippocampus and can be divided into two sublayers based on their connectivity. The area adjacent to the hippocampal sulcus is the outer molecular layer that receives fibres from the entorhinal cortex targeting the proximal aspect of GC dendrites. The inner layer adjacent to the GCL contains fibres coming from the septal area and from the contralateral hippocampus (inner molecular layer) (Lynch and Cotman, 1975; Cerbone et al., 1993). In between the two blades is the third layer of the DG, the polymorphic cell layer (syn. stratum plexiforme; from Latin “*plexiformis*”: grid-like). It contains a variety of neuron types and intermixed abundant unmyelinated nerve fibres. It is now recognized that there is no clear-cut difference or border between the pyramidal neurons of CA4 and the neurons of the polymorphic layer. They are now considered to be the same neuronal population (see above). The neurons in the hilus are also called “mossy cells”, as they have analogous thorny excrescences on their dendrites as the neurons of CA3.

The DG is one of three areas in the brain where neurogenesis occurs. Neuronal stem cells reside in a thin layer at the border between the granule- and polymorphic cell layer, which is called the subgranular zone. They provide a reservoir for the turnover and replacement of GCs that are functionally integrated into the granular cell layer (Taupin and Gage, 2002; van Praag et al., 2002). This process continues to occur throughout life and provides plasticity, which plays a crucial role in learning and memory. The progenitor cells undergo large-scale changes in gene expression, which helps in identifying them using immunohistochemical methods. Neuronal activity stimulates neurogenesis which is an important factor for the memory functions of the hippocampus.

### **3.1.5 Septo-temporal axis of the hippocampus**

Traditional studies regarding the hippocampal structure and function have treated this brain part as a whole (Stephan, 1975). However, the predominant view in modern neuroscience is that the hippocampus presents subdivisions along its longitudinal, or septo-temporal axis (Fanselow and Dong, 2010). The concept that the hippocampus may not act as a unitary structure, was suggested based on several findings. Although its cellular structure and architecture are largely conserved along the longitudinal axis, the packing density of GCs is higher septally than temporally in rodents (Gaarskjaer, 1978). Differences also exist with regard to connectivity (Swanson and Cowan, 1977). The septal (dorsal) pole of the rat hippocampus rather communicates with the retrosplenial- and cingulate cortex (Cenquizca and Swanson, 2007), which is involved in processing of visuospatial information and spatial navigation (Harker and Whishaw, 2004). The temporal (ventral) hippocampus primarily receives input from the primary olfactory cortex and amygdala (Cenquizca and Swanson, 2007). The septal and ventral temporal subregion of the hippocampus also take on different functional roles. The temporal pole seems to contribute to emotional reactions and stress responses (Henke, 1990), whereas spatial memory appears to rather depend on the dorsal hippocampus (Moser et al., 1993). Last, different patterns of gene expressions suggest that the hippocampus is composed of three distinct molecular subdomains - a dorsal, an intermediate, and a ventral domain (Thompson et al., 2008; Fanselow and Dong, 2010; Dong et al., 2009).

### **3.2 Epilepsy in cats and dogs**

IE is one of the most common neurological, chronic diseases of cats and dogs. It has been estimated to have a prevalence of 0,6-0,75% in dogs (Kearsley-Fleet et al., 2013; Shorvon, 2014) and 0,5-2% in cats (Schriefl et al., 2008; Stanciu et al., 2017). IE must be differentiated from structural epilepsy, caused by a structural disease of the central nervous system (vascular, inflammatory, infectious, traumatic, neoplastic), and an epilepsy of unknown cause (once cryptogenic epilepsy), in which the presence of an underlying cause is suspected but cannot be demonstrated (Berendt et al., 2015). Moreover, seizures can be also provoked by metabolic or toxic causes and in this case, they are classified as reactive seizures.

IE is a complex pathology of the brain, in which a sudden, abnormal activity of the neuronal networks leads to seizures. It's a genetic disease, with complex genetic and epigenetic influences (Berendt et al., 2015). The genetic defect responsible for IE has been recognised just in a few dog breeds, in many others is just highly suspected (Jokinen et al. 2007; Seppala et al., 2011; Seppala et al., 2012; Stassen et al., 2013).

An animal is considered to be affected by IE if the following states are respected (Thomas and Dewey, 2016):

- Suspected or confirmed genetic aetiology.
- Seizure onset between 6 months and 6 years of age in dogs (De Risio et al., 2015) and between 1 and 7 years in cats (Stanciu et al., 2017).
- Unremarkable general examination.
- Unremarkable interictal neurological examination.
- Unremarkable blood works (haematology, biochemistry, ammonia and bile acids).
- Absence of cerebral structural lesions in magnetic resonance imaging (MRI) and computed tomography (CT).
- Unremarkable liquor examination.

Semiologically, we can distinguish focal (characterized by lateralized and/or regional signs), and generalized (both sides of the body and therefore with an involvement of both cerebral hemispheres) epileptic seizures (Berendt et al., 2015). The first ones occur more often in cats (Schriefl et al., 2008) whereas dogs are more often affected by generalized

tonic-clonic seizures with loss of consciousness and focal seizures with secondary generalisation (Thomas and Dewey, 2016).

Unlike in dogs, in which epilepsy has already been described and investigated in depth, in cats this topic is still quite unknown and has been studied more in depth just in the last years. The prevalence of IE or epilepsy of unknown origin (EUC) has been estimated to range from 25 and 54% in the feline epileptic population (Barnes et al., 2004; Pakozdy et al., 2010; Rusbridge, 2005; Schriefl et al., 2008; Wahle et al., 2014). A discussion as to whether EUC prevalence in cats has been overestimated due to the limitations of current magnetic resonance imaging protocols, to the use of low-field MRI, to the lack of post-mortem histopathologic examinations is still opened. Considering the recent findings regarding feline HS and immune-mediated limbic encephalitis with voltage-gated potassium channel (VGKC) complex antibodies (Pakozdy et al., 2011; Pakozdy et al., 2013a), it is logical to speculate that part of the cases previously classified as idiopathic were actually the result of a cerebral structural disease which has not been recognised (Barnes et al., 2004; Pakozdy et al., 2010; Schriefl et al., 2008). Moreover, temporal lobe changes, attributable to HS or necrosis detected in the MRI scans, have been already described in an early study (Sato, 1975) concerning feline temporal lobe epilepsy. This has been further confirmed in recent articles and significantly associated to focal seizures with orofacial involvement (OI), which is a typical clinical presentation of temporal lobe epilepsy (TLE) also in human patients (Claßen et al., 2016). A large part of cats with EUC shows OI (Wahle et al., 2014; Pakozdy et al., 2011), which leads to the consideration that possibly many cats belonging to this class are actually affected by a structural epilepsy: mesial temporal epilepsy (MTE).

Regarding a possible involvement of temporal lobe structures in the development of seizures in dogs, only a few reports of hippocampal malformation can be found in the veterinary literature. One report (Cantile et al., 2001) describes the presence of unilateral cortical hippocampal hamartia in a Pekingese dog with concurrent necrotizing meningoencephalitis (NME). Buckmaster et al., (2002) reported in its study population of dogs with medically intractable epilepsy one dog with abnormal heterotopic cells clusters in the molecular layer of the DG. A Shi-Tzu dog with porencephaly and cortical dysplasia (supposed cause of seizures) was reported by Machado et al., (2012) and finally Klang et al., described in 2014 a case of a mixed breed dog with bilateral hippocampal malformation and concurrent granulomatous meningoencephalitis. This last one was very

similar to the case report of the Pekingese dog of 2001. In these cases, it can be postulated that the hippocampal malformations of these dogs acted as a contributing factor for the development of seizures and the encephalitis as actual trigger of these. Nevertheless, also in dogs with IE and a completely normal temporal lobe, it is possible that the hippocampus contributes to the development of antiepileptic drugs resistance or in the propagation of the abnormal electrical activity through the brain, as it is known to have the highest *basic epileptogenic level* (BEL) in humans (Lüders et al., 2009).

### **3.2.1 Diagnostic investigations in patients with seizures**

While investigating an animal affected by epileptic seizures, attention should be put first on signalment and anamnesis, since many other disorders (such as narcolepsy/cataplexy, neuromuscular diseases, metabolic collapse, vestibular events) may be misinterpreted as seizures. Seizures can in fact manifest in many different ways and while animals with tonic-clonic generalized seizures can be quite easily identified and classified, dogs with generalised myoclonic, atonic, absence and focal seizures are rarely correctly assessed (De Risio, 2014). The direct examination of a seizure episode through an electroencephalographic study is in most cases not possible in veterinary medicine; for these reasons, the signalment and the anamnesis are very important to reach a diagnosis. The neurologist has to rely on the pet owner's accurate description of the events and sometimes on videos, which are a really helpful tool. The presence of clinical signs, like postictal signs, a peracute and unpredictable onset and termination of the event, the presence of involuntary motor activity and/or abnormal mentation and behaviour and/or autonomic signs are suggestive of seizure episodes (De Risio, 2014). Based on this information (signalment and anamnesis) and on the general and neurological examination, the clinician can formulate a list of differential diagnosis and consequently choose the more appropriate diagnostic test to further investigate the patient (De Risio, 2014).

A first, quite cheap test, which in some cases can help to formulate a diagnosis (for example in case of diabetes), is a complete blood count and biochemistry panel. Moreover, these tests will provide general information about the health of the patient, which are very important in order to perform further investigations in anaesthesia and before starting any antiepileptic treatment (De Risio, 2014).



In order to rule out hepatic encephalopathy, also fasting plasma ammonia and fasting and post-prandial total serum bile acid concentrations should be assessed, together with the hepatic function. Toxicological tests can be performed if an intoxication is suspected (De Risio, 2014). Some infectious agents (like herpesvirus, FIP) can lead to the development of seizures as well and above all if the blood count indicates a possible infection, further tests should be performed in order to rule them out (De Risio, 2014).

Radiographs of the thorax and radiographs or an ultrasound of the abdomen are indicated, above all in old animals, in order to rule out the presence of a primary or metastatic neoplastic disease or of a metabolic disorder (for example insulinoma associated hypoglycaemia, encephalopathy related to a portosystemic shunt), capable of causing seizures (De Risio, 2014).

The MRI is the golden standard to evaluate directly cerebral structures. It should be performed any time structural epilepsy is suspected (i.e., presence of interictal neurological abnormalities) and to support the diagnosis of IE in animals with normal interictal general and neurological examination, normal blood tests and early seizure onset as well. It's the most sensitive and specific medical imaging issue in the diagnosis of cerebrovascular, inflammatory and neoplastic brain diseases (Cervera et al., 2011; Wolff et al., 2012). The ability to recognise the presence of MRI abnormalities in the brain depends on many factors like the magnetic field strength, the choice of the image acquisition protocols and the experience of the radiologist (the person who examines and reports the MRI). There are many different pulse sequences, which can be used in the investigation of an epileptic patient. The most commonly used are spin echo T1-weighted pre-contrast (T1W) and post-contrast (T1WC), T2-weighted (T2W), T2-weighted fluid attenuated inversion recovery (FLAIR) and T2-weighted gradient echo (T2\*W GRE) images (De Risio, 2014).

Another important test which can help to reach a diagnosis even if structural abnormalities cannot be detected in the MRI is the liquor analysis. Nevertheless, in most of cases the results of MRI and liquor examination are associated (normal versus abnormal) and together lead to an exact diagnosis, as the study from Bush et al. (2002) showed. While examining the MRI of an epileptic patient after a seizure occurred, attention must be specifically paid to distinguish which changes induced the epileptic fit and which are its consequences. In fact, it is well known that up to 10-14 weeks after a seizure, MRI

changes produced by this one, can be detected (De Risio, 2014). These abnormalities are represented by vasogenic and cytotoxic oedema, usually localized unilaterally or bilaterally in the piriform and temporal lobes, but also in the olfactory bulb, in the frontal lobe and in the hippocampus and correspond to areas of maximal electroencephalographic abnormalities (Cole, 2004). Repeating the MRI after a period of seizure freedom, may help to differentiate seizure-induced changes from inflammatory or neoplastic epileptogenic structural lesions (Mellema et al., 1999; Pakozdy et al., 2013b). Moreover, in the last years an increasing number of functional imaging studies have been carried out also in veterinary medicine. In human medicine, diagnostic devices like magnetic resonance spectroscopy (MRS), positron emission tomography (PET), single-photon emission computed tomography (SPECT) and functional MRI (fMRI) are commonly used in the investigation of epileptic patients. The hope is that sooner or later these devices will be available also for the workup of our epileptic animals, above all considering the high percentage of AEDs resistant patients, which could benefit from the surgical resection of the epileptogenic focus. These diagnostic investigations could be in fact necessary for the precise localization of the focus and of the structures that are mostly involved in the seizure (De Risio, 2014). Finally, we cannot forget to mention electroencephalography (EEG), whose use is still limited in veterinary medicine. EEG is the recording of spontaneous electrical cortical activity generated by the pyramidal neurons and it could be also useful to help localizing the focus epilepticus. Its applications include the detection of epileptiform activity and of functional, focal or diffuse abnormalities of the brain and the monitoring of antiepileptic drugs' effect (Poncelet and Poma, 2013).

### **3.2.2 Medical therapy of seizures in cats**

The aim of the therapy is to reduce the frequency and the severity of the seizures (at least with an interictal period longer than 6 months) or even better to induce a state of seizure freedom with the less collateral side-effects possible. At present, the mainstay of therapy used for IE in veterinary medicine is the medical treatment and the first line antiepileptic drug is phenobarbital with an initial dose of 2,5-3 mg/kg BID. If this one alone is not enough to control seizures, a second antiepileptic drug is introduced. Potassium bromide (KBr) is the most often used add-on therapy. These two drugs have represented for a long time the primary treatment for epileptic dogs due to their long-standing history,

widespread availability, and low cost (Bhatti et al., 2016). Cats unluckily do not tolerate KBR as good as dogs and therefore in cats it cannot be employed as second line drug. In fact, it induces in a high rate of feline patients lower airway disease and many other severe side effects. Two alternative drugs, which can be used safely in cats as monotherapy or add-on drug are levetiracetam and imepitoin (Charalambous et al., 2018). Tipold et al. demonstrated in a recent (2015) randomised, controlled, blinded study that imepitoin has the same efficacy in controlling seizures in dogs but it leads to less adverse effects if compared to phenobarbital. Imepitoin is an active substance originally developed for the therapy of epilepsy in humans (Rundfeldt and Löscher, 2014). Its favourable pharmacokinetic profile in dogs led to the decision to use it for the treatment of canine IE and in 2013, thanks to randomized, controlled, clinical trials, which demonstrated its efficacy, it was approved for this indication (Löscher et al., 2004; Rieck et al., 2006; Tipold et al., 2015). At present imepitoin is recommended as monotherapy for dogs with recurrent generalized epileptic seizures, but still not as adjunct to another AED. Its efficacy has not been proven in patients with cluster seizures yet. Other drugs with a good safety profile which can be used as second line in cats and dogs are: levetiracetam, zonisamide and gabapentin (effective only in dogs). These have been rarely used as first-line drugs as well (Thomas and Dewey, 2016).

### **3.2.3 Antiepileptic drug resistance**

A task force of the International League against Epilepsy (ILAE) has recently defined pharmacoresistant epilepsy as a "*failure despite adequate trials of two (or more) well-tolerated, correctly chosen and used AED regimens (whether as monotherapies or in combination) to achieve sustained seizure freedom*" (Kwan et al., 2010).

In humans, as well as in animals, despite a therapy with at least two AEDs, 23% of the patients continue having seizures (Picot et al., 2008). In dogs the rate of AEDs' resistance is even higher: between 75-85% (Arrol et al., 2012; Berendt et al., 2002, 2007; Heynold et al., 1997); of these about 20-30% will experience a reduction of the seizure frequency inferior to 50% despite adequate treatment with phenobarbital and/or potassium bromide (Podell and Fenner, 1993; Schwartz-Porsche et al., 1985; Trepanier et al., 1998). This leads to a quite poor quality of life of the patients and often to euthanasia. Many studies showed in fact that dogs with epilepsy, especially refractory epilepsy with a high seizure

frequency, have an increased risk of premature death, behavioural changes and a reduced quality of life (Berendt et al., 2007; Chang et al., 2006; Shihab et al., 2011; Wessmann et al., 2012). Moreover, seizures do not only affect the quality of life of the affected animals, but also of the pet owners (Chang et al., 2016; Wessmann et al., 2012). The same considerations can be made for cats as well. Many risk factors for refractory epilepsy have already been recognised. For example, the high prevalence of epilepsy in many breeds (Jaggy et al., 1998; Kathmann et al., 1999; Berendt et al., 2002, 2009; Casal et al., 2006; Gullov et al., 2011) arises the suspect that genetic factors are involved in drug-responsiveness. Disease-related factors are also of importance, and these include the aetiology, the clinical course of the disease, and pathophysiology underlying the seizure disorder, changes in drug targets or binding sites, drug uptake into the brain and changes of the epilepsy circuit. Finally, drug-related factors such as ineffective pharmacodynamics or -kinetic properties and/or development of tolerance can also play a role in the development of pharmaco-resistance (Volk, 2014). Epilepsy is just a manifestation of a structural or functional brain abnormality and therefore to be able to treat it and improve the outcome of our patients, it is necessary to better understand the pathophysiological mechanisms that induces it and treatment failure. Drug resistance in fact is more a dynamic process rather than a fixed condition and it is strictly dependent to its underlying pathophysiology (Kwan et al., 2010).

Most pharmaco-resistant patients will often not respond to multiple antiepileptic drugs despite the individual differences in their mechanism of action (Regesta and Tanganelli, 1999; Löscher and Potschka, 2002). The probability that a patient, who do not respond to the first standard therapy, responds to the subsequent chosen antiepileptic drug is only 3% (Kwan and Brodie, 2000).

### 3.3 Temporal lobe epilepsy (TLE) in cats

Temporal lobe epilepsy first report in cats dates back to 2000 in Switzerland (Fatzer et al., 2000). Since then, the evidence that seizures originating from the temporal lobe are a typical form of structural epilepsy in cats has been growing (Brini et al., 2004; Gelberg, 2013; Marioni-Henry et al., 2012). Seizures in cats frequently manifest as complex focal seizures with or without secondary generalization (Kline, 1998; Parent and Quesnel, 1996; Rusbridge, 2005; Schriebl et al., 2008). Such epileptic fits are characterized by drooling, facial twitching, lip smacking, chewing, licking tremor, rapid running, mydriasis, hypersalivation, vocalizations, aggression, urination and defecation (Kitz et al., 2017; Pakozdy et al., 2014). During these seizures, cats can remain in sternal recumbency or be very active, like climbing or running (Rusbridge, 2005). Many of the aforementioned signs (oro-facial automatism and behavioural changes) are also typically observed in human patients with temporal epilepsy (Ko and Sahai-Srivastava, 2017; Santana et al., 2010), which is in humans often associated with degenerative or immune-mediated changes of the hippocampus, like HS or limbic encephalitis. The latest ILAE commission even proposed precise criteria to define temporal sclerosis: “*Neuronal cell loss and gliosis at the CA1 segment with relative sparing of other hippocampal regions, synaptic reorganisation that is not limited to mossy fiber sprouting and dispersion of the granule cells; extrahippocampal pathology can be present and special staining is recommended (i.e. Timm’s stain or glial fibrillary acidic protein)*” (Wieser, 2004).

In the last years similar changes have been detected in epileptic cats as well (Brini et al., 2004; Fatzer et al., 2000; Gelberg, 2013; Marioni-Henry et al., 2012; Pakozdy et al., 2010; Schriebl et al., 2008). Recently an immune mediated form of limbic encephalitis provoked by voltage-gated potassium channel complexes (VGPC-complexes) antibodies has been described as well in cats with complex partial seizures (CPS) and orofacial involvement (Pakozdy et al., 2013a; Pakozdy et al., 2014). The same condition has been recognised also in humans with acute onset of seizures (Graus et al., 2010; Vincent et al., 2004; Vincent and Crino, 2011). All these conditions in cats just like in humans are often associated with a poor control of seizures.

The reason which can explain why the temporal lobe is so prone to generate seizures in cats can be found in an old experimental study performed on the feline brain. In this study a relatively low threshold against electrical stimulation has been observed along the fornix, amygdaloid nucleus and near the alveus of the temporal lobe (Gibbs and Gibbs,

1936). In general, it is known that the temporal lobe is very susceptible to generating and perpetuating seizures, due to the low excitability threshold of the hippocampus (Manford et al., 1996).

The role of the hippocampus in maintenance and perpetuation of seizure activity seems to be universal (concept of a final common seizure pathway). Therefore, hippocampal surgical resection seems to be a promising technique for the treatment of refractory epilepsy in cats. Nevertheless, an early study (Estey et al., 2017) indicated that hippocampal asymmetry is a frequent finding (47 %) also in dogs affected by IE in comparison to non-affected dogs (20%). Whether the hippocampal abnormalities were a cause or a consequence of seizures, the authors of this study reflected on the possibility that also in dogs the hippocampus could be involved in the epileptogenesis or in the perpetuation of seizures and for this reason its surgical resection should be considered also in a sizeable proportion of dogs, above all in the ones presenting AED resistance.

### **3.3.1 Temporal lobe pathologies underlying TLE in cats**

#### **3.3.1.1 Congenital malformations**

In literature, just a few cases of hippocampal or temporal malformation have been described in cats and dogs. Porencephaly consists in the presence of congenital cerebrospinal fluid filled brain cavities, usually connecting the subarachnoid space with the brain ventricles. In humans, congenital hippocampal atrophy is often associated with porencephaly (Grattan-Schmith et al., 1993; Ho et al., 1998). This association has been described in veterinary medicine as well (Hori et., 2015). In cats and dogs with porencephaly hippocampal asymmetry was also present and the side with the greater hippocampal atrophy was always contralateral to the larger porencephalic defect (Hori et al., 2015). The patients affected by these anomalies usually present secondary mesial temporal lobe epilepsy (MTLE) (Ho et al., 1998; Hori et al., 2015).

Another malformation which has been associated with temporal lobe epilepsy is focal cortical dysplasia (FCD) (Blumcke et al., 2017), whose classification has been recently updated (Najm et al., 2018). This anomaly induces seizures mostly in children, but the seizure onset may occur also in older patients, up to the fifth or sixth decade of life (Fauser

et al., 2006). The same anomaly has been described bilaterally in a 10-year-old Golden Retriever referred for generalized epileptic seizures, preceded some months before by intermittent focal facial twitching (Casey et al., 2014). Klang et al. reported another example of temporal lobe congenital malformation in 2015. This was consistent with a bilateral DG structural alteration in a 13-year-old cat with a history of focal epileptic seizures (seeking behaviour, anxiety, orofacial automatism, hypersalivation) and occasional generalized epileptic fits. Nevertheless, in this case seizures were more probably the result of an intraventricular meningioma and associated HS (dual pathology). The malformation observed in this cat was similar to that of tectonically deformed dentate gyri in a subgroup of human patients with temporal lobe epilepsy affected by bulbous expansion of the CA1 pyramidal cells and subicular layers (Sloviter et al., 2004)

Another case report of hippocampal dysplasia in a dog was described by Cantile et al. (2001): a 4-year-old pug referred with a history of recurrent seizures and progressive abnormal gait and behaviour. The dog was euthanized due to poor response to medical treatment and in the histopathological examination post-mortem changes compatible with necrotizing meningoencephalitis and unilateral hippocampal cortical hamartia were evidenced. Also in this case, the signalment and the progression of the clinical signs suggested that the dysplastic changes in the hippocampus were just incidental findings.

Regarding HS, which is often involved in refractory epilepsy in human medicine, the discussion is still opened whether this should be considered a disorder resulting from developmental errors (Blumcke et al., 2012), above all when associated with other congenital abnormalities like FCD, or a secondary change induced by seizures of extrahippocampal origin, like in children with febrile convulsion (Briellmann et al., 2005; Mueller et al., 2006; Parmar et al., 2006).

### **3.3.1.2 Acquired pathologies (sclerosis/necrosis)**

HS refers to loss of hippocampal neurons and astrogliosis in various degree and is the main pathological abnormality associated with MTLE (Mathern et al., 1997). In one study performed at an epilepsy centre in Paris half of the examined epileptic patients had a diagnosis of temporal lobe epilepsy and of these the half had radiological evidence of HS

(Semah et al., 1998). Considering that MRI is not 100% accurate in evidencing HS, it is likely that its real prevalence has been even underestimated, confirming that temporal lobe epilepsy with HS is likely to be the most common form of epilepsy in humans (Engel, 1998). As mentioned before, it is still unclear if this should be considered a congenital abnormality and/or a secondary change induced by seizure. Moreover, it is still unknown how far hippocampal pathology contributes to epileptogenesis and disease progression. In veterinary medicine, HS is mostly known to affect cats (Figure 5), which, just like people with temporal lobe epilepsy, show limbic seizures with or without orofacial involvement. In one study performed on a population of 93 epileptic cats, 25,8 % of these were affected by HS and no other changes were detected during brain histopathologic inspection (Wagner et al., 2014). The aetiology of HS in absence of other brain pathologies (primary or idiopathic HS) in cats just as in humans is still unknown. Nevertheless, HS can be also the consequence of structural pathology disrupting hippocampal architecture (secondary HS), like neoplasia or bacterial, parasitic, viral and immune-mediated encephalitis (Wagner et al., 2014). Another hippocampal pathology which leads to the development of seizures in cats is in fact the encephalitis-hippocampal necrosis complex (LEHN) also known as limbic encephalitis or VGKC-complex/LGI1 antibody-associated limbic encephalitis. This has been firstly described by Pakozdy et al. in 2013 (a). In this study, the presence of the same VGKC complexes antibodies which are responsible for limbic encephalitis in humans was demonstrated in cats with limbic seizures: the leucine-rich glioma inactivated 1 (LGI1) protein. These antibodies are responsible for neuronal hyperexcitability in the hippocampus, interfering with the expression of LGI1, which is an important modulator of VGKC in the hippocampus (Pakozdy et al., 2014).



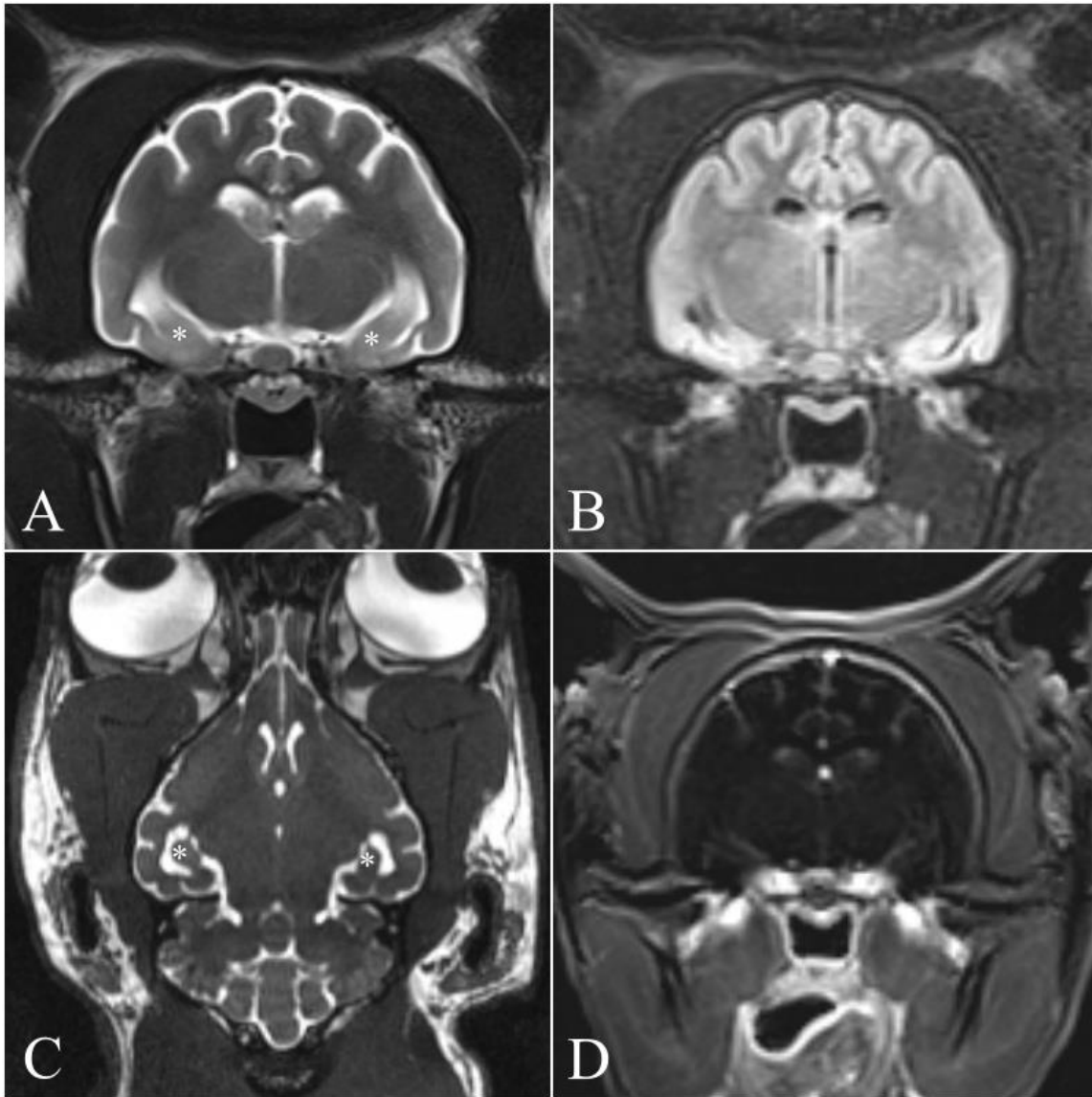


**Figure 5. Magnetic resonance imaging of a cat with suspected HS. 5-year-old male castrated Domestic Shorthair cat, which was presented in the small animal hospital of the JLU in Giessen due to chronic, refractory epileptic seizures. In the magnetic resonance imaging of the head, the hippocampus (star) presented a mild to moderate atrophy, with multiple, irregular, hyperintense areas in the T2-weighted (A) and FLAIR (B) images. The atrophy is also evident in the 3D CISS sequence. No contrast enhancement was present (D). The findings were suggestive for HS, possibly secondary to the chronic epileptic activity. In the figure above, transverse T2-weighted (A), FLAIR (B) and T1-weighted SUB after application of gadolinium (D) images, and a dorsal section of a CISS sequence (C) are shown.**

Previously many cases of feline hippocampal necrosis (FHN) have been reported (Fatzner et al., 2000; Fors et al., 2015; Gelberg, 2013; Schmied et al., 2008) but until 2013 the aetiology was not known. A possible involvement of hippocampal pathology also in dogs affected by IE has been suggested by Estey et al. (2017). In this study, hippocampal volumes were evaluated in a group of dogs with IE and compared with a control group of

non-epileptic dogs. There was no significant difference between IE and non-IE groups with regard to overall hippocampal volume but dogs with IE have a greater hippocampal asymmetry than non-IE dogs. In human medicine around 60-70 % of patients with MTLTLE who undergo surgical treatment of refractory seizures present hippocampal asymmetry, resulting from unilateral HS (Farid et al., 2012). Another study evidenced a correlation between the radiologic evidence of reduced hippocampal volume and ipsilateral temporal EEG findings in a population of epileptic dogs (Czerwik et al., 2018): 35 % of the dogs with MRI evidence of hippocampal atrophy (56 % of dogs in the IE group) had temporal epileptiform discharges on the same brain side. So, in the light of these new evidence HS may play an important role also in canine epileptogenesis.

### **3.3.1.3 Dual Pathology**

Dual pathology refers to the presence of HS together with an additional epileptogenic extrahippocampal lesion (temporal or extratemporal-like a tumour or focal cortical dysplasia type II) in the same epileptic patient. In animals, dual pathology has been described just in a few cases (Vanhaesebrouck et al., 2012; Klang et al., 2014), whereas in human medicine it is often observed in patients with refractory epilepsy. Its real prevalence is however unknown. In fact, the associated changes are not always visible using neuroimaging and they can often be revealed only by pathologic examination (Eriksson et al., 2005).

Two reports exist in veterinary medicine: in both cases the patients were affected by seizures. The first one was a 14-years-old cat with a pyriform lobe oligodendroglioma and FHN, presented because of partial complex seizures with orofacial involvement refractory to medical treatment (Vanhaesebrouck et al., 2012) and the second one was also a cat with intraventricular meningioma and HS, affected by seizures resembling temporal lobe epilepsy and euthanised for unrelated reasons (Klang et al., 2014). The last one, as aforementioned, showed bilateral DG congenital structural alterations as well.

Kim et al. showed that patients with dual pathology consisting of FCD and HS have a better surgical outcome when both dysplastic tissue and sclerotic hippocampus are removed (2010). The author suggested though that intracranial EEG monitoring should be performed in all patients in order to decide whether the hippocampus should be

resected or not, since its intrinsic epileptogenicity may otherwise remain undetected. In fact, hippocampal resection in all FCD patients with radiologic evidence of HS cannot be justified with the better surgical outcomes observed in this study. A small proportion of these patients may in fact become seizure-free even after hippocampal sparing resection and preserve hippocampal function.

## 3.4 Epilepsy surgery

### 3.4.1 Surgical techniques in human medicine

In human medicine two surgical approaches are available for the resection of temporal structures (Figure 6), with cortico-amygdalohippocampectomy (CAH) and selective amygdalohippocampectomy (SAH) being the most common procedures.

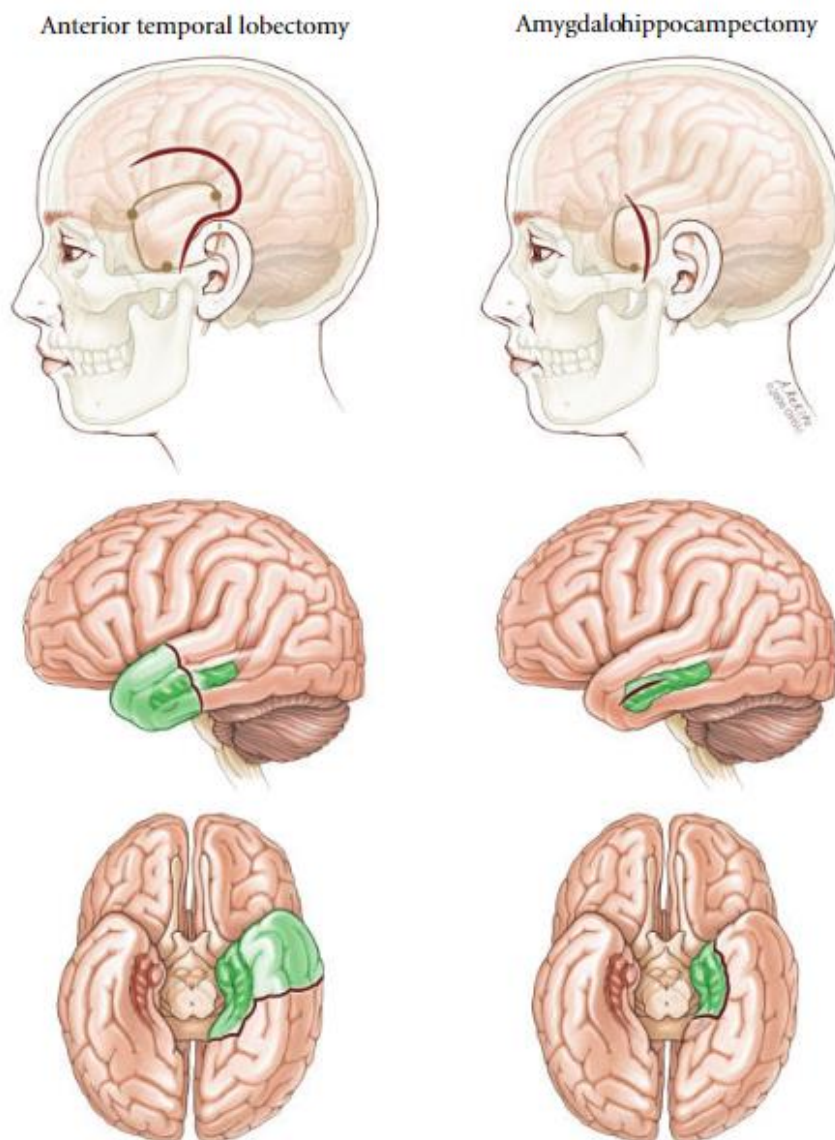


**Figure 6. Comparison of anterior temporal lobectomy and selective amygdalohippocampectomy (Spencer and Burchiel, 2012). On the left an anterior temporal lobectomy or cortico- amygdalohippocampectomy can be observed, while on the right the much less invasive selective amygdalohippocampectomy can be seen.**

The choice of the technique depends on the patient and in particular on the functional and structural abnormalities displayed with the diagnostic investigations (EEG, MRI, spectroscopy, magneto-encephalography). In fact, there is no consensus so far as to which approach is best, with respect to seizure outcome, neuropsychological impact and complications (Olivier et al., 2012b). Since mesial temporal structures are supposed to be the most epileptogenic of the temporal lobe (So et al. 1989; Gloor et al., 1982), it appears logical to perform a selective resection of these. Nevertheless, their localisation in the depth of the temporal lobe makes it more difficult.

In general, the selective approach seems to be more indicated in the cases with evidence of mesial temporal sclerosis and of seizures onset in the mesial temporal structures. On the other hand, the non-selective should be preferred in patients with no clear evidence of mesial temporal lobe epilepsy or when the lesion that is responsible for seizures is located outside the mesial temporal structures (Olivier et al., 2012b).

#### **3.4.1.1 Cortico-amygdalohippocampectomy**

The CAH or anterior temporal lobectomy consists of an antero-lateral temporal neocortical resection followed by the removal of the mesial temporal structures (hippocampus and amygdala mainly) (Muzumdar et al., 2016; Olivier et al., 2012a). Concerning the surgical technique, the patient is in supine position with the head rotated towards the opposite side, slightly extended and fixed in the head clamp. This allows a better exposition of the temporal lobe and minimizes its retraction. Then, a standard question mark incision is performed upwards from the zygoma and one centimetre in front and above the pinna, ending along the superior temporal line. Care must be taken in this phase to avoid the superficial temporal artery and the facial nerve. The scalp is reflected anteriorly, the temporal fascia is opened and after that, blunt dissection of the temporal muscle with the help of periosteal elevators is carried out. The superior limb of the temporal fascia, which is attached to the superior temporal line, should be preserved in order to facilitate the closure at the end of the surgery. Bleeding from the deep temporal vessels can be stopped applying pressure on them or using a bipolar coagulator. The monopolar should not be used because of the higher risk of tissue necrosis. The muscle is reflected anterior-inferiorly (Muzumdar et al., 2016; Olivier et al., 2012a). At this point the craniectomy can be performed: the root of the zygoma should be visualised in order

to ensure a sufficient exposure of the middle fossa. The craniectomy could be extended superiorly up to the superior temporal line and not over. In fact, thanks to the neuronavigation, it is not necessary to expose the sylvian fissure but the access should be centred on the middle temporal gyrus (T2). Then the dura is opened circumferentially and reflected away (Muzumdar et al., 2016; Olivier et al., 2012a).

Depending on the experience of the surgeon, the corticectomy can be approached in many ways, with a different extension of the resected tissues and using different tools. Olivier (2012) for example describes an incision line which starts from T1, crosses the temporal stem and is brought downwards to the basis of the temporal lobe, through the collateral sulcus. After transecting the lateral temporal cortex through this line medially and removing it en bloc, the surgeon has access to the temporal horn. Then, an incision in the lateral ventricular sulcus can be performed to allow the endopial emptying of the parahippocampus. At this stage, the hippocampal sulcus is visible through the medial border of the parahippocampus (Olivier et al., 2012a). The cortical resection can be carried out also using the technique of gyral emptying that consists of a subpial aspiration performed with the help of an ultrasonic dissector. To avoid bleeding from the opercular branches of the middle cerebral artery that run towards the superior temporal sulcus, these can be coagulated using a bipolar coagulator and divided with scissors (Olivier et al., 2012a).

Another way to reach the hippocampus is described by Muzumdar (2016), who opts for a corticectomy of the middle temporal gyrus (T2), circa 4 cm above the midpoint of the zygoma. The temporal horn is identified approximately 3-3,5cm under the surface of the cortex. Neuronavigation can be used to identify the temporal horn, depending on the ability of the surgeon. In some cases, in which the MRI has showed extended cortical dysplasia or structural abnormalities of the hippocampus, this device can be very helpful (Muzumdar, 2016). If neuronavigation is not used, to properly recognise the temporal structures, it is very important in any moment of the surgery to verify the anatomic landmarks (the ascending gyri of the central area, the middle cerebral vessels, the sylvian fissure, the wing of the sphenoid bone, the floor of the middle fossa) (Olivier et al., 2012a).

Once the corticectomy is terminated and the temporal horn has been reached with the exposition of the mesial temporal structures, the fimbria can be transected and the

hippocampus incised at the junction of body and tail and disconnected from its vascular pedicle. The subpial dissection is then carried forward in the hippocampal sulcus until the entire head, body and tail are disconnected and the en bloc removal or subpial emptying is made possible. Any residual hippocampal tissue is aspirated off the sulcus. If required, the uncus can be removed as well using the ultrasonic dissector (Olivier et al., 2012a). To ensure that the epileptogenic tissue has completely been resected and improve the outcome, especially in patients with cortical dysplasia, in some cases intraoperative electrocorticography could be used. To allow the histo-pathological examination of the resected structures, it is preferable to remove these en bloc (Muzumdar, 2016).

### **3.4.1.2 Selective amygdalo-hippocampectomy**

This surgical technique was firstly introduced in the mid-1950s by Dr. P. Niemeyer who, moving off the standard temporal lobectomy in vogue at that time, postulated that the resection of the only temporal mesial structures would be sufficient to reach a good outcome in many patients affected by temporal epilepsy. He demonstrated through surface and intraventricular registrations that these structures were within the temporal lobe the most involved in the epileptogenesis and he elaborated a procedure of transcortical, transventricular SAH through the second temporal gyrus (Figure 7). Moreover, he showed that the spiking activity in the remaining tissue became slowly non-epileptic in the days after surgery (Niemeyer, 1958; Niemeyer and Bello, 1973). Successive studies have further demonstrated the prominent role of structures such as the hippocampus, amygdala, uncus, entorhinal cortex, dentate gyrus, parahippocampus, entorhinal cortex, piriform and perirhinal areas in the genesis of epileptic activity (Gloor et al., 1982; Rasmussen and Branch, 1962; Sato et al., 1990).

Moreover, important in patients with temporal lobe epilepsy is to consider in which hemisphere seizure start. In fact, in the 77% of cases originate exclusively or with a strong predominance in one temporal lobe only. In the remaining cases, the focus is located bilaterally (23%) or independently in either temporal lobe without significant lateralization (14%) and just a small percentage (9%) of cases has multiple seizures patterns (So et al., 1989).

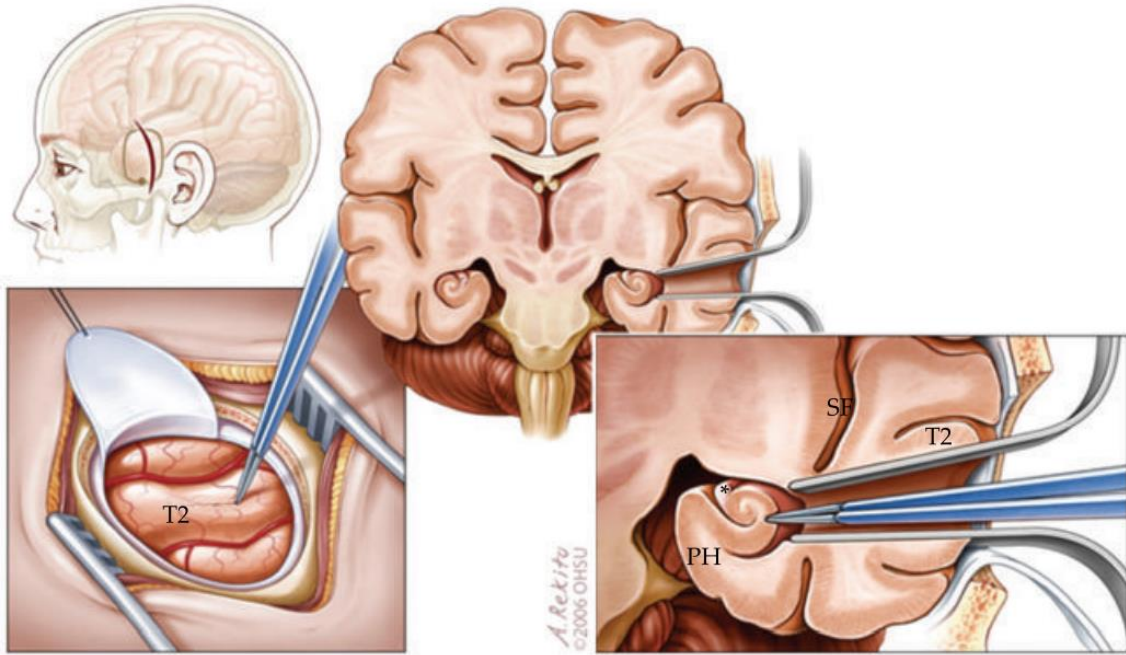


**Figure 7. Selective transcortical amygdalohippocampectomy through the second temporal gyrus (Spencer and Burchiel, 2012). Surgical approach (left) and coronal views of the brain, temporal lobe and nearby structures (centre and right). A retractor is placed along the white matter corridor in T2 after opening the lateral ventricle to fully expose the hippocampal formation. The first step in the SAH is to enter the lateral ventricular sulcus to empty the parahippocampus in a subpial fashion. Then, the hippocampus is separated from the fimbria (\*), tail and removed en-bloc. Lastly, the subpial emptying of the uncus and the resection of the amygdala are carried out. The mesial temporal structures that are removed in this technique are the hippocampal complex and parahippocampus. SF = Sylvian Fissure; T2 = middle temporal gyrus; PH = parahippocampal gyrus (T5).**

Nowadays, many different approaches for the SAH have been described: the transventricular (Niemeyer, 1958), the transsylvian (Yasargil et al., 1985), the subtemporal one (Hori et al., 1993; Park et al., 1996), the stereotactic ablation (Parrent and Blume, 1999) and the MNI selective amygdalohippocampectomy (Niemeyer, 1958; Niemeyer and Bello, 1973; Olivier et al., 1992). The second one above mentioned technique requires the transection of the temporal peduncle to reach the hippocampus through the sylvian fissure. This one is then exposed and resected en bloc with a suction device and the amygdala is removed subpially (Yasargil et al., 1985). The third approach has the advantage to reduce the amount of transected tissue (cortex and white matter) since it implies the retraction of the temporal lobe and of the bridging vessels. The last one consists of the stereotactic insertion of an electrode in order to damage the mesial temporal structures. With this approach the seizure outcome is not as positive as with the



other techniques, maybe because of the limited resection of epileptogenic tissue or residual scar tissue formation

At the Montreal Neurological Institute (1928) many different approaches have been adopted over the years. There, many leading neurologists and neurosurgeons, who have contributed to develop most of the present knowledges in this field, worked in the last century. At the beginning they performed a transcortical SAH through the first temporal gyrus (T1), then through the superior temporal sulcus and afterwards through the second temporal gyrus (T2), with an approach much similar to the one proposed by Niemeyer in 1958. In 1992, Olivier adopted and modified this approach using neuronavigation, which has allowed refining the technique and improving the outcome, and a system of ultrasound dissection to perform the endopial emptying of the mesial temporal structures.

### **3.4.2 Post-operative complications after epilepsy surgery**

The presence of blood in the temporal horn can cause fever. People can experience mild local pain and mild to moderate headaches. These symptoms should resolve over few days. In case they persist, it is indicated to perform a CT examination and a liquor study in order to rule out meningitis (Muzumdar et al., 2016). The development of a hematoma after resection is also a possible complication, but this can be hopefully removed in a second surgery (Helmstaedter et al., 2004). Salanova et al. reported in another study (2002) the occurrence of infection of the bone lap (1.3 %), a mild hemiparesis (0.9 %), hemianopia (0.4 %), transient cranial nerve palsies (3.2 %), transient postoperative language difficulties (3.7 %), verbal memory deficits (8.8 %), postoperative psychosis (2.3 %) and postoperative depression (5.5 %). Global memory deficits occur rarely (1%), however after dominant hemisphere resection verbal memory deficits as well as language deficits happen very often (25-50% and 25-60% respectively) (Muzumdar et al., 2016).

### **3.4.3 Outcome in human patients**

Regarding seizures outcome, surprising results has been obtained in the last 50 years: a remarkable percentage (75-90%) of AEDs' resistant patients were seizure free after surgery for the whole duration of the follow-up period at least (Cuckiert et al., 2009; Dupont et al., 2006; Lutz et al., 2004; McIntosh et al., 2004; Nayel et al., 1991; Salanova

et al., 2002; Tanriverdi et al., 2009; Wieser et al., 2003; Yam et al., 2010). In the study of Cuckiert et al. (2009), 77% of the patients had no seizures during the follow-up year after the surgery, whereas another 15% of the patients still suffered from simple partial seizures (SPS), 4% from SPS and generalized tonic-clonic seizures (GTC) and the remaining 3% just from GTC. An important point to improve the seizure outcome is the completeness of the hippocampal resection (Hori et al., 1993) and above all of its posterior part, which seems to be one of the most epileptogenic tissues of the brain (Spencer et al., 1984). In fact, the recurrence of epilepsy is either due to a remnant of dysplastic tissue or to residual hippocampal tail; both of them can lead to recurrent epileptic seizures after surgery (Muzumdar et al., 2016).

With regard to neuropsychological outcome, global memory deficits occur rarely (1 %) (Clusmann et al., 2002); instead, verbal memory deficits have been more often observed and in particular after performing the trans-sylvian or the subtemporal approaches (Lutz et al., 2004; von Rhein et al., 2012). The transsylvian SAH is in fact associated to a quite extensive dissection of the middle cerebral artery branches and consequently to the risk of vascular injury and retraction injury which can result in stroke and language deficits (Adada, 2008; Yasargil et al., 1993; Yasargil et al., 2004). For this reason, the transcortical approach shows a better outcome in many studies in comparison to the trans-sylvian one. Moreover, verbal memory deficits occur above all (in 25-50% of cases) after dominant hemisphere resections (Clusmann et al., 2002; Helmstaedter et al., 2004). Indeed, verbal memory impairment have been described above all with left-sided resections (Bonelli et al., 2010; Gleissner et al., 2004; Lee et al., 2002; Sherman and Guillery, 2011; Tanriverdi et al., 2010).

Controversially, more recent studies showed (Gül et al., 2017; Oddo et al., 2012) a better outcome with impaired recall phase of verbal memory but improved recognition phase, which leads therefore to the absence of verbal memory dysfunction also after left-sided resections. An improvement of verbal memory was also observed in other studies after left-sided resections (Grammaldo et al., 2009; Schramm, 2008; Vojtěch et al., 2012). Gül et al. reported also significant improvements in executive functions, like preservative responding, abstraction and problem-solving difficulties as well (2017).

In general, an improvement in memory function related to improved contralateral temporal lobe function (on the non-operated side) has been observed in 60% of the

patients. 59% of the patients experienced even an improvement in general IQ (Cuckiert et al., 2009). Lutz et al. (2004) observed above all improvements in memory span and in working memory task; in his opinion, verbal fluency improved above all after a transcortical approach. The transsylvian SAH in fact is associated to an extensive manipulation of the frontal lobe and is consequently related to the so-called “collateral damage”, possibly responsible for the verbal fluency task deterioration (Helmstaedter et al., 2004). Visual memory deficits have been sometimes reported as well (Bonelli et al., 2010; Grammaldo et al., 2009; Helmstaedter et al., 2011; Tanriverdi and Olivier, 2007; Tanriverdi et al., 2010).

### 3.5 Epilepsy surgery in cats and dogs

The resection of temporal lobe structures in dogs and cats has already been described in the past years. In the study of Kowalska and Kosmal (1992), the resection of the hippocampus has been carried out with experimental purposes. Indeed, the researchers used it with the aim to investigate the cognitive functions of the temporal lobe. In another experimental study, amygdalo-hippocampectomy was attempted in cats after induction of limbic status epilepticus through the microinjection of kainic acid into the unilateral amygdala (Tanaka et al., 1989). Moreover, in a case report a novel approach for temporal lobectomy has been described with the aim to remove a cavernous haemangioma in a dog (Shihab et al., 2014). Noteworthy is the recently published case of a cat which underwent a focal cortical resection and total hippocampectomy due to refractory temporo-occipital seizures (Hasegawa et al., 2021).

In the first aforementioned experimental work, a dorsal approach through the parietal, visual, associative area with the aid of an operating microscope was employed in dogs: the skin was cut along the midline with a rostro-caudal direction; then, the temporal muscle was resected along its aponeurosis and retracted laterally. After performing a small circular craniectomy 11-30mm from the midline, a round defect (about 7mm in diameter) in the parietal cortex was created between the *fissura ectolateralis* and the *f. suprasylvia*. In this way, the author was able to reach the hippocampus in the temporal horn of the lateral ventricle and to resect most of it by suction. With this technique the removal of the anterior part of the dorsal and ventral hippocampus were just partially possible (Kowalska and Kosmal, 1992). The same approach was used by the author in a later behavioural study (Kowalska, 1995), which investigated the role of hippocampus in spatial memory. Here, it was demonstrated that a bilateral hippocampectomy in dogs impairs the performance of a delayed response task involving memory for the spatial location of an auditory cue. This impairment depends also on the length of the delay. Unluckily, a control group, in which the unilateral resection of the hippocampus was performed was missing in this investigation (Kowalska, 1995).

In the first abovementioned case report, a lateral approach to the temporal lobe was described. The haemangioma was in fact located ventrally and mesially in the temporal lobe, caudally to the amygdala and was involving the ventral part of the hippocampus. First a “T” shaped incision was obtained in the skin and in the temporal muscle using a combination of sharp dissection and bipolar diathermy. After that, the muscle was

retracted. During dissection the superficial temporal artery was isolated and ligated. A square craniectomy was performed with a pneumatic drill over the lateral aspect of the ventral part of the temporal bone. In order to reach the tumour located mesially, the temporal cortex over the mass was resected with an ultrasonic aspirator. The dog was discharged two days after surgery. At the time of discharge, he was ambulatory but showed a mild generalized ataxia; the mentation was normal, and no seizure activity was recorded. On re-examination, two weeks after surgery the neurologic status of the dog was unchanged. No seizure episodes have been reported by the owner. Five months after surgery, the dog showed a recurrence of focal seizures, but thanks to the surgical therapy these were now responsive to the pharmacotherapy. One year after surgery, general and neurological examinations were still unremarkable and blood panels as well (Shihab et al, 2014).

Lastly, a recent case report described the first surgically treated case of a cat affected by refractory temporo-occipital epileptic seizures (Hasegawa et al., 2021). This innovative study demonstrated that epilepsy surgery is a feasible treatment option also for epileptic animals with antiepileptic drug resistance. The cat underwent before surgery a 3-days video EEG examination with electrocorticographic (ECoG) electrodes, which allowed to localise the epileptogenic area. In view of the MRI, electroencephalographic and electrocorticographic findings, a two-step surgical approach was planned: first a cortical resection of the temporo-occipital cortex was carried out, and then, due to the persistence of epileptic seizures, a total hippocampectomy and an additional cortical resection were conducted. No postsurgical complications were recorded, and the cat experienced a notable reduction in seizures frequency under antiepileptic therapy (> 85%).

Regarding earlier surgical attempts to treat non-temporal epilepsy or epileptic seizures in general, to date in veterinary medicine an experimental study (Bagley et al., 1995) and few case reports (Glass et al., 2000; Martlé et al., 2009; Oliver, 1965; Parker and Cunningham, 1971) can be found in literature. Bagley's research focused on determining morbidities associated to the longitudinal division of the *corpus callosum* in dogs (Bagley et al., 1995). This surgical procedure was chosen with the aim to be potentially employed as surgical treatment in animals with AED resistance. Indeed, the corpus callosotomy is well known in humans to eliminate a potential pathway for seizure propagation and may, therefore, help to decrease the severity of seizure activity. Moreover, preventing seizure generalization, this technique may improve responsiveness to antiepileptic drugs (Asadi-

Pooya et al., 2008). Lastly, a modified bilateral transfrontal sinus craniotomy was described in 5 dogs to approach the canine olfactory bulbs and frontal lobes for removal of lesions in these areas of the brain (Glass et al., 2000).

### **3.5.1 Morphological differences between human and feline temporal lobe structures**

The biggest obstacle to overcome in veterinary medicine is the size of the brain. In fact, the dimensions of an animal's brain (above all of a cat) are much smaller than those of a human brain. This itself makes the surgical approach much more difficult in our domestic animals. A subtemporal approach for example is unlikely to be performed in our pets. A bigger attention must be paid to avoid the tiny blood vessels and for this reason, an intraoperative microscope should be employed in the future to perform these surgeries in our pets, above all if a microinvasive approach is attempted. Another difference which can possibly have a clinical relevance is the incompleteness of the orbital bony structures in domestic animals: in fact, in dogs there is caudo-laterally to the orbita no conjunction between the zygomatic and the frontal bone and in cats there are only two incomplete processi departing from both bones. This may expose the ocular bulb to possible trauma through the positioning of a retractor in the temporal musculature.

When approaching the temporal lobe of a dog or a cat, the surgeon must be aware that the morphology of the gyri is completely different. Indeed, in humans the temporal lobe is composed by 7 gyri, whereas in pets by just 5 gyri (ectosylvian gyrus, sylvian gyrus, parahippocampal gyrus, dentate gyrus and hippocampus itself). This is very important in order to correctly localize the mesial temporal structures without a stereotactic device.

### **3.6 Histopathology of hippocampal sclerosis**

HS is a very frequent histo-pathologic finding in adults affected by drug-resistant temporal lobe epilepsy. In one study 5,392 epileptic patients who underwent surgical resection for various aetiologies, HS was diagnosed in 33.6% and another 5.1% showed dual pathology, which consists of HS in combination with cortical malformations, tumors, vascular lesions or scars (Blumcke and Spreafico, 2012). Similarly, in another hospital-based study, 25% of the patients with TLE presented MRI findings indicative of hippocampal atrophy (Semah et al., 1998). Because of the high percentage of patients affected by hippocampal pathology, the necessity to reach an international consensus in its classification was impending in human medicine. For this reason, the ILAE elaborated in 2013 a histological classification scheme for HS. All specimens were firstly stained with haematoxylin-eosin and then with at least NeuN and GFAP in order to evaluate neuronal and glial cell densities in the specimens. The ILAE recognized three types of HS which could be identified by visual histopathologic examination of en-bloc resected surgical hippocampal specimens (Blümcke et al., 2013):

- In the type 1 HS, which is the most encountered in human medicine (around 60-80 % of all TLE-HS cases), the CA1 segment is the most severely affected (with >80 % neuronal loss) (Blümcke et al., 2012). Other segments may be affected as well: 30-50 % of pyramidal cell loss in CA2, 30-90 % of neuronal loss in CA3 and 40-90 % in CA4. The loss of the 50-60 % GCs can be detected in the DG as well.
- Type 2 HS presents predominantly pyramidal cell loss (almost 80 %) in the CA1 sector. The other areas are just marginally affected. Granular cells dispersion in the DG can be observed as well. This type is present just in the 5-10 % of all surgical cases.
- Type 3 HS is characterized by a predominant cell loss in C4 (circa 50 % of cell loss) and in the DG (35 % of cell loss). It is also considered a rare pattern of HS (4-7,4 %).
- 20% of TLE cases show just reactive gliosis but no significant neuronal cell loss (no hippocampal sclerosis, gliosis only).

GCs dispersion is observed in approximately 50 % of all TLE cases. It is associated in human medicine with greater cell loss in the hilus, an older age at epilepsy surgery and

longer epilepsy duration. The involvement of GC can be related to memory impairment in these patients.

Moreover, during the histopathological examination of hippocampal specimens from epileptic patients with HS, other stainings (i.e. MAP2, CD34, Vimentin, Ki-67) could be required to rule out the presence of other pathological abnormalities (i.e. neoplastic, inflammatory) underneath (dual pathology).

In veterinary medicine, so far only one study tried to describe the patterns of HS in cats and to evaluate its prevalence (Wagner et al., 2014). The authors underlined the fact that HS occurs very often together with pathologies disrupting the hippocampal architecture (76.3 %), whereas only 23.7% of the affected cats had a concurrent extrahippocampal forebrain lesion. Most of the intrahippocampal lesions were of inflammatory origin (48.4%). Moreover, all cases of bilateral HS were associated with the presence of inflammatory or neoplastic infiltrates invading both hippocampi. Only a very small number of animals were affected by “HS-only pathology”.

Regarding the histopathological pattern of the lesions, 80% of the cats showed polysegmental HS. CA3 and CA4 were most commonly affected areas, being involved in 63.4% and 53.6% of all cases, respectively. On the other hand, CA1 in contrast to humans does not seem to be a vulnerable region in the feline hippocampus, whereas CA2 is more often affected by neuronal cell loss and gliosis than in people (Wagner et al., 2014). Nevertheless, a detailed, complete classification of the pathology has not been undertaken, yet.

### **3.6.1 Hippocampal cellular densities**

While in humans and rodents a lot of research about this topic has already been conducted, there is no study that systematically investigated the cellular densities in the feline hippocampus. A very interesting systematic review of mouse cerebral cellular densities has been recently published (Keller et al., 2018). This work includes all published studies regarding neuronal and glial cells density in the hippocampal formation of the mouse. By analysing the different studies, it becomes evident that in the past many different methods were used for cell counting: optical disector (Jinno and Kosaka, 2010; Ogata and Koasaka, 2002), optical fractionator (Fabricius et al., 2008), using a counting software (Kurt et al., 2004), with the aid of a grid or a counting box (Geisert et al., 2002), or manual count (Shimada et al., 1992). In addition, it should be mentioned that most works on mice



were performed on mouse models of human pathology and not on healthy animals, or aimed at evaluating particular cell populations (i.e. ErbB4 expressing interneurons in Neddens and Buonanno, 2010). Moreover, not all hippocampal areas were always taken into consideration but in many studies only CA1, CA3 and the DG were evaluated (Keller et al., 2018). This can be a consequence of the difficulty to adequately delimit CA2 from the surrounding areas. Nevertheless, the end folium (CA4) was also rarely examined. On the other hand, most studies performed in humans aimed at investigating the influence of age, sex, or pathological brain conditions on hippocampal cellular densities. Dam et al., underlined that cellular densities decrease in general from CA3 to CA1 and that CA4 is the area with the lowest one (1979). The low cell density of CA1 in comparison to CA2 and 3 is probably related to the high vulnerability of this area in relation to various pathological conditions, especially hypoxia in humans (Meldrum and Brierley, 1972). Moreover, one study showed a higher vulnerability of the posterior part of the hippocampus in comparison to the anterior one (Ball, 1977); this diversity may be related to a difference in cell density. Regarding the influence of race, sex and age on hippocampal cellular population, no racial or sexual influence was found in humans so far (Ball, 1977; Dam et al., 1979; Devaney and Johnson, 1984), whereas age seems to influence hippocampal cellular density. To this regard, opposing results can be found in literature. Indeed, whereas some studies suggested that with age a decrease in neuronal and glial density occurs in the brain (Ball, 1977; Dam et al., 1979), others shown that the relative proportions of neurons and glia actually remain stable throughout life and so cellular densities, although cellular loss occurs. This is due to a progressive shrinkage of the brain just like of the hippocampus (Shefer, 1977). Due to cerebral and hippocampal age-related atrophy, in another study even increased neuronal densities were found in the hippocampus of old people (Devaney and Johnson, 1984). Lastly, a regional selectivity of neuronal loss was reported in another study in which age-related losses were recorded only in the subiculum and in the hilus of the DG; the three remaining examined hippocampal subdivisions (CA1, CA2-3 and GCL) showed no significant changes (West, 1993).

## **4 Study 1**

### **4.1 Aims and objectives of the study**

The aim of this study is to establish and evaluate a new surgical approach for the resection of mesial temporal structures and in particular of the hippocampus in cats; in fact, cats, similar to humans, are known to be affected by HS, potentially causing AED resistance. In humans, temporal lobe resection is a standardized therapy in patients with refractory temporal lobe epilepsy (TLE). The majority of TLE patients are seizure free after surgery.

The surgical procedure developed in the study will be accurately described and documented with photos. Important cortical and subcortical structures within or close to the surgical site, as well as the structures which have to be resected will be identified through the use of different diagnostic imaging techniques and the software ARMIRA<sup>®</sup>. These devices will be indeed used for pre-surgical planning. Moreover, a micro-CT (mCT) examination will be performed to assess temporal vasculature as a reason for possible intraoperative complications. Post-resection MRI and histological examination of the resected tissues will show the exact extension of the resection and evidence any damage to the surrounding structures. In addition, it will be evaluated if the resected tissues are feasible to be histologically examined.

## 4.2 Materials and methods

### Animals

Fourteen cats of different age were collected from the Department of Veterinary Clinical Sciences, Clinic for Small Animals of the Justus-Liebig-University, Giessen. The cats were euthanized or had died from diseases unrelated to the skull and central nervous system. Written consent was obtained from all owners that donated their animals for the study, and actual cats remained anonymous. The clinical history of all of them was known. The protocol used for euthanasia was the following: premedication with 0,5 mg/kg of Diazepam administered intravenously [IV], followed by induction of anaesthesia with 2-4 mg/kg of Propofol [IV] and finally administration of 60 mg/kg of Pentobarbital [IV]. Cadavers were eligible for the current study if they did not present morphologic brain abnormalities, as assessed through a neurologic examination ante-mortem and the pre-surgical MRI examination. Two cats were excluded due to the presence of cerebral disease in the pre-surgical MRI. Of the remaining twelve cats, ten were enrolled to perform the surgical procedure and the other two were used for the mCT study of vascular supply in the surgical field. The cats were all but two (British Shorthair, Persian) Domestic Shorthair cats (DSH), weighing between 0.5 and 5.6 kg (median weight: 3.79 kg). Median age was 4.9 years (range: 1 month to 10 years). Of the twelve cats, six were females (3 spayed and 3 sexually intact) and six were neutered males (Table 1).

**Table 1. Signalment and cause of death of the study cats (surgical study).**

Animals	Breed	Weight (kg)	Age	Sex	Cause of death
1	Domestic Shorthair	5.2	5 y	Male, neutered	Spinal fracture Th10
2	Domestic Shorthair	3.5	10 m	Male, neutered	Fractures of both femurs, fracture of the ileo-sacral joint on the right, fracture of the ileus, fracture of the 3rd coccygeal vertebra
3	Domestic Shorthair	3.7	4 y	Male, neutered	Suspected rupture of the trachea with pneumomediastinum
4	Domestic Shorthair	3.5	9 y	Female, entire	Subcutaneous emphysema and pneumothorax due to ribs fracture after trauma

<b>5</b>	Domestic Shorthair	3.75	8 y	Male, neutered	Tarsal luxation and mandibular luxation
<b>6</b>	Domestic Shorthair	2.7	10 y	Female, neutered	Inguinal wound and hypothermia after trauma
<b>7</b>	British Shorthair	0.5	1 m	Female, entire	Atresia ani
<b>8</b>	Domestic Shorthair	3.8	7 y	Female, neutered	Intestinal neoplasia
<b>9</b>	Domestic Shorthair	4.2	5 y	Female, entire	Aortic thromboembolism
<b>10</b>	Domestic Shorthair	5.6	9 y	Female, neutered	Aortic thromboembolism
<b>11</b>	Domestic Shorthair	4.8	1 y	Male, neutered	High-grade mediastinal lymphoma
<b>12</b>	Domestic Shorthair	4.2	11 m	Male, neutered	Pulmonary contusion and pneumothorax after trauma

## MR- and CT imaging of the head

A standardized MRI protocol was used to examine the brain before and directly after removal of the hippocampus using a 3.0-T superconductive system and a flex-mini sensitivity-encoding coil (Siemens Healthcare). Sagittal, dorsal, and transverse T2-weighted (TE = 120 ms, TR = 2.900 ms) and T1-weighted 3D sequences were acquired in all cats pre- and post-operatively. Slice thickness varied from 1-2 mm. The field of view measured 180 x 180 mm. The matrix was 288 x 288. Before surgery, CT data sets were also acquired with a 16-slice helical CT scanner (CT Brilliance, Philips, Hamburg, Germany; 120 kV, 350 mAs, matrix 512 x 512, slice thickness 0.8 mm, pitch 1).

## Image processing

In order to find the appropriate surgical approach to the hippocampus, 3D models of the head were built on the basis of MR- and CT images. Image processing for volume rendering of the volumes of interest was achieved using specialized graphical software (AMIRA<sup>®</sup>, Mercury Computers Systems, Berlin, Germany). This program can combine image information of CT and MRI into 3D models. The hippocampus, brain surface, skull and skin surface were extracted from the digital images by manually tracking the

boundaries of the structures as described previously (Schmidt et al., 2017). Using landmark tools, the hippocampus was highlighted within the brain model and its position was projected on the surface of the brain and skull.

### **mCT Study**

In order to visualize the blood vessels of the surgical area, the cerebral vasculature of two cats was perfused with Solutrast®. Directly after death the chest was opened, the brachiocephalic trunk was prepared, and a blunt 18 gauge cannula was inserted into the vessel. After tight fixation of the cannula and ligation of the vessel caudal to the cannula, the animals were first perfused with heparin (25000 UI) diluted in crystalloid solution (500 ml) to prevent the blood from clotting in the vessels. The blood in the cerebral vessels was drained out through an incision on the right auricle. Solutrast® was infused into the vascular system with a perfusion rate of 1 ml/min after complete drainage of blood. After exit of the Solutrast® from the right atrium, the chest was tamponed, and the carcass was stored at room temperature with the head hanging down for one night. Then, the brains were removed from the skull and fixed in formalin. The brains of the perfused cats were examined with the mCT System Skyscan 1173 of the company Brucker Microct (Kontich, Belgium). The SKYSCAN 1173 is a high energy mCT scanner which includes a 130 kV microfocus (< 5 µm), X-ray source (Hamamatsu 130/300), flat panel sensor (detector), and a precision object manipulator. Before scanning, the brains were wrapped in parafilm in order to avoid dehydration and fixed into the sample holder with styrofoam. The sample holder was then positioned on the sample stage, between the X-ray source and detector, within the mCT. The voltage and current source selected for the acquisition were respectively 70 kV and 114 µA. The detector had a matrix size of 2240x2240 pixel, with a pixel size of 20.1 µm. In order to reduce the beam hardening, a 1.00 mm aluminium filter was used. For each brain, two scans were necessary in order to obtain a complete 3D image. The samples moved with a rotation step of 0.25–0.30° on their vertical axis with a “step and shoot” type of motion, whereas the detector was still. The exposure time was between 950–1100 ms. The result of the acquisition process was raw data in TIFF format with a depth of 16 bits. Next, the raw data was reconstructed using a modified Feldkamp algorithm. As a result, three-dimensional data sets with isotropic voxels and 8-bit grey tone distribution were obtained and saved as BMP files. The digital processing and analysis of the 3D images was then performed with the program Analyze© 12.0, produced by the company Biomedical Imaging Resource (BIR) (Mayo clinic in

Rochester, MN, USA). For the identification of the hippocampal vasculature and its isolation from the surrounding tissues, a grey threshold on a grey scale was set. Once the vessels of the hippocampus were extracted, they were inserted in the cerebral frame in order to allow better orientation. Relevant arteries in the surgical field were identified on the basis of published investigations (Gillilan, 1976; Goetzen and Sztamska, 1992; Nilges, 1944).

### **Tissue samples processing and examination**

All resected hippocampus specimens were fixed in 10% neutral-buffered formalin for at least 5 days at room temperature. Before paraffin embedding, the samples were taken off formalin and pre-treated with phosphate buffered saline (PBS), in order to wash out formalin. This process lasted 72 hours, and the PBS solution was replaced twice in order to optimize formalin diffusion out of the samples. The resected specimens were infiltrated with paraffin wax and then embedded into wax blocks. These were then sectioned with a Leica RM2125RT Microtome. Seven  $\mu\text{m}$  thick sections were mounted on standard microscope slides. Before staining, the sections had to be deparaffinized through a passage in a 100% xylene solution and then hydrated.

The slides were stained using Nissl staining (cresyl-violet). In order to obtain this staining, after the hydration process (Table 2) the sections had to be put in a 50% potassium-disulphite solution for 15–20 minutes before being washed with distilled water. Following this, the sections were ready for staining in a 1.5% cresyl-violet solution for 20 minutes at room temperature. After staining, a quick rinse in PBS was performed. The next step was a differentiation in alcohol: the slides were immersed first in a 70% ethanol solution, then twice in a 96% ethanol solution, and finally twice in a 100% ethanol solution to remove the excess stain. The dehydration process was then completed through a passage in xylene (Table 3).

**Table 2. Hydration process. Before staining all slides undergo a hydration process as shown.**

<b>Repetition</b>	<b>Duration (minutes)</b>	<b>Solution used</b>
2x	10	Xylene
1x	5	100% Ethanol

1x	5	96% Ethanol
1x	5	80% Ethanol
1x	5	70% Ethanol
1x	5	Distilled water

**Table 3. Dehydration process (Nissl staining). After staining with cresyl violet, all sections undergo a differentiation process, which ends two passages in xylene 100%. During this process, part of the stain is washed away from the slides.**

Repetition	Duration (minutes)	Solution used
1x	10-20	70% Ethanol
1x	5-7	96% Ethanol
1x	5	96% Ethanol
1x	3-5	100% Ethanol
2x	10	Xylene

After resection of the hippocampus, all brains were fixed in formalin and processed in the same way as described above. 10–15 slides (76x52 mm) at different levels of the corticotomy were obtained and stained with the cresyl-violet staining. These slides were used to evaluate the extent of the resection and the presence of accidental traumatic injury in the structures mesial to the hippocampus.

## 4.3 Results

### Localization of the hippocampus within brain and skull

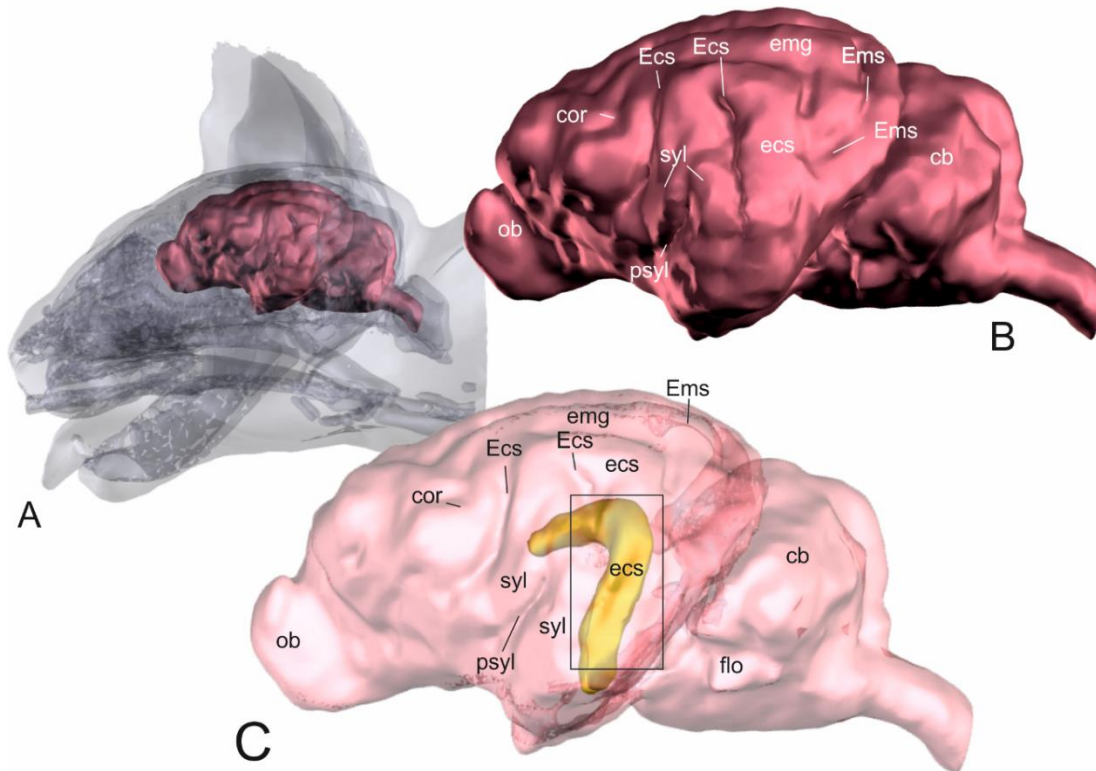


**Figure 8. Localization of the hippocampus within the brain. 3D models of the skull and brain of a domestic shorthair cat based on CT- and MRI-images. Model A shows the whole brain (red) within the skull. Model B gives an overview of the neocortical sulci and gyri of the same brain. The brain surface is transparent in model C that displays the hippocampus (yellow) within the brain. Most of the hippocampus (head, body and parts of the tail) is situated underneath the caudal ectosylvian sulcus. ob: olfactory bulb; cor: coronal sulcus; Ecs: ectosylvian sulcus; ecs: ectosylvian gyrus; syl: sylvian gyrus; psyl: pseudosylvian fissure; emg: ectomarginal gyrus; Ems: ectomarginal sulcus; cb: cerebellum; flo: flocculonodular lobe.**

Using transparent skull and brain models, the opaque hippocampus could be clearly visualized within the brain (Figure 8). The body and part of the tail of the hippocampus were identified underneath the caudal ectosylvian gyrus in mesocephalic as well as in brachycephalic cats (Figures 8-9). The most lateral point of the body of the hippocampus was localized at the level of the dorsal part of the caudal ectosylvian sulcus. Using landmark tools, the position of this part of the hippocampus was projected to the bone and skin surface (Figure 9). It was then localized using an imaginary line between the external occipital protuberance and the tip of the frontal process of the zygomatic bone.



The middle of this line marked the centre of the craniectomy site, approximately 0.5–1 cm rostral to the lateral cantus of the pinna.

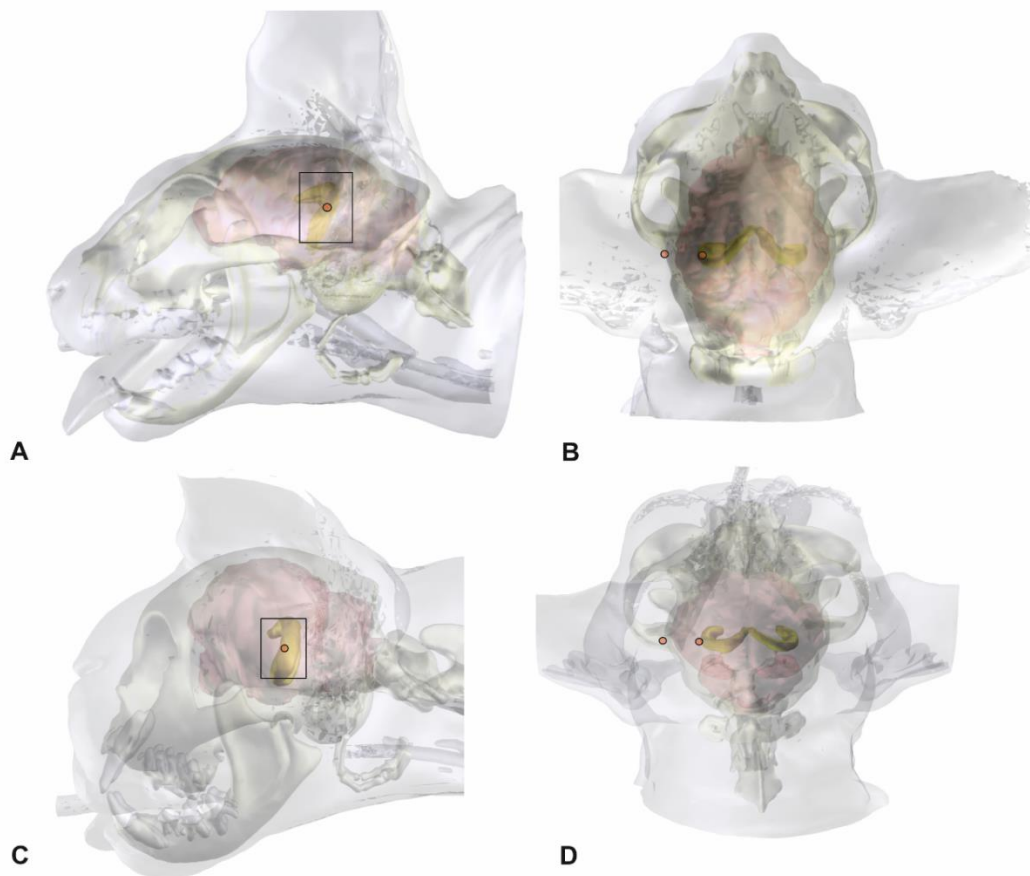


**Figure 9. Localization of the ectosylvian sulcus and the hippocampus from the skin surface and skull. 3D models of the head, skull, and brain of a mesocephalic Domestic Shorthair cat (A, B) and a brachycephalic Persian cat (C, D), in lateral (A, C) and a dorsal view and a dorsal view (B, D). The graphical software combines MRI- and CT-images. The hippocampus can be localized within the brain and the position can be projected on the brain and skull surface.**

Compared to mesocephalic cats, the brain of brachycephalic cats is distorted to accommodate their altered skull (Schmidt et al., 2017). Due to the reduction in its longitudinal extension, the hippocampus is less curved but has the same position underneath the caudal ectosylvian gyrus. The concave side is slightly tilted towards the midline. The orbit of brachycephalic cats in this study was closed, and thus the tip of the frontal process could not be used as an orientation point. The external occipital protuberance and the base of the frontal process of the zygomatic bone, where it merges with the zygomatic process of the frontal bone can be used as a landmark in brachycephalic cats (Figure 9).

## Surgical technique

The cats were placed in sternal recumbency with the head positioned at a 45-degree rotation to the right. Silicone cushions were used to hold this position. Using the landmarks explained above, a straight dorso-ventral skin incision was made, from the sagittal crest, at the level of the medial canthus of the *pinna auricularis*, to the temporomandibular joint (5–6 cm). The underlying fascia and the temporal muscle were sharply dissected, and the two edges of the muscle were retracted using Weitlaner retractors to expose the parietal and temporal bone (Figure 10). A blunt dissection of the musculature to reduce bleedings is possible as well. During muscular retraction, the ocular orbit rostrally must be preserved. After spreading the temporal muscle, the cranial sutures between the frontal, parietal, and sphenoid bone could be used as landmarks. The coronal suture (fronto-parietal suture) marks the rostral boundary, and the squamous suture (sphenoparietal suture) marks the ventral boundary of the craniectomy (Figure 10).

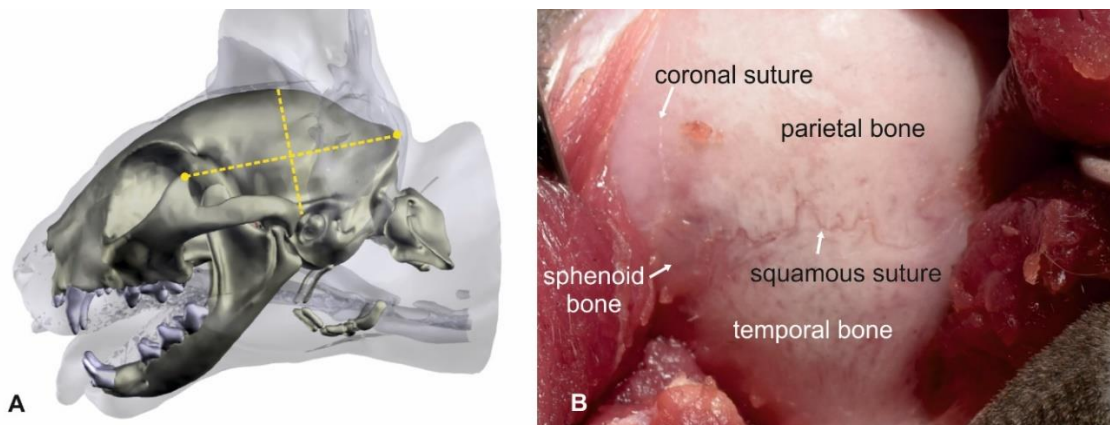


**Figure 10. Pterional craniotomy: Bony anatomical landmarks.** The cat's head is turned 45° to the side in order to place the zygomatic arch at the highest point. Landmarks for skin incision are the frontal process of the zygomatic bone and the external occipital protuberance. A skin incision is made in the middle of an imaginary line connecting the two landmarks (A). After dissection and spreading of the temporalis muscle, the left parietal and temporal bone is exposed. The crossing of the coronal and squamous suture is visible (B). The same landmarks that can be used for the orientation on the skin surface can be used at the calvaria as well. The middle point of these imaginary line marks the position of the craniectomy site with the hippocampus body at the centre.

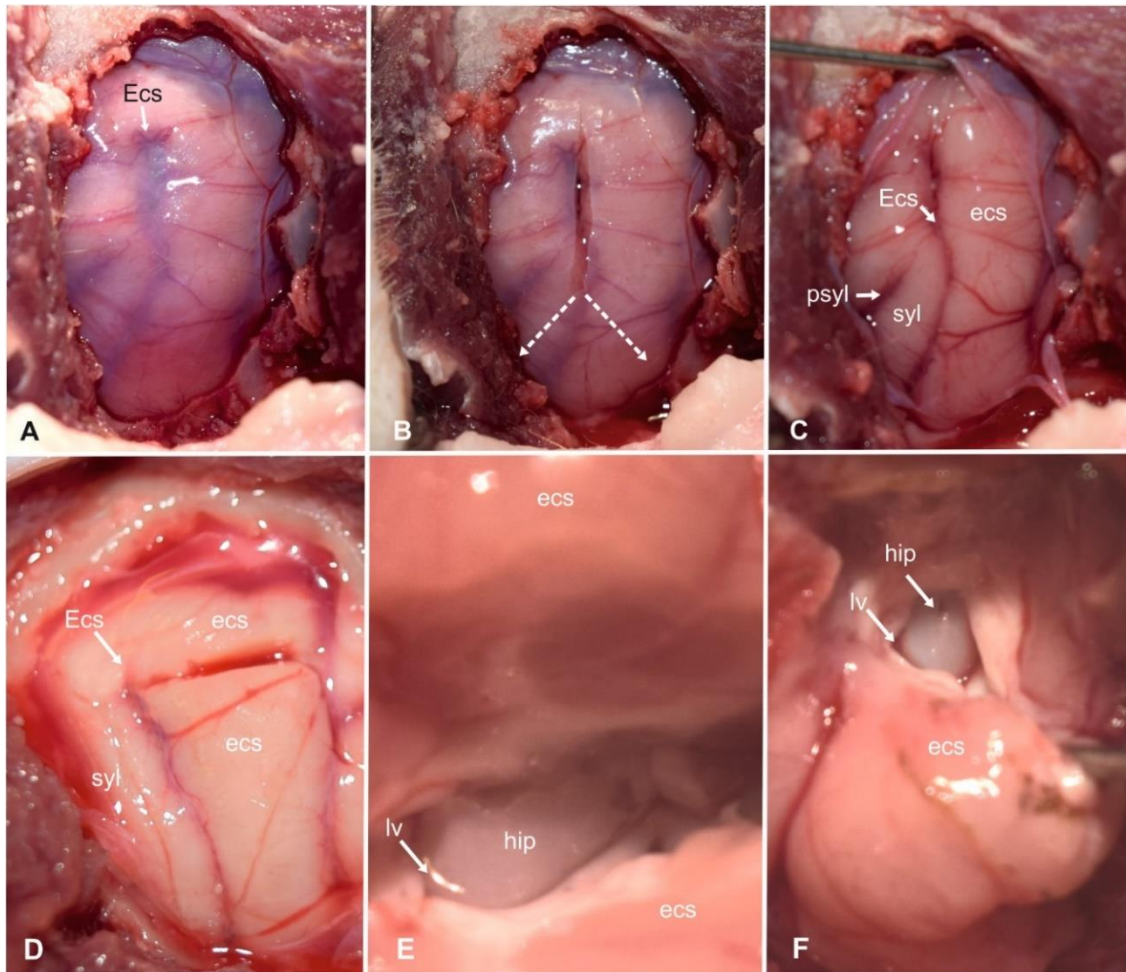


**Figure 11. Transcortical approach to the hippocampus (part 1). Intraoperative photograph showing the view on the left Sylvian and ectosylvian gyri and corresponding sulci after craniectomy and dural exposure (A). Tripartite dural incision (B). View of the brain surface after reflection of the dura (C). Magnified view on the incision in the dorsal ectosylvian gyrus (D). High magnification photograph of the transcortical access to temporal horn (E) and exposure of the hippocampal body (F). Ecs: ectosylvian sulcus; ecs: caudal ectosylvian gyrus; hip: hippocampus; lv: lateral ventricle syl: caudal Sylvian gyrus.**

A rectangular opening (ca. 1.5 x 3 cm) over the caudal Sylvian and ectosylvian gyri was created 0.5–1 cm caudal to the coronal suture using a power-assisted drill and was enlarged as necessary using a Kerrison rongeur (Figure 11A). During this procedure, the sigmoid sinus, located ventro-caudally to the surgical field, should be avoided. The orientation on the cranial sutures worked well in both mesocephalic and brachycephalic cats.

The underlying dura mater was opened with an upside-down X-shaped incision using an 11-scalpel blade and Castroviejo scissors (Figure 11B). The large meningeal branches from the caudal and medial cerebral arteries were spared. The four parts of the dura could

then be easily reflected to expose the caudal sylvian and caudal ectosylvian gyri (Figure 11C). Unlike in other species, the caudal and rostral part of the ectosylvian sulcus does not have connective middle part in cats (Pakozdy et al., 2015). Thus, the upper end of the caudal ectosylvian sulcus was used as a leading structure for the incision into the cortical surface (Figure 11D). On the surface of the temporal lobe, at the level of the pseudosylvian fissure, the medial cerebral artery splits into three to four main branches (Gillilan, 1976). From this point, the caudal main branch traverses the caudal sylvian gyrus and divides into subbranches, which run over the caudal sylvian and ectosylvian gyri. In some cats used in this study, the caudal ectosylvian gyrus also received vessels from branches of the caudal cerebral artery that approached from the dorsolateral aspect of the occipital lobe. These vessels were cauterized on both sides of the caudal ectosylvian gyrus. The cortex of the ectosylvian gyrus was horizontally transected using an 11-scalpel blade 3–5 mm below the upper end of the ectosylvian sulcus (Figure 11D). The underlying white matter was gently dissected and gradually removed until cerebrospinal fluid emerged from the lateral ventricle. The alveus of the hippocampus contrasted with a glistening ebony colour against the matt-white myelin of the surrounding cortical white matter (Figures 11E,F). The ependymal lining of the ventricle appeared greyish in colour. The opening in the pallium was ventrally enlarged on each side of the first cortical incision to further expose the hippocampus by gradually cutting the caudal ectosylvian gyrus left and right parallel to the adjacent sulci using the scalpel blade and Castroviejo scissors. The parenchyma of the ectosylvian gyrus was gently pulled laterally and ventrally using a spatula or a nerve hook and further dissected until the temporal horn of the ventricle was exposed (Figure 12A). The gyrus was cut on its ventral aspect and then fully removed. The cortical window could be mildly enlarged by reducing the adjacent white matter of the sylvian gyrus using surgical suction, exposing the transition from the hippocampus to the fimbria and the rostral choroidal artery, which was cauterized dorsally and ventrally on the exposed part of the hippocampus. A 1 x 2 cm neurosurgical patty (Neurosorb1) was moistened and placed at the ventral edge of the excised ectosylvian gyrus. A horizontal incision was made in the dorsal part of the exposed



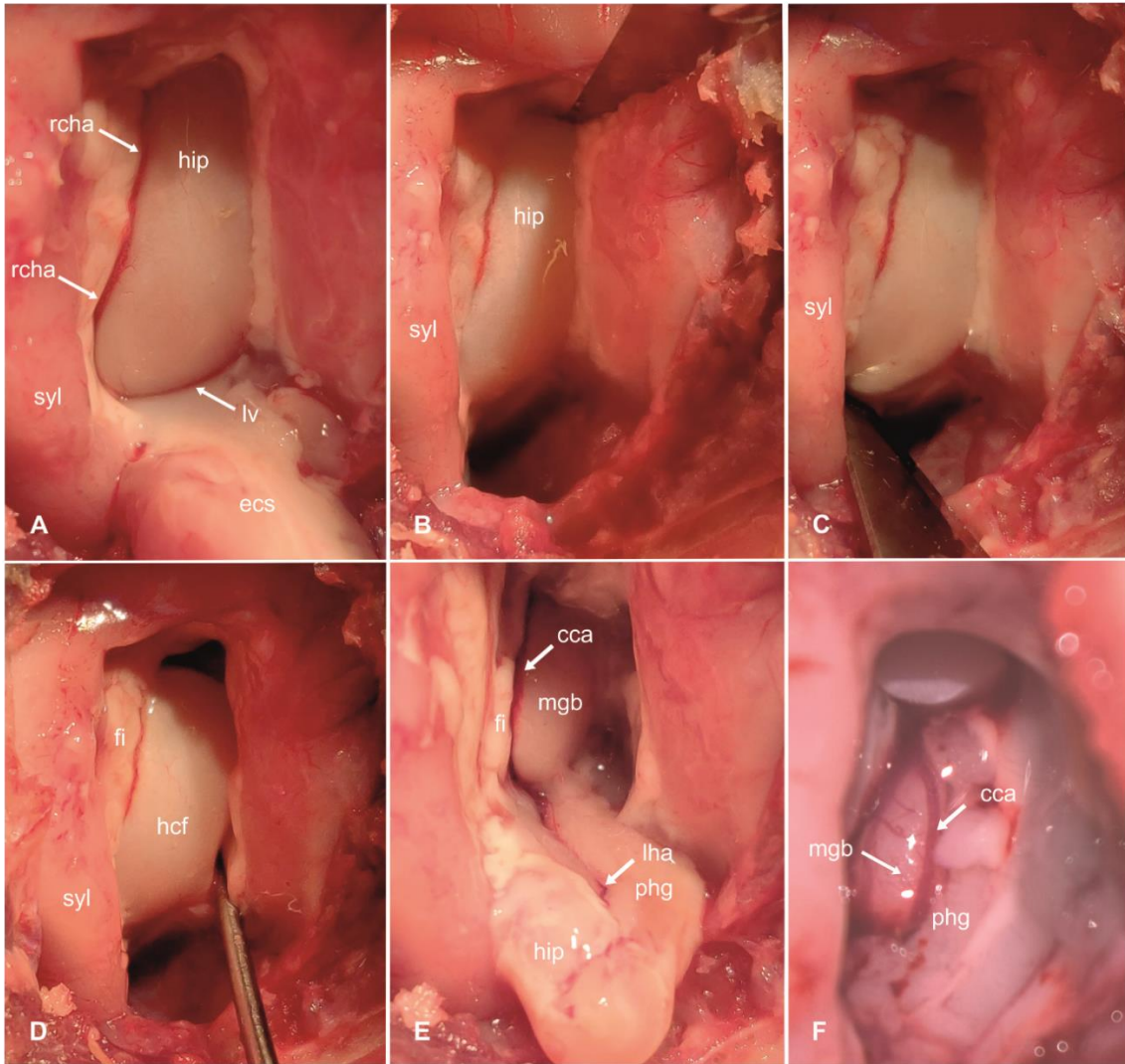


**Figure 12. Transcortical approach to the hippocampus-hippocampal resection (part 2). Intraoperative photograph showing the hippocampus after resection of the temporal neocortex (caudal ectosylvian gyrus). The hippocampus is cut off dorsally (B) and ventrally (C) with an 11-scalpel blade; then its mesial connections are carefully transected with the help of a nerve hook (D) and the hippocampus is pulled out and removed (E). After completing the resection, the medial geniculate body and the caudal cerebral artery become visible (F, enlarged view). ecs: caudal ectosylvian gyrus; syl: caudal sylvian gyrus; rcha: rostral choroidal artery; hip: hippocampus; lv: lateral ventricle; fi: fimbria; hcf: hippocampal fissure; phg: parahippocampal gyrus; mgb: medial geniculate body; cca: caudal cerebral artery; lha: longitudinal hippocampal artery.**

hippocampus and the cut was deepened and enlarged until the longitudinal hippocampal artery on the caudo-medial side was ruptured (Figure 12B). The procedure was repeated on the ventral aspect of the exposed hippocampus (Figure 12C). Next, the fimbria was transected. The isolated middle part was then gently pulled out by transecting its mesial connections with the help of a nerve hook and placed on the surgical patty (Figure 12D and 10E). The head and tail of the hippocampus were removed using surgical suction as

much as possible under visual inspection. At the end of the procedure, the dura mater was closed with a running suture using 5–0 Polyglactin. A standard closure method was then used to suture the temporal fascia, the subcutaneous tissues, and the skin. Operating time was approximately 120 minutes on average with this technique.

### **Possible intraoperative complications**

During the procedure, intraoperative complications were recorded. While opening the temporal fascia, the superficial temporal vein was damaged in one cat provoking hemorrhage. This vessel lies over the ventral border of the temporal muscle and should be avoided during this phase. Blunt dissection of the temporal musculature is preferable in order to prevent muscular bleeding and disruption, even if sharp dissection is faster and allows to prepare a wider bony surface. Excessive retraction of the temporal muscle rostrally could provoke a bulbus prolapse with traumatic damage to the optic nerve and secondary blindness can occur. While drilling the craniectomy, the transverse sinus was opened in one cat. For this reason, the craniectomy should not reach the level of the nuchal crest. In all cats, the longitudinal hippocampal artery must be transected during the procedure which can cause considerable hemorrhage.

### **Vascular supply of the hippocampus**

mCT of the contrast-injected cat brains revealed the vascular supply of the hippocampal formation. The main blood supply to the hippocampus comes from the caudal cerebral artery which emits the longitudinal hippocampal artery at the medial base of the piriform lobe (Gillilan, 1976; Goetzen and Sztamska, 1992). Both vessels follow the convex longitudinal axis of the medial side of the hippocampus (Figure 13). The large caudal cerebral artery runs more rostrally and curves around the medial geniculate body. The longitudinal hippocampal artery is much smaller. In all cats in this study, there was not a single artery, but rather this vessel was divided into two to three arteries sitting in the hippocampal fissure between the dentate and parahippocampal gyrus (Figures 12E,13). From the longitudinal hippocampal artery, numerous segmental vessels run nearly parallel towards the hippocampal fissure and supply the parenchyma of the hippocampus (as internal transverse hippocampal arteries) by penetrating the DG and connecting with the rostral choroidal artery (Gillilan, 1976; Goetzen and Sztamska, 1992). The rostral choroidal artery runs on the rostral side of the hippocampus in the shallow sulcus between fimbria and the hippocampus. This artery does not contribute to the hippocampal blood

supply but gives rise into the choroid plexus of the third ventricle (Gillilan, 1976; Goetzen and Sztamska, 1992). However, this artery must be considered as a source of hemorrhage during hippocampus resection.

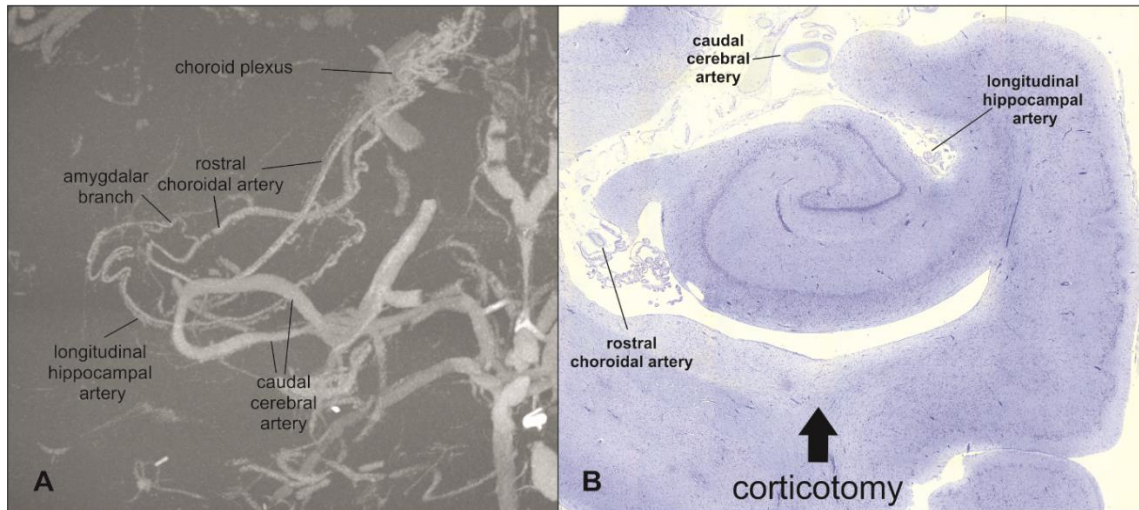


**Figure 13. Illustration of the blood supply of the hippocampus. Maximum intensity projection of the contrast-injected vascular supply of the hippocampus in a dorsal view reveals the major blood vessels of the hippocampus (A). The brain and other vessel images have been removed using a grey threshold. The histopathological section of the hippocampus shows the relevant arteries in the surgical field (B).**

### **Postoperative MRI and histological evaluation of the resected tissue**

Postoperative MRI and histopathological examination revealed that in all cats the whole body of the hippocampus could be resected en bloc (Figures 14A-B). In nine cats, there was no evidence of alterations in the surrounding structures. In one animal, the presence of a laceration in the thalamus was evidenced in the histopathological examination of the brain. The same lesion was not visible in the MRI post-resection.

The entorhinal cortex and the amygdala adjacent to the hippocampus could not be removed. All hippocampal specimens could be histologically examined and identification of the pyramidal and granular cell bands of all hippocampal fields was possible in five cats. In the other five, partial loss of these was evident. The subiculum, presubiculum and parasubiculum were in all cats damaged to a varying degree. In 3 specimens, the infrapyramidal blade of the DG was also disrupted (Figure 14C-E). The entorhinal cortex was not included in the specimen. The fimbria was in all cats torn off the hippocampus and was just partially visible.

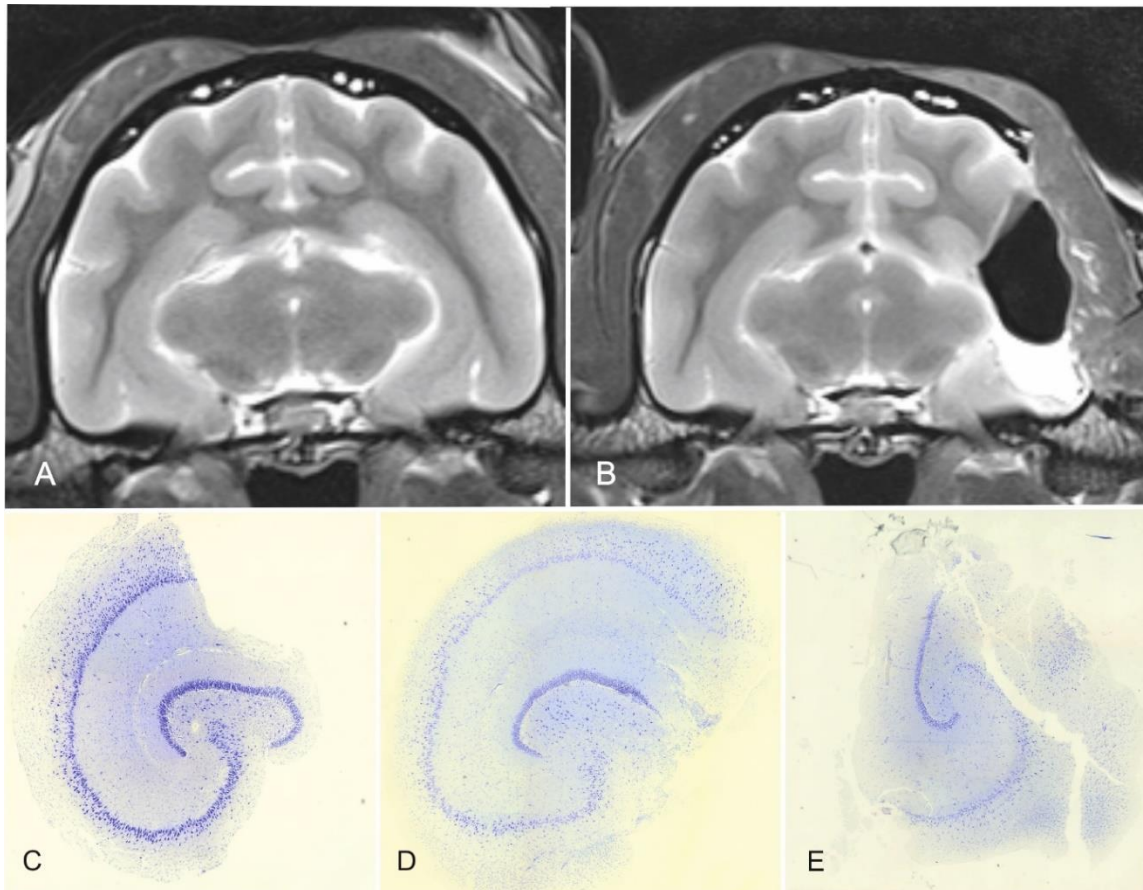


**Figure 14. MRI before (A) and after (B) surgery and histological sections of the resected hippocampus (C-E). In the MRI post-resection, the left hippocampus (body) as well as the temporal neocortex are absent. Nevertheless, most of the hippocampal tail and the whole head are still in situ (B). Histological sections of the hippocampus after resection show that the specimen allow the examination of all CA-fields in most cases (C, D), but in some of them not all fields are preserved and can be examined (E). The completeness of the resected specimens is also related to the surgeon's learning curve.**



## 4.4 Discussion

Feline HS may occur as a primary disease of the hippocampus, or as a consequence of status epilepticus or chronic cluster seizures (Fors et al., 2015; Sloviter, 2008; Vanhaesebrouck et al., 2012; Wagner et al., 2014; Yu et al., 2018). Regardless of whether HS is cause or the consequence of seizures, the change in the cellular architecture is assumed to predispose for seizure development, propagation, and enhancement as well as for refractoriness to medication (Martlé et al., 2014; Rusbridge et al., 2015; Wagner et al., 2014). Surgical resection of the hippocampus and associated temporal lobe structures is considered an effective treatment for refractory seizures originating from HS in humans, and seizure freedom rates after temporal surgery range between 69–90% in humans (Muzumdar et al., 2016; Salanova et al., 2002). Cats with seizures and HS may also benefit from hippocampal resection, which is why an evaluation of possible surgical techniques is the first step towards the establishment of systematic epilepsy surgery in animals. Due to morphological differences, the standard technique described for humans cannot be directly adopted for cats. In humans, massive expansion of the temporal cortex caudal to the non-growing insula creates a structurally distinct temporal lobe that is somewhat separated from the rest of the hemisphere by the deep sylvian fissure (Nieuwenhuys et al., 1998). The hippocampus head and body follow this curved movement during development and the bulk of the hippocampus and amygdala lie separated from the rest of the hemisphere within the temporal lobe, which can be resected en bloc (Olivier et al., 2012). In cats and other domestic carnivores, the temporal lobe has not developed to a comparable extent. The feline hippocampus lacks a distinct tapering from a head into a tail (Ellenberger and Baum, 1977; Schober and Brauer, 1974). The left and right hippocampi have a rather uniform shape in their dorsoventral course around the thalamus. The tail sits far dorso-medially underneath the corpus callosum, and the head, associated with the amygdala, sits deep in the cerebral hemisphere adjacent to the thalamus (Ellenberger and Baum, 1977; Olivier et al., 2012; Snider and Niemer, 1961). The standard technique of anterior temporal lobectomy (also called cortico-amygdalohippocampectomy) is therefore not applicable for cats, as a structurally distinct temporal lobe has not evolved. Destruction of the hippocampus used to be frequently performed in dogs and cats in experimental studies. Aiming to understand the physiology of the hippocampus, researchers partially or totally removed the structure to study the effects of the lesions in living dogs and cats (Andy et al., 1967; Kowalska, 1995; Kowalska, 1999; Kowalska, 2000; Kowalska and Kosmal, 1992; Tanaka et al., 1989;

Tartygin, 1996). The main approach used in such studies was a dorsal paramedian craniectomy in the parietal bone. The hippocampus was destroyed inside the brain through a cortical resection window in the suprasylvian- and/or ectosylvian gyrus and aspirated using surgical suction (Andy et al., 1967; Kowalska, 1995; Kowalska, 1999; Kowalska, 2000; Kowalska and Kosmal, 1992; Tartygin, 1996; Teitelbaum, 1964). Access to the hippocampus is limited in this approach and resection was incomplete in many animals. Furthermore, structural damage of the lateral and medial geniculate body occurred in some of the operated cats (Brown et al., 1969). Indeed, Hasegawa et al., required an even larger focal cortical resection than the one proposed in this cadaveric study to allow performing a total hippocampectomy without harming the surrounding structures (2021). Although the cortical corridor may differ, the technique used in the old experimental studies resembles SAH in humans, in which hippocampus and amygdala are removed through different cortical corridors using an ultrasonic aspirator, a bipolar cautery, or suction (Olivier et al., 2012). If histological examination of the resected tissue is not desired, such a minimally invasive transcortical approach at variable sites might also be appropriate. In this case, the use of neuronavigational systems and an intraoperative microscope are most likely necessary to carry out a successful surgery. In fact, thanks to these facilities, which are largely available in human neurosurgery, SAH, the less invasive approach to mesial temporal structures, can be performed in humans (Olivier et al., 2012). However, there is disagreement regarding as to whether this approach or the more invasive CAH also known as anterior temporal lobectomy is correlated with a better outcome and less post-operative complications (Bate et al., 2007; Bujarski et al., 2013; Hu et al., 2013; Loiselle et al., 2012; Nascimento et al., 2016; Paglioli et al., 2004; Wendling et al., 2013). In veterinary medicine, the use of these devices could also be of great help while performing mesial temporal resections, above all considering the aforementioned anatomical and size differences existing between human and feline brains (Long et al., 2014; Shores and Brisson, 2017; Snider and Niemer, 1961; Wininger, 2014). However, we consider pathologic examination of the resected tissue of paramount importance to verify the presumptive diagnosis of HS and to clarify the role of HS in epileptogenesis and/or seizure perpetuation (Wagner et al., 2014). In this study, we designed an approach to remove the hippocampus and obtain specimens usable for histological examination at the same time. This approach, which is highly similar to the one recently described for hippocampectomy and partial cortical resection in a cat affected by AED resistant seizures (Hasegawa et al., 2021), is partly built upon existing

craniectomy techniques that were slightly refined. To access most of the forebrain lobes, a standard rostro-tentorial craniotomy is described for dogs and cats (Shores and Brisson, 2017). Using the crossing of the squamous suture and the coronal suture as a landmark, opening of the skull in this approach resembles the pterional approach in humans. The Greek word “pterion” describes a localization on the lateral calvarium where the squamous suture meets the coronal- and speno-squamosal suture. These sutures are also present on the skull of cats (Ellenberger and Baum, 1977) and thus we suggest referring to the craniectomy used for hippocampectomy in cats as pterional craniectomy. A T-shaped incision of the temporal muscle was proposed to access the temporal lobe in dogs (Shihab et al., 2014), but such an incision was not necessary to sufficiently expose the skull in the cats of this study. However, the tri-partite, or even better X- or U-shaped, incision of the dura was vital to expose enough of the sylvian and ectosylvian gyri and to orientate in the surgical field. A simple straight incision did not allow sufficient exposure of all cortical landmarks. Particularly, the ventral end of a straight dural incision hindered preparation and removal of the caudal ectosylvian gyrus and placing of the surgical patty on which the hippocampus bloc comes to lie after resection. Removal of the caudal ectosylvian gyrus was necessary to achieve resection of the hippocampus tissue en bloc. Spreading the cortical mantle after vertically cutting the caudal ectosylvian sulcus might also be possible to spare some of the structural integrity of the gyrus. However, spreading the ectosylvian gyrus to an extent that allows removal of the hippocampus en bloc could anyway lead to damaging the cortex in this gyrus and, more importantly, compressing the medial cerebral artery in the adjacent pseudosylvian fissure with devastating consequences for the vascular support of the hemisphere. Spreaders might also further limit approachability to the hippocampus. In this study, the presence of a thalamic laceration possibly due to manipulation during surgery was evident in one cat. Since the same abnormality was not observed in the post-operative MRI, it was speculated that this could also be an artefact related to the histological preparation of the tissues. In fact, this is more likely to occur with less invasive approaches, in which the hippocampus cannot be directly visualized by the surgeon, in absence of neuronavigational systems as we know from the older studies (Brown et al., 1969). With the approach described here it is indeed more likely to provoke ischemic damage or swelling of the surrounding structures due to vascular impairment and/or manipulation of the parenchyma. The head and tail of the hippocampus could not be resected as a whole. However, as they were visible as a distinct structure, they could be removed using suction. In addition, as underlined in a

recent case report of a cat affected by temporo-occipital seizures, the mesial temporal structures are usually characterised by a certain degree of atrophy (2021). This atrophy should facilitate the surgeon's manoeuvre within the lateral ventricle and therefore allow a total hippocampectomy. This was not achievable in the present study since all operated cats had healthy brains with normal volumes. Moreover, it is still not clear whether a total resection of the hippocampus is in general required in these patients.

Sclerosis of the hippocampus can occur in combination with neuronal loss and gliosis in the amygdala (Miller et al., 1994; Yu et al., 2018). The epileptogenic role of the amygdala in cats has been emphasized in experimental studies (Delgado and Sevillano, 1961; Shouse et al., 2004; Tanaka et al., 1989). Thus, additional resection of the amygdala could provide more effective seizure control than resection of the hippocampus alone (Miller et al., 1994). The nuclear masses of the amygdaloid body lie further rostro-ventrally underneath the sylvian gyrus (Ellenberger and Baum, 1977; Schober and Brauer, 1974). Removal of the sylvian gyrus in order to expose the amygdala might again carry the risk of damaging the medial cerebral artery. An approach to the amygdala might be possible by undermining the sylvian gyrus from the corticotomy site laterally, but the view into this area is extremely limited. Furthermore, the medial aspect of the amygdala lies in close proximity to the cavernous sinus. Removal of this brain section is hardly feasible using the approach described here. Nevertheless, as already underlined for total hippocampectomy, also the practicability of a concurrent amygdalectomy may depend on the available space in the surgical field in each case (Hasegawa et al., 2021).

The excised tissue did not include all parts of the hippocampal formation. The cutting line is through the subiculum and parahippocampal gyrus, which is why examination of these parts and the entorhinal cortex is not possible with this technique. The ILAE classifies HS into three subgroups based on neuronal loss and gliosis in the subfields of the hippocampus (Blümcke et al., 2013). The subiculum and entorhinal cortex are not included in this classification system, and thus absence of these parts in the resected tissue seems to be acceptable at this time. A pioneering study investigating the hippocampus in a large cohort of cats with HS demonstrated that all CA fields can show cytopathological changes with the CA3 region being most frequently affected (Wagner et al., 2014). The quality of the specimen increased with increasing experience with the technique. In the end, almost all CA fields were well preserved in the tissue specimen and would therefore be sufficient to allow reproducible examination according to standards in human

neuropathology (Blümcke et al., 2013). Diagnosis of HS relies mostly on documentation of reduced pyramidal cell density and astrogliosis, which may differ throughout the hippocampal axis, also in healthy cats. If only the body of the hippocampus is available for examination, reference values on cellular density and cytoarchitecture for this part of the feline hippocampus would be necessary to establish standardized examination and diagnosis of feline HS.

The expected clinical manifestations of the loss of hippocampal tissue have been demonstrated in the resection studies of the past century. The caudal ectosylvian gyrus is part of the primary auditory cortex, which is tonotopically organized (Reale and Imig, 1980). Unilateral loss of hearing frequencies between 2.5 and 9 mHz must be expected after resection of the caudal ectosylvian gyrus, but there is no reason to expect total hearing loss on one side. Removal of the hippocampus was associated with deficits in motivation, spatial memory, and orienting response, as well as loss of conditioned reflexes and learned behaviors (Andy et al., 1967; Gambarian et al., 1979; Jarrard, 1973; Kowalska, 2000). Cats can get hyperactive and aggressive (Adamec and Stark-Adamec, 1983a,b) and may have a disruption of their diurnal cycle (Andy et al., 1967; Brown et al., 1969). Moreover, due to the greater development of the temporal muscle in cats in comparison to humans, it can be speculated that cats could develop problems with chewing and food uptake after invasive dissection of this muscle. Nevertheless, no studies evaluating surgical procedures of the temporal area with involvement of the temporal muscle recorded such complications (Cheung, 1996; Forterre et al., 2009; Mestrinho et al., 2015; Wouters et al., 2010). Furthermore, in our approach neither the muscular insertions nor its vascularization is compromised. In the recently published first case report of an epileptic cat treated with hippocampectomy and partial cortical resection, no significant postoperative complications were recorded (Hasegawa et al., 2021). Moreover, an excellent seizure outcome was documented, with a reduction of seizures frequency of more than 85%. However, the cat died for unknown reasons 1 year and 5 months after surgery. Even in the necropsy a cause for the sudden general deterioration of the animal could not be found. The known postoperative complications in human medicine can include fever, mild local pain, and mild to moderate headaches. These symptoms normally resolve over few days. In case they persist, it is indicated to perform a CT examination and a liquor study in order to rule out meningitis (Muzumdar et al., 2016). The development of a hematoma after resection is also a possible complication,

but this can be removed in a second surgery (Helmstaedter et al., 2004). In another study, the occurrences of infection of the bone lap (1.3%), mild hemiparesis (0.9%), hemianopia (0.4%), transient cranial nerve palsies (3.2%), transient postoperative language difficulties (3.7%), verbal memory deficits (8.8%), postoperative psychosis (2.3%) and postoperative depression (5.5%) are described as rare complications (Salanova et al., 2002). Global memory deficits occur rarely (1%), however after dominant hemisphere resection verbal memory deficits and language deficits happen very often (25–50% and 25–60%, respectively) (Muzumdar et al., 2016). Controversially, more recent studies showed (Gül et al., 2017; Oddo et al., 2012) an absence of verbal memory dysfunction after left-sided resection and even an improvement of this was observed in other studies after left-sided resection (Grammaldo et al., 2009; Schramm, 2008; Vojtěch et al., 2012). Gül et al. reported also significant improvements in executive functions, like preservative responding, abstraction, problem-solving difficulties (2017). Moreover, functional MRI studies have recognised an activation contralateral to the resection side and enhanced connectivity to the remaining hippocampus in patients after epilepsy surgery (Cheung et al., 2009; Hertz-Pannier et al., 2002; McCormick et al., 2013). This neuroplasticity mechanism may support memory improvement above all in patients with right-sided resection (Simons and Spiers, 2003).

The limitations of this study are mostly related to its nature as cadaveric study. Indeed, it is difficult to evaluate possible intraoperative and postoperative complications of a surgical procedure on dead animals. Further studies are indeed required on alive animals to more precisely evaluate these aspects and also the seizure and cognitive outcome.

Suitable candidates for surgical resection must be selected based on convergent lines of evidence implicating the hippocampus as epileptogenic region. Feline HS in association with feline partial seizures with orofacial involvement (FEPSO) seems to be a unique seizure disease because the structurally abnormal brain area (epileptogenic lesion), the area from which the abnormal electrical activity arises (epileptogenic zone), and the area that is responsible for the clinical manifestations of the seizures related to FEPSO (symptomotogenic zone) (Hasegawa, 2016) are combined into a single structure (Kitz et al., 2017). Resective surgery might be most successful in these cats. However, a consensus about presurgical evaluation of a potential candidate for hippocampectomy will be necessary. Nevertheless, the surgical approach used in this report was highly similar to the one described in our cadaveric study.

## **5 Study 2**

### **5.1 Aims and objectives of the study**

Cats are known to be affected by HS, potentially causing AED resistance. This can occur as a consequence of longstanding seizure activity secondary to trauma, inflammatory or idiopathic diseases or even be primary. In humans, temporal lobe resection is a standardized therapy in patients with refractory temporal lobe epilepsy and HS is a frequent finding.

Diagnosis of HS relies mostly on reduced pyramidal cell density and astroglial activation at hippocampal specimen. These cell populations may differ throughout the hippocampal axis, also in healthy cats. For this reason, normal reference values on neuronal and astrocytes cellular densities and cytoarchitecture for the different parts of the feline hippocampus (CA1 to CA4) and for the GCL of the DG are needed to establish a standardized examination protocol for the diagnosis of feline HS. In Veterinary Medicine, such data are still missing, therefore the purpose of this study is to evaluate feline hippocampal pyramidal layer cellular densities and cytoarchitecture at different levels. For this purpose, the neuronal marker NeuN and the glial marker GFAP will be employed to stain dorsal, middle and ventral transversal sections of the hippocampal formation of normal cats. Differences in cellular density and layer thickness (LT) between the hippocampal head, body and tail will be evaluated. Human standard recommendations for the diagnosis of HS will be observed during the assessment.

As surgical treatment for epileptic cats with AED resistance may become as in humans a therapy option in the future, this study will help in the standardized examination of hippocampal specimen with suspected HS.

## **5.2 Materials and methods**

### **Animals**

This study was performed on the cadavers of 17 cats at the Small Animal Clinic-Department for Surgery and Neurology of the Justus Liebig University in Giessen. The clinical history of all of them was known. The animals were euthanized for reasons unrelated to the study. The protocol used for euthanasia was the following: premedication with 0.5 mg/kg of diazepam administered intravenously [IV], followed by induction of anesthesia with 2-4 mg/kg of propofol [IV] and finally administration of 60 mg/kg of pentobarbital [IV]. Cadavers were eligible for the current study if they were free from clinical signs of brain disease (including seizures), evaluated through a neurologic examination before death. Animals with brain pathology at post-mortem analysis were excluded.

One additional epileptic cat, which was euthanized due to refractory seizures and failure of antiepileptic therapy, was enrolled to compare the obtained reference values from normal animals with those achieved from a cat with temporal seizures.

### **Classification of the animals**

The cats were divided into sex categories (male and female) and into age categories according to the feline stage guidelines provided by the American Animal Hospital Association (AAHA) and the American Association of Feline Practitioners (AAFP) (Vogt et al., 2010): prime (3-6 years) and mature (7-10 years) cats were considered together as “adult” animals and senior (11-14 years) and geriatric cats (15 years +) were considered together as “senior” animals. Moreover, breeds were subdivided into mesocephalic and brachycephalic. Since almost all animals were neutered, the influence of the entire/neutered status was not taken into consideration.

### **Tissue sampling and processing**

Within 12 hours after death or euthanasia, all brains were removed from the cats’ skulls and fixed in 10% formaldehyde at least for one week before sectioning. Three 2-4 mm thick specimens were obtained from the dorsal (at the level of the hippocampal tail),



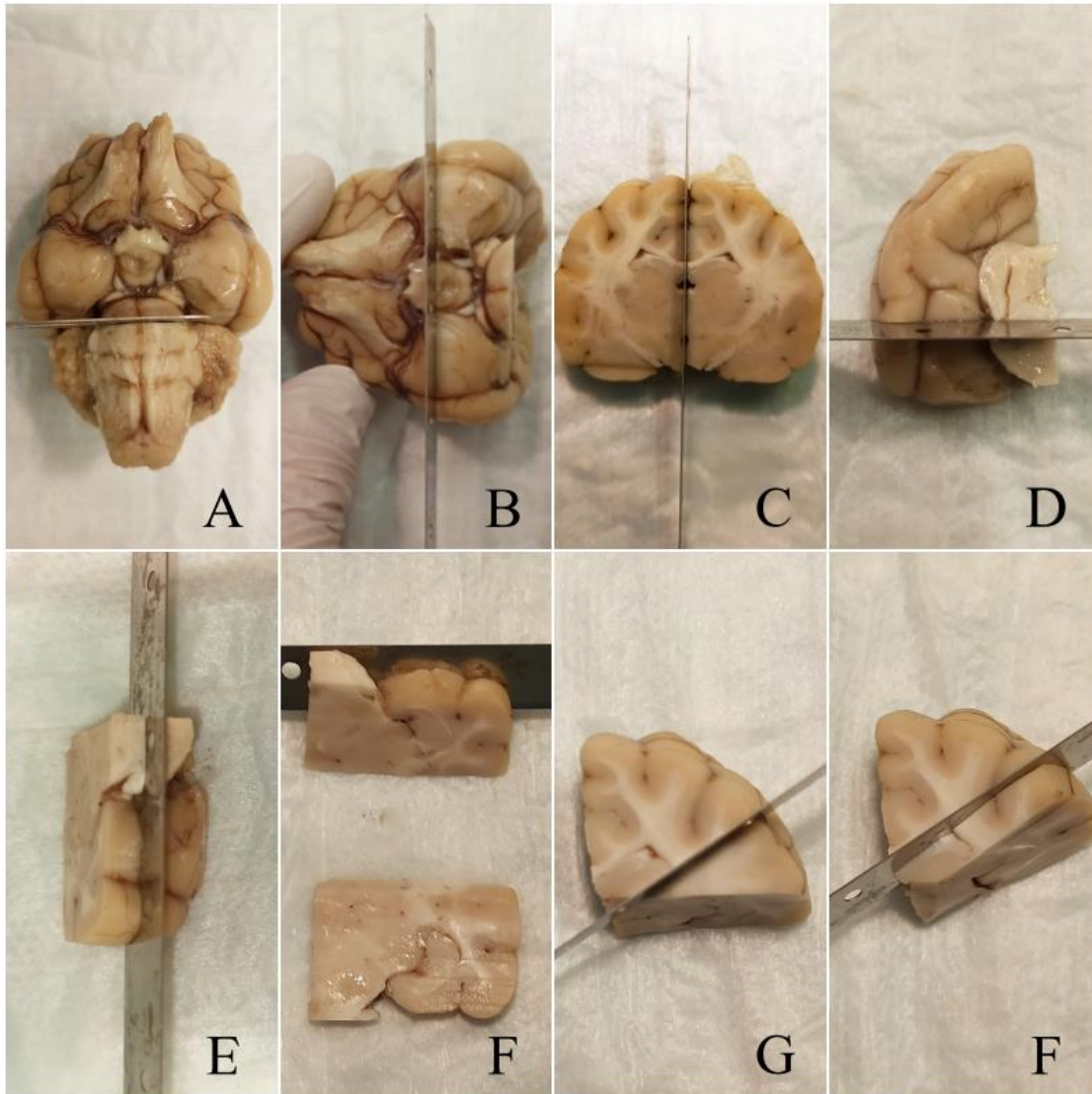


**Figure 15. Standardized brain processing for obtaining head, body and tail sections from a hippocampus. First, the brainstem was approached ventrally and a ventro-dorsal section at the level of the rostral cerebellar colliculi and pons was trimmed with a scalpel blade in order to separate the cerebellum and medulla oblongata from the region of interest (A). Then, a transverse cut at the level of the pituitary gland was obtained with a long blade (B). Subsequently, the right and left hemispheres were separated over the midline with the same blade (C). At this point, the left hippocampal body was dissected through a 90° cut directly underneath the mesocephalic aqueduct (D). Two further parallel sections, respectively 2-4 mm under (E) and 2-4 mm over (F) the previous cut were made, in order to obtain a specimen from the head and one from the body of the hippocampus, respectively. Finally, from the residual dorsal part of the temporal lobe a section from the hippocampal tail was obtained: the cut line was set through the vertex of the occipitotemporal flexure with an inclination of 45° (G). Once done, a further cut parallel and dorsal to the previous one was performed, obtaining the dorsal hippocampal specimen (F).**

middle (at the level of the hippocampal body) and ventral (at the level of the hippocampal head) part of each left temporal lobe (Figure 15), following the recommendations for

systematic sampling and processing of brains from epileptic animals provided by the international veterinary epilepsy task force (Matiasek et al., 2015).

First, the brainstem was approached ventrally and a ventro-dorsal section at the level of the rostral cerebellar colliculi and pons was trimmed with a blade (scalpel blade no. 10) in order to separate the cerebellum and medulla oblongata from the region of interest (temporal and occipital lobes) (Figure 15A). Then, a transverse brain cut at the level of the pituitary gland was obtained with a long blade (Figure 15B). Subsequently, the right and left hemispheres were separated through a cut over the midline with a long blade (Figure 15C). For the next part, only the left hemisphere was used. At this point, the hippocampal body was dissected through a 90° cut directly underneath the mesocephalic aqueduct: the blade was inserted into the caudal surface of the rostral mesencephalic stump in a tilted caudoventral to rostradorsal fashion (90°), to create a perpendicular section of the entorhinal cortex and temporoventral hippocampal body (Figure 15D). At this stage, two further parallel sections, respectively 2-4 mm over and 2-4 mm under the previous cut were made, in order to obtain a specimen from the body and one from the head of the hippocampus, respectively (Figure 15E-F). Finally, from the residual dorsal part of the temporal lobe a section from the hippocampal tail was obtained: the cut line was set through the vertex of the occipitotemporal flexure with an inclination of 45° (Figure 15G). Once done, a further cut parallel and dorsal to the previous one was performed, obtaining the dorsal hippocampal specimen (Figure 15F). All obtained temporal lobe samples were post-fixed in 10% neutral-buffered formalin for at least a further 5 days at room temperature and paraffin embedded according to standard procedures.

### **Histology and immunohistochemistry stainings**

Wax blocks were sectioned with a Leica RM2125 RTS microtome® (Leica Biosystems, Wetzlar, Germany) at seven µm. The slides were stained using hematoxylin-eosin (HE), Nissl staining according to standard procedures. The completeness and quality of the histological sections was evaluated with the HE staining and in case the hippocampus was damaged or partly missing, the specimen was trimmed again, and new slides were prepared for the HE assessment and the other staining (Nissl, NeuN and GFAP). In brief, to perform Nissl staining, the slides were pre-treated with a 50% potassium disulfite solution for 15-20 minutes before applying a 1.5% cresyl-violet solution for 20 minutes

at room temperature. Immunohistochemical analyses were performed using the staining platform BenchMark XT ULTRA (Ventana, Heidelberg, Germany) with the following antibodies: monoclonal mouse anti-NeuN MAB377 (1:500; Merck, Darmstadt, Germany) and polyclonal rabbit anti-GFAP Z0334 (1:2000; Dako Agilent, Santa Clara, United States) with 3,3' diaminobenzidine (DAB) as chromogen.

### **Histological examination**

All sections were scanned with the digital slide scanner NanoZoomer S360® (Hamamatsu Photonics, Herrsching am Ammersee, Germany). Morphometric analysis of the hippocampus was performed on three sections: dorsal or tail (1), middle or body (2) and ventral or head (3). According to the feline HS assessment by Wagner et al. (2014), the cellular density and LT were analysed on the CA subfields (CA1, CA2, CA3 and CA4) and the GCL of the DG. Since the borders of CA2 are mostly not well-defined, this area was evaluated both individually and in combination with CA3 (Figure 16A-C). To obtain cell densities, in each evaluated region, two rectangular areas from all CA areas of the pyramidal cell layer and from the GCL were extracted using the program QuPath-0.2.3® and sent to the Fiji® processing package (version 1.8; <https://imagej.net/software/fiji/>). The cell counter plug-in of this software was then used to run cell counts in each area. The surfaces ( $\mu\text{m}^2$ ) of the evaluated areas were extracted from Fiji® as well and then used to calculate cellular densities (cells/ $\text{mm}^2$ ). Due to the difficulty in distinguishing the borders of CA2 with GFAP staining, the astrocyte density (AD) was not evaluated in this single region, but rather by combining CA2 and CA3. LTs were assessed by using QuPath-0.2.3®. For each CA region and GCL, the thickness ( $\mu\text{m}$ ) was measured on two different, randomly selected points, in order to take account of any potential, intrinsic variability of the layers (Figure 16C). In CA4, this evaluation was not possible, due to the form of this area.

Cellular densities were evaluated both for the pyramidal cells (NeuN) and the astroglia (GFAP), and the LTs were evaluated using both Nissl and NeuN staining in order to point out any differences in the two methods.

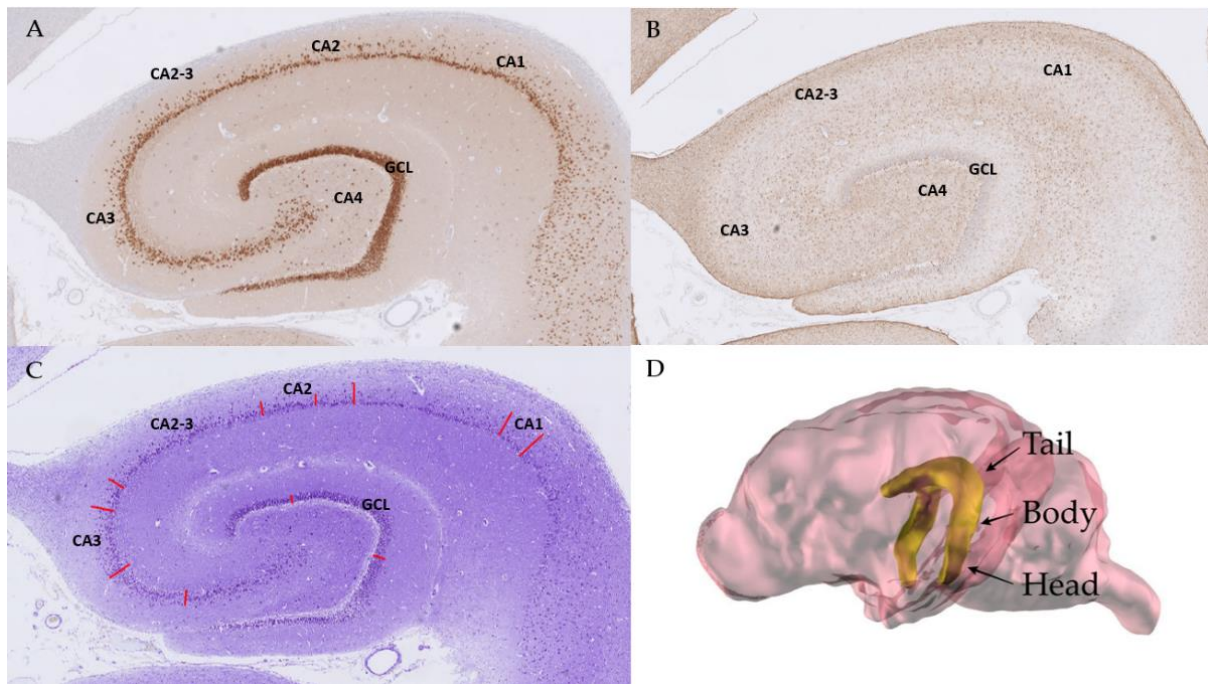


**Figure 16. Hippocampal areas of the assessed sections. From each hippocampus two rectangular areas were selected from the regions CA1-4 and GCL for cell counting at NeuN (A) and GFAP (B) stained slides. CA2 alone was not assessed for GFAP. Evaluation of the LTs of the different areas at Nissl-stained sections (C). A 3D model of the skull of a Domestic Shorthair cat based on CT and MRI images showing the localization of the hippocampus and its divisions (tail, body and head) (D).**

### Statistical analysis

Statistical evaluation was performed under the supervision of a biostatistician (KB) and computed with a commercial statistical software package (SAS® 9.4 Procedures Guide: Statistical Procedures, 2<sup>nd</sup> edition ed., Statistical Analysis System Institute Inc., Cary, NC, USA). Data were acquired by the author and submitted in an Excel table.

Both cellular densities and LT data were examined for normality by the Shapiro-Wilk test for each group, since one repeated measurement was conducted for every parameter in each measured area (CA1-4 and GCL) and section (tail, body and head). Then, data were evaluated via t-test for repeated measurements to determine whether any statistically significant differences between the two measurements were present. Similarly, the presence of significant differences between the LTs measured from the Nissl- or from NeuN-stained slides was assessed. If the t-test did not show any evidence of significant differences, the mean values of the repeated measurements could be then used for the further statistical assessment. The data was normally distributed for almost all repeated measurements. In fact, only in the evaluation of AD did the Shapiro-Wilk test show no

normal distribution for the CA3 body ( $p=0.03$ ) and in the evaluation of the LT for CA1 dorsal and ventral ( $p=0.04$ ). Nevertheless, a visual inspection of the data showed that these were almost normally distributed and since the related  $p$ -values were below 0.05, the  $t$ -test was applied for these exceptions as well. The  $t$ -test showed a statistically significant difference in some cases between the repeated measurements. This was evident in CA3 dorsal ( $p = 0.03$ ), CA4 dorsal ( $p=0.01$ ) and body ( $p=0.002$ ) in the evaluation of neuronal density (ND), in CA3 ventral ( $p=0.01$ ) in the evaluation of AD and in CA3 dorsal ( $p = 0.048$ ) in the evaluation of LT. Nevertheless, mean values for cellular densities and LT were used in the further analysis. To compare cellular densities and LTs of the CA areas and GCL between the hippocampal tail (1), body (2) and head (3), a variance analysis of repeated measurements according to sections 1, 2 and 3 was performed. In this assessment, the factors age and breed were also included as variables. Sex was not included in the analysis due to the absence of female animals in the age group “adult”. The  $p$ -value for significance was set at  $< 0.05$ . Descriptive statistics were provided for estimates of hippocampal layer cell densities and thickness differences, also correlated to breed and age. A description of the quantitative data characteristics is given by mean ( $\pm$  standard deviation).

Due to the deficient or absent NeuN staining in cats 5, 6 and 10, these animals were excluded from the assessment of ND. Regarding LT, while comparing the measurements from Nissl- and NeuN-stained slides, the Shapiro-Wilk test showed that all data except in CA3 ventral ( $p=0.004$ ) were normally distributed. Since almost none statistically significant differences were detected via  $t$ -test between the values obtained from NeuN or Nissl-stained slides, the LTs were only assessed from the latter, in order to evaluate the whole study population. Indeed, only in CA2-3 body were relevant differences ( $p=0.015$ ) found between the two staining methods.

## 5.3 Results

### Characteristics of the animals included in the study

Seventeen cats were enrolled in the study. The mean age of the animals was 10 years (range 3-17 years). In one cat the exact age was not known. Four cats were female (all neutered) and 13 were male (1 entire and 12 castrated). Eight animals (100% males) were classified as adults and nine as senior (55.6% females and 44.4% males). Eleven cats were mesocephalic (8 Domestic Shorthair, 1 Domestic Longhair and 2 Maine Coon) and six were brachycephalic (3 British Shorthair, 2 Persian and 1 British Longhair). Weight ranged from 2.5-7.1 kg (median weight: 4.47 kg). Cause of death was due to different diseases (Table 4).

**Table 4. Signalment and cause of death of the study cats.**

Animal s	Breed	Weigh t (kg)	Age	Sex	Cause of death
1	Domestic Shorthair	4.1	13 years	Male, entire	Feline asthma
2	Domestic Shorthair	3.0	17 years	Female, neutered	Suspected nasal neoplasia
3	Domestic Shorthair	5.2	3.5 years	Male, neutered	Hypertrophic cardiomyopathy, aortic thromboembolism
4	Persian	2.5	11 years	Female, neutered	Suspected lymphoma
5	Domestic Shorthair	4.0	13 years	Male, neutered	Aortic thromboembolism
6	Domestic Longhair	6.1	Unknown (prime/mature)	Male, neutered	Vertebral fracture and luxation at the level of Th 5-6, sternal luxation of the 5 <sup>th</sup> and 6 <sup>th</sup> sternebrae
7	Domestic Shorthair	3.0	14 years	Female, neutered	Chronic kidney disease
8	British Longhair	4.7	7 years	Male, neutered	Recurrent feline urinary tract disease and uroabdomen
9	British Shorthair	2.6	15 years	Male, neutered	Aortic thromboembolism

<b>10</b>	British Shorthair	4.8	7 years	Male, neutered	Liver insufficiency
<b>11</b>	Domestic Shorthair	4.7	7 years	Male, neutered	Chronic otitis externa, suspected otitis media and interna, suspected diabetes
<b>12</b>	Domestic Shorthair	4.4	3 years	Male, neutered	Haemolytic anaemia
<b>13</b>	British Shorthair	7.1	13 years	Male, neutered	Septic abdomen
<b>14</b>	Main Coon	5.9	16 years	Male, neutered	Bladder neoplasia
<b>15</b>	Domestic Shorthair	3.7	10 years	Male, neutered	Aortic thromboembolism
<b>16</b>	Main Coon	4.7	3 years	Male, neutered	Aortic thromboembolism
<b>17</b>	Persian	5.6	11 years	Female, neutered	Lung oedema

## Morphometric analysis

The results of the repeated measurements variance analysis revealed that age and breed did not exhibit any statistically relevant influence either on cellular densities or on LT. Nevertheless, brachycephalic cats seemed to have a higher ND than mesocephalic cats (Appendix; Figure 21A). In contrast, ADs were higher only in CA2-3 and CA4 in mesocephalic cats than in brachycephalic cats (Appendix; Figure 21B), whereas in the GCL the opposite was observed (Appendix; Figure 21C). Moreover, the hippocampal tail and body of mesocephalic cats seemed to have thicker layers (Appendix; Figure 21D). However, all these results showed no statistical differences.

Regarding the variance analysis of NDs evaluated in Neun-stained slides, mean values, standard deviations and minimum and maximum values are summarized in Table 5 (Appendix). The analysis revealed that no statistically significant difference was present in CA1 between the head (3), body (2) and tail (1) (Figure 17A), whereas densities were significantly different between all three sections in the GCL (Figure 17F). Specifically, the values increased in the ventro-dorsal direction along the hippocampal axis. In addition, sections 1-3 had different NDs also in CA2-3, CA3 and CA4, but while density values were higher in the hippocampal tail for CA2-3 and CA3 and increased in ventro-

dorsal direction, in CA4 the NDs were higher at the level of the hippocampal head and decreased in the ventro-dorsal direction (Figure 17C-E). Between sections 1-2 in CA2, CA2-3 and CA3, a significant difference was also evident (Figure 17B-D). The hippocampal body and head (2-3) had significantly different densities only in CA4 and in the DG, as aforementioned, whereas sections 1-3 were significantly different in all areas apart from CA1 and CA2 (Figure 17A-F). In comparison to the CA areas, at the level of the GCL, the standard deviations for the mean density values were overall lower. The GCL showed the highest NDs, whereas CA4 had the lowest (Appendix; Table 5).

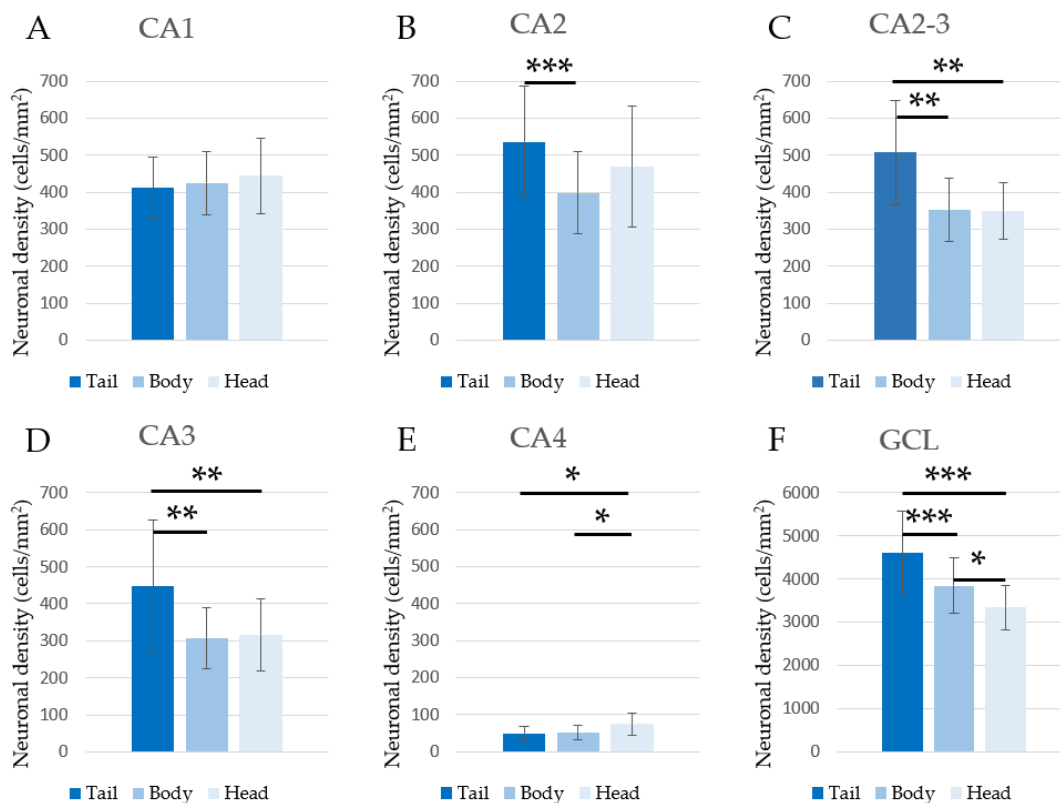


**Figure 17. Estimated ND values (LS-means +/- standard error) (Least-Squares-means) from the variance analysis for repeated measurements comparing the hippocampal tail, body and head. The data are relative to all examined areas and show the presence of statistically significant differences. \* p < 0.05, \*\* p < 0.01, \*\*\* p < 0.001.**

Regarding the variance analysis of ADs evaluated in GFAP-stained slides, the mean values, standard deviations and minimum and maximum values are summarized in Table 6 (Appendix). The AD values were statistically significantly different only between the tail and head (1-3) in CA1, and in the GCL, between the body and head (2-3) in CA1 and between the body and tail (1-2) in the GCL (Appendix; Figure 22A,E). In all remaining



hippocampal areas, the astroglial population did not show quantitatively significant differences between 1, 2 and 3 (Appendix; Figure 22B-D). In CA1, ADs were significantly higher at the level of the head (3). In the GCL, the density values were higher in the head (3) if compared to the tail (1) and in the body (2) in comparison to the tail (1) (Appendix; Table 6).

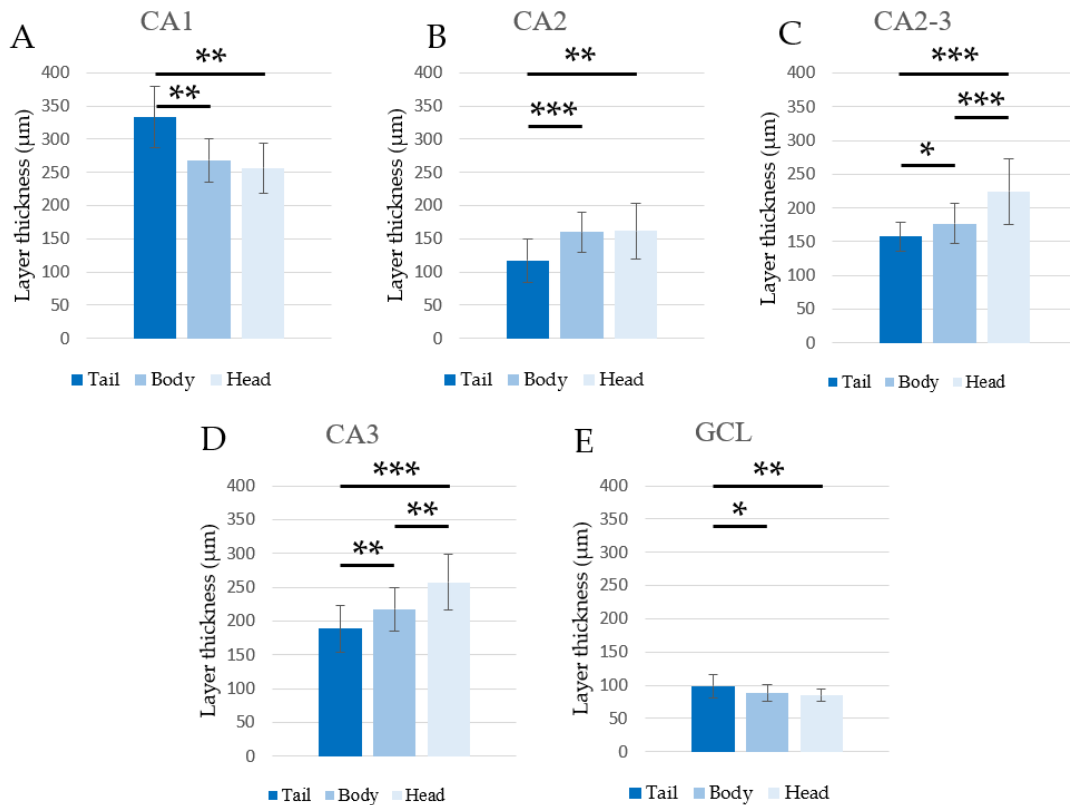


**Figure 18. Estimated LT values (LS-means +/- standard error) from the variance analysis for repeated measurements comparing the hippocampal tail, body and head. The data are relative to all examined areas and show the presence of statistically significant differences. \*  $p < 0.05$ , \*\*  $p < 0.01$ , \*\*\*  $p < 0.001$ .**

The LTs evaluated with Nissl staining showed significant differences in almost all regions. Mean values, standard deviations and minimum and maximum values for LTs are summarized in Table 7 (Appendix).

Between the body and head (2-3) at the level of CA1, CA2 and GCL, no difference was found (Figure 18A-B,E). In CA1 and in the GCL the LT values were larger in the tail (1) than in both the body (2) and the head (3) (Figure 18A,E). In general, LTs seemed to decrease in the ventro-dorsal direction at the level of CA2, CA2-3 and CA3 (Figure 18B-

D). In addition, despite the significant differences observed in the GCL, the LTs appeared more homogenous than in the CA areas (Table 7).

### **Hippocampal pyramidal cell layer and granule cell layer cytoarchitecture in cats**

Analysing the morphology of the examined areas (NeuN and GFAP), a marked difference in cytoarchitecture was observed (Figures 19-20). The pyramidal cell layer was divided, as in other species (i.e. mouse, human), into a superficial (closer to the stratum radiatum) and deep layer (closer to the stratum oriens). This division was evident in CA1 and CA2, whereas it disappeared along CA3 and was completely absent in CA4. CA1 was thicker than CA2, CA2-3 dorsal and body, CA3 dorsal and body and the GCL in all animals. CA2-3 ventral (16.7% of the animals) and CA3 ventral (38.9%) showed LTs that were higher than in the corresponding section of CA1. In this area, the neurons presented an elongated to roundish form and were smaller than in the other CA areas. CA2 was a small transitional area whose extension differed along the hippocampal axis and from individual to individual as well. Its borders were not always easy to identify. In this area, the superficial layer was usually very thin and dense with polygonal to round pyramidal cells, whereas in the deep layer, neurons were sparser. Overall, CA2 was thinner than CA1 and usually also thinner than CA3. Indeed, only in one cat was CA2 thicker than CA3 (body). CA3 neurons were also roundish to polygonal cells. This neuronal population usually showed dispersion to some degree at the border with CA4. Beneath the pyramidal layer in the CA3 area, mossy fibres coming from the GCs of the DG could be consistently observed in the stratum lucidum. These structures and the related layer tended to disappear at the border with CA2.

In CA3, the distinction between deep and superficial layers was less evident, above all in proximity to CA4, which is the area in contact with the DG. Here, the neurons had a rather polygonal form, were generally small and very dispersed, and showed as a very cell-poor area in the NeuN staining. Indeed, the AD in this layer was much higher than the ND (Figure 19-20).

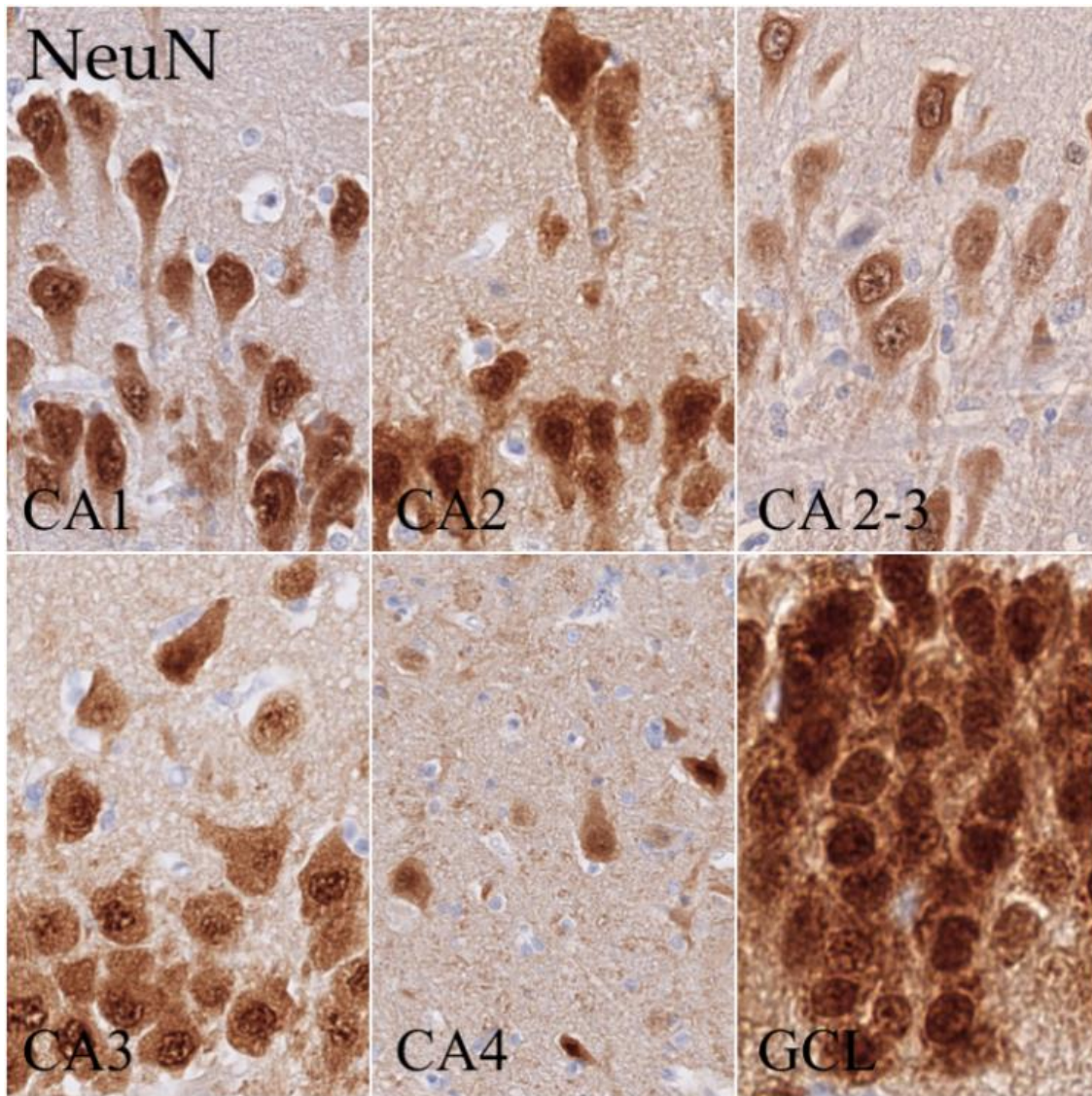


**Figure 19. Neuronal morphology of the pyramidal cell layer areas and GCL in NeuN. All examined areas, including the four CA regions (CA1-4), the GCL and an example of the combination of CA2 and 3 can be seen. Significant morphological differences were present along the pyramidal cell layer. Both cell form and distribution meaningfully changed along the transverse hippocampal axis.**

Finally, the GCs in the GCL of the DG were very small, round neurons. Overall, this layer was very thin and compact, showing the highest neuronal densities. It did not reveal any division, as shown in the hippocampal CA areas. Here, the astrocytes were mostly located at the bottom of the layer, i.e. at the conjunction between the hilus (CA4) and the DG, whereas in the hippocampal pyramidal cell layer, the astroglia was homogenously sparse throughout the full thickness of the stratum (Figure 20).



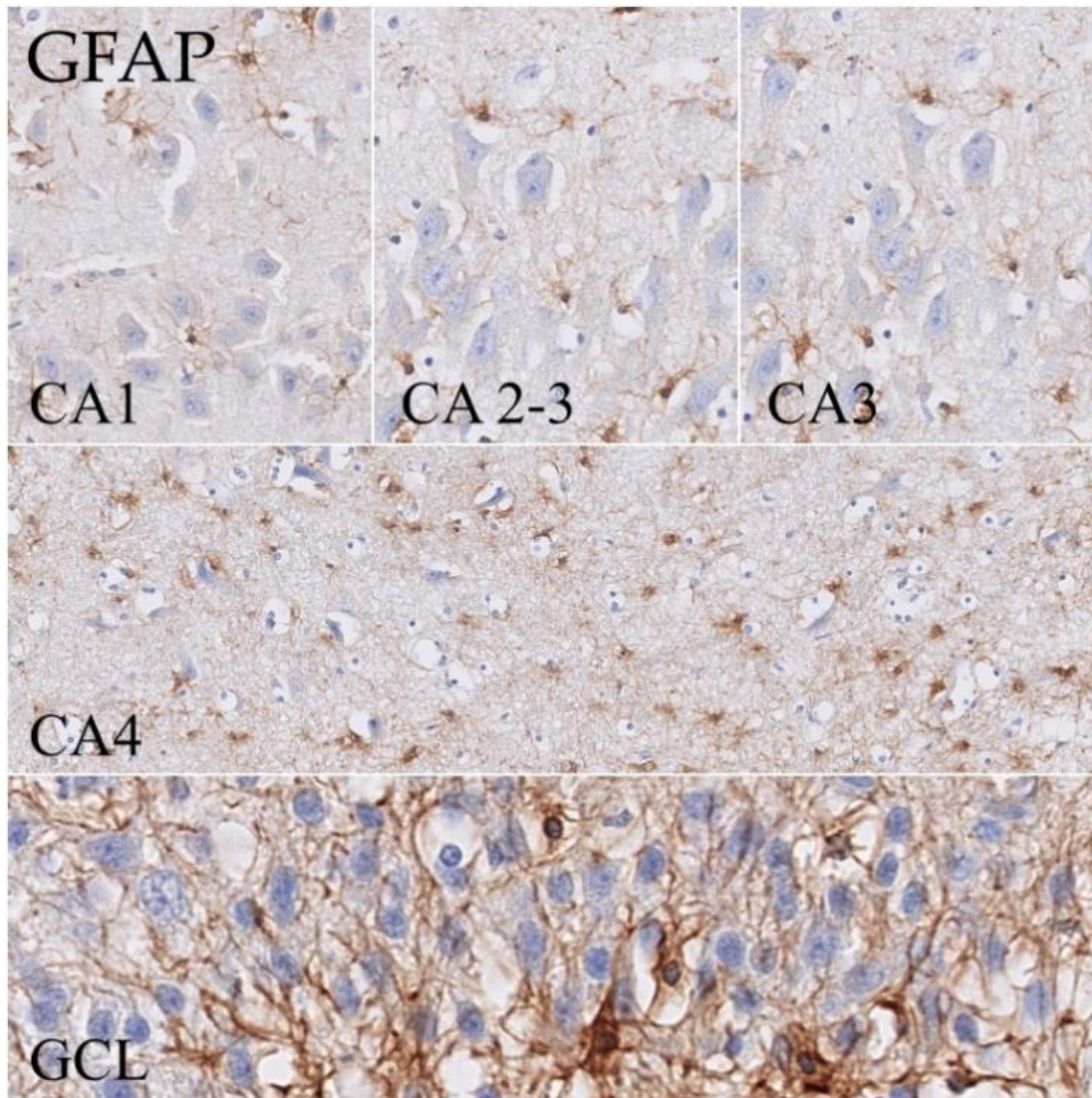


**Figure 20. Astroglial cell morphology of the different hippocampal pyramidal layers and GCL. All examined areas, including CA1, CA3 and CA4, the GCL and an example of the combination of CA2 and 3 can be seen. The distribution of astroglia was homogenous throughout the pyramidal cell layer. Nevertheless, in CA4, astrocytes were more abundant compared to the other CA areas. In the GCL, astroglial cells were mainly located at the border towards CA4.**

### **Clinical history and quantitative histopathological examination of an epileptic cat**

The epileptic animal was a 2-year-old, female neutered, Domestic Shorthair cat (weight: 4.7 kg) that was euthanized due to chronic, refractory, complex, focal epileptic seizures with OI, which did not respond adequately to antiepileptic drugs. No comorbidities were known. The owner refused to perform a MRI of the head and cerebrospinal fluid examination ante-mortem. One day after death, the brain was removed from the skull and then processed in the same manner as described above. The stained sections from the

hippocampal samples were markedly damaged and presented multiple lacerations and fissures, which were not observed on the specimens from normal brains. Due to excessive damage, it was not possible to perform two repeated measurements in all areas. The examination of ND, AD and LT evidenced the presence of a mild to moderate decrease in ND (47.71-60.33% lower than the mean values for normal ND; see table 5) and increase in LT (19.77-88% higher than the mean values for normal LT; see table 7) at the level of the GCL in all three sections (tail, body and head) and all CA areas except CA1 at the level of the tail. These changes could not be appreciated visually without reference. Moreover, an increase in AD (22.33-122% higher than the mean values for normal AD; see table 6) above all at the level of the hippocampal body and head, which was also subjectively evident (astrogliosis), was noted. Based on the reference values obtained in this study, this cat was diagnosed with a mild form of HS.

No statistical analysis was performed on these data.

## 5.4 Discussion

Feline HS continues to be of great interest to researchers in veterinary epileptology but so far, little is known about this pathology in cats. Pathological studies have defined different patterns of HS, as well as its clinical course and the presence of associated brain diseases in affected cats (Wagner et al., 2014). Partial cortico-hippocampectomy is an emerging surgical technique in veterinary medicine, which will not only provide hippocampal specimens for histopathological investigations but will also for conclusive correlations to be made between clinical signs, disease course, imaging and histopathology. Furthermore, these correlations will secondarily aid in advancing and refining the identification of suitable candidates for surgery (Hasegawa et al., 2021; Zilli et al., 2021). Lastly, feline HS might also offer a model to study human TLE (Pakozdy et al. 2017). In the current study, a further step in the diagnostic process of HS has been made. In fact, considering the possibility of performing surgical treatment on these animals in the near future, important considerations regarding the normal cytoarchitecture of the hippocampal pyramidal cell layer and the GCL have been made. Indeed, it has now been demonstrated that the hippocampal pyramidal cell population as well as the thickness of the pyramidal cell layer and GCL differ throughout the longitudinal hippocampal axis independently from age and breed in healthy cats, which is an important consideration to take into account while performing the histopathological examination of hippocampal specimens. In fact, the diagnosis of HS in both humans and cats is mostly based on the recognition of pyramidal cell loss and astrogliosis in hippocampal specimens (Wagner et al., 2014; Blümcke et al., 2013). In addition, normal reference values on neuronal and astrocyte cellular densities as well as LT for the different CA areas (CA1 to CA4) and for the GCL of the DG were provided and compared between the dorsal (tail), middle (body) and ventral (head) sections of the hippocampus. Such an analysis aimed to support the standardized histopathological diagnosis of HS in cats with AED resistant MTLE. Overall, no such evaluation has been undertaken in cats so far. However, a similar investigation has been performed in mice and demonstrated differences mostly in CA1 and in the suprapyramidal blade of the DG along the dorso-ventral hippocampal axis (Jinno and Kosaka, 2010). In this case, only the neuronal densities of glutamatergic principal neurons were estimated. The presence of significant cytoarchitectural differences along the longitudinal hippocampal axis is also supported by evidence that lesions in the hippocampal tail affect learning and memory in rats (Moser et al., 1993), while lesions in the hippocampal head reduces fear-related behaviour but do not impair

spatial learning in rats (Kjelstrup et al., 2002). This functional differentiation along the dorso-ventral hippocampal axis is actually well-known in monkeys (Colombo et al., 1998) and humans (Small et al., 2001) as well. In addition, a systematic review of cellular densities in the mouse brain, including the hippocampus, has been recently published (Keller et al., 2018). In human medicine, some older studies investigated this topic, mostly aiming to find relations between neuronal densities in the hippocampus and pathological conditions, age or other possible influencing factors (Ball, 1997; Dam, 1979; Devaney and Johnson, 1984; Shefer, 1977; West, 1993).

Since the study aimed to define a standardized examination protocol for the diagnosis of HS in cats, the relevant hippocampal and DG areas examined in human medicine classification of this pathology were taken into consideration (Blümcke et al., 2013): CA1-4 and the GCL. Regarding the method used for cell counting and for measuring LTs, a purposely simple technique was developed, so that this could be also employed in the diagnostic process for the histopathological examination of surgical hippocampal specimens, if needed. The technique is similar to the one used by Shimada et al. in 1992 for evaluating astroglial cell densities in the mouse (Shimada et al., 1992). In order to ensure a more precise analysis and reduce any bias, two measurements were made for all examined areas. Nevertheless, the t-test evidenced a statistically significant difference between some repeated measurements. These were the ND data in CA3 dorsal and CA4 dorsal and body, the AD data from CA3 ventral, the LT values from CA3 dorsal and the data obtained from the comparison between Nissl and NeuN staining for the evaluation of LTs from the CA2-3 area. Since most differences involved CA3, it can be postulated that a higher intrinsic variability is present in this CA area, which lies at the border between two very diverse regions (CA2 and CA4). Another speculation that can be made is that the method used for cell counting as well as the one used for the evaluation of LTs in this study could be responsible for this variability and therefore may not be completely appropriate for this type of assessment. Nevertheless, the intention of the authors was to use a technique that can be easily reproduced for the analysis of pathologic samples from animals with suspected hippocampal pathology. Such a method, like that of the optical disector (Jinno and Kosaka, 2010; Jinno et al., 2007; Mayhew and Gundersen, 1996; Ogata and Kosaka, 2002), would have likely been more accurate but inadequate for standard laboratory analysis. In contrast to a previous study (Wagner et al., 2014) in which age, responsible for mild neuronal loss, displayed a significant impact on the parameter

interneurononuclear distance (INND) throughout CA1 to CA3, here age and breed did not show any statistically significant influence on ND, AD or LT comparing the hippocampal sections in the tail, body and head. In general, it is possible that these data would acquire a statistical significance if the study population was larger. In human medicine, contrasting opinions can be found in the literature regarding the influence of age on hippocampal cellular densities. Indeed, whereas in one study a decrease in pyramidal cell density in people over 68 years was found (Dam, 1979), in a later investigation exactly the opposite results were obtained (Devaney and Johnson, 1984). Nevertheless, the two studies used different cell counting techniques and are therefore not strictly comparable. Moreover, in the second study, they supposed that the apparent increase in ND with age could also be attributed to the fact that the whole hippocampal formation (grey and white matter) was analysed. In fact, these two components of the central nervous system, and in particular the white matter, undergo senescent shrinkage. Indeed, in agreement with some older studies (Dam, 1979; Shefer, 1977), it is rather unlikely that the proliferation of neurons takes place in the brains of adult humans. Senescent shrinkage could also explain the apparent increase in AD in senior cats, which was observed in this study in the hippocampal tail.

With regards to the variance analysis, a statistically significant difference in ND was observed along the dorsoventral hippocampal axis above all between the head and tail, and the body and tail, whereas the body and head seemed to have a more similar neuronal population. This difference was evident between all three sections (1, 2 and 3) in the GCL and completely absent in CA1. CA4 constituted an exception, since in this area, no differences in ND were observed only between the body and tail. Overall, ND was higher at the level of the tail in CA2-3 and CA3 if compared to the body and head. The opposite trend was visible in CA4, where ND values were larger in the hippocampal head. With regard to the GCL, the ND showed at this level a net growth in the ventro-dorsal direction along the whole hippocampal axis. On the contrary, the astroglia exhibited a rather uniform cellular population, since only in CA1 and in the GCL were statistically significant differences found. Here, in both cases, AD was higher at the level of the hippocampal head. This trend is opposite to the one shown by neurons at the level of the GCL; indeed, ND was higher in the hippocampal tail. Regarding LTs, net differences were pointed out between the head and tail, as well as between the body and tail in all areas, whereas only CA3 and the combination of CA2-3 showed differences between the



hippocampal head and body. The LTs tended to increase in the dorsoventral direction in the CA2, CA2-3 and CA3 areas. Instead, the opposite trend was observed in CA1 and in the GCL. Overall, this analysis suggests that, in the evaluation of hippocampal specimens, the hippocampal section (tail, body or head) to which the examined tissue sample belongs should be taken into consideration, since many differences were observed, above all in ND and LT.

With regard to the clinical relevance of this study, although the diagnosis of HS is normally reached without a proper assessment of cell densities in human medicine, it has to be considered that human patients, who are affected by this pathology, usually have a long clinical history of seizures before undergoing surgical treatment. Indeed, it has been reported in a large multicenter study that the average interval between the onset of epilepsy and surgical intervention is 24 years among epileptic people (Engel, 2003). Furthermore, in another study, in which only patients with MTLE were investigated, the average period of time was 18 years (Benbadis et al., 2003). Now, considering that most domestic cats, even if completely healthy, do not live so long, it can be postulated that some of the cats affected by HS would present border-line hippocampal changes, which are not so obvious as in affected human hippocampi. This discrepancy could lead to misinterpreting the histopathological findings from some animals affected by HS. For this reason, in those cases with subtle hippocampal changes, the quantitative evaluation of cellular densities and LT could be helpful to obtain a definitive diagnosis. Nevertheless, it must be taken into consideration that the assessment of cellular densities alone can be sometimes not an easily interpretable indicator of disease state, as differences can rely on both changes in cell number and cell distribution (i.e. presence of layer dispersion) (West, 1999) and therefore it is recommended to evaluate both ND and LT. The recently published first case report of focal cortical resection and hippocampectomy in a cat with non-induced, refractory tempo-occipital seizures showed that the examination of such small and surgically deteriorated specimens may not be easy. Indeed, in this case, an accurate assessment of neuronal cell loss was not possible and therefore it could not be determined whether the cat was affected by typical HS (Hasegawa et al., 2021). This first example of a surgically treated cat as well as the epileptic cat examined as part of this study further confirmed the hypothesis that whereas substantial cellular loss like the one observed in hippocampal specimens from affected human patients does not require a quantitative examination to obtain a diagnosis of HS, on the other hand, in veterinary

medicine, it can be supposed that a large number of patients would present only subtle evidence of neuronal loss. In addition, considering that resected specimens can undergo a certain degree of damage during surgery, this makes a subjective examination of resected tissues even more difficult. Therefore, we suggest that a quantitative analysis should be performed in dubious cases. In the epileptic cat examined here, the extensive damage to the tissues was probably of artefactual origin, due to delayed fixation in formaldehyde.

The choice of staining (Nissl, NeuN and GFAP) was also in agreement with the standard investigation protocol used in human medicine in patients with suspected HS (Blümcke et al., 2013). However, it must be considered that the use of the anti-GFAP antibodies to identify non-reactive astrocytes may have led to an undercounting of the astroglial cell population (Wu et al., 2005). Indeed, not all astrocytes express this marker in the cortex and hippocampus of adult animals (Kitamura et al., 1987; Ling and Leblond, 1973; Savchenko et al., 2000; Walz and Lang, 1998). For this reason, it cannot be excluded that the astrocyte cell count was underestimated in this study as well as the astroglial densities. In this regard, a comparative examination with the astroglial marker S100 $\beta$  should be performed to verify this hypothesis. In fact, in contrast to GFAP, it seems that all astrocytes express S100 $\beta$ , which is on the other hand less specific than GFAP. In fact, it can also be found in some types of neurons, at least in rats (Rickmann and Wolff, 1995).

The main limitation of the study is related to the small population examined, which could of course have led to a bias. Moreover, the difficulties performing NeuN staining led to the consequence that ND was evaluated in an even smaller group of 14 animals. A hypothesis for the failure of the NeuN immunostaining in some cats is that this was the consequence of overfixation of the examined tissues in formaldehyde or delayed fixation of the tissues (even if within 12 hours of death), which led to a neuronal nuclear damage. Other explanations could not be found since all brains were processed in the same manner and stained using the same kits and staining system.

The hippocampus from only one epileptic cat was examined in this study to compare the normal reference values obtained from the statistical analysis with pathological ones. As a next step, a statistical analysis including an adequately large population of epileptic cats with suspected hippocampal pathology should be considered in order to assess relevant

differences in comparison to normal cats and to further evaluate the clinical importance of a quantitative histopathological examination of the hippocampus in these animals.

## 6 Conclusions

The partial temporal cortico-hippocampectomy has demonstrated to be a feasible technique for the resection of the hippocampus and of the temporal neocortex in cats. Resected tissue does not include subiculum, entorhinal cortex, or amygdala. If seizures fail to respond to medication, then epilepsy surgery may be an option for cats with intravital diagnosis of HS, in order to improve the prognosis. In this context, an important role is also played by hippocampal neuropathology. Therefore, the present study introduced a guide for processing post-mortem feline brains in order to perform a standardized morphological analysis of the hippocampal areas. The data provided for the first-time reference values for neuronal and astroglial densities as well as for LT of the hippocampal pyramidal cell layer (CA1-4) and GCL in adult and senior cats. Normal values are crucial to estimate the hippocampal pathology. As surgical treatment (i.e., hippocampectomy and/or cortical resection) for epileptic cats with AED resistance and seizures of temporal origin may become a therapy option in the future, this study will help in the standardized histopathological examination of resected hippocampal specimens.

## 7 Summary

Cats, like humans, are known to be affected by HS, potentially causing AED resistance. In humans, temporal lobe resection is a standardized therapy in patients with refractory TLE. Therefore, the purpose of this prospective cadaveric study is to establish a surgical technique for hippocampal resection in cats as a treatment for AED resistant temporal seizures and to define normal reference values on cellular density and cytoarchitecture for the different parts of the feline hippocampus, which is a necessary premise for a standardized examination of post-surgical hippocampal specimens. First, ten cats of different head morphology were examined. A pre-surgical 3D reconstruction of the head, brain, and hippocampus was obtained. The resected hippocampal specimens and the brains were examined histologically and with MRI for tissue injury adjacent to the surgical site. The feasibility of the established surgical procedure, as well as the usability of the removed specimen for histopathological examination, was assessed. In all cats but one, the resection of the temporal cortex and the hippocampus was successful. In one cat, the presence of mechanical damage of the thalamic surface was evident in the histopathologic examination of the brain post-resection. All hippocampal fields and the GCL were identified in five cats via histological examination. The second part of the study focused on the evaluation of the cytoarchitecture in the pyramidal layer of all CA areas and the GCL of the DG, which are known to undergo profound structural changes in cases of HS. Three transverse sections (head, body and tail) of each left hippocampus were obtained from 17 non-epileptic cats of different brachycephalic and mesocephalic breeds and age classes. Histological (H&E, Nissl) and immunohistochemical (NeuN, GFAP) staining was performed to investigate neuronal and astroglial cell populations, and LT of the pyramidal cell layer and GCL. Significant differences in ND and LT could be evidenced throughout the longitudinal hippocampal axis ( $p < 0.05$ ); on the other hand, the AD did not differ. Moreover, reference ranges for these parameters were defined. The factors breed and age did not influence ND, AD or LT. The study describes a new surgical approach offering a treatment for cats with AED resistant TLE, which may become a therapy option for these animals. Moreover, estimating normal values of the hippocampal cytoarchitecture will help in the standardized histopathological examination of resected hippocampal specimens to reach a diagnosis of HS.

## 8 Zusammenfassung

Katzen können Veränderungen des Hippocampus analog der humanen Hippocapussklerose entwickeln, welche potenziell eine Resistenz auf antiepileptische Medikamente auslösen kann. In der Humanmedizin ist die Resektion der Temporallappen eine standardisierte Therapie bei Patienten mit refraktärer temporaler Epilepsie. Ziel dieser prospektiven Studie ist es eine chirurgische Technik für die Resektion des Hippocampus von Katzen als Therapie gegen refraktäre temporale Anfälle zu entwickeln und normale Referenzwerte für die Zelldicke und die Zytoarchitektur unterschiedlicher Anteile des felines Hippocampus festzulegen, um eine standardisierte Untersuchung von postoperativen Proben des Hippocampus zu erreichen. Im ersten Teil, wurden zehn tote Katzen unterschiedlicher Kopfmorphologie untersucht. Präoperative 3D-Rekonstruktionen der Köpfe, Gehirne und Hippocampi wurden erstellt. Die resezierten Proben aus den Hippocampi und die operierten Gehirne wurden auf Gewebeschäden evaluiert. Die Durchführbarkeit der erprobten chirurgischen Methode, so wie die Verwendbarkeit der resezierten Proben für eine histopathologische Untersuchung wurden beurteilt. Die Resektion des temporalen Kortex und Hippocampus ist in neun Katzen erfolgreich gewesen. In einem Fall fiel ein oberflächiger Riss des Thalamus im Rahmen der histologischen Untersuchung auf. Alle untersuchten Felder wurden in fünf Katzen histologisch identifiziert. Im zweiten Teil wurde der Fokus auf die Evaluierung der Zytoarchitektur aller CA Bereiche und des GCL gelegt. Drei Transversalschnitte von jedem linken Hippocampus 17, nicht-epileptischer, toter Katzen unterschiedlicher brachycephalen und mesocephalen Rassen, sowie Altersgruppen wurden angefertigt. Histologische (H&E, Nissl) und immunhistochemische (NeuN, GFAP) Färbungen wurden verwendet, um die Neuronen und Astrozyten Populationen, sowie die Dicke der Pyramidenschicht und GCL zu untersuchen. Signifikante Unterschiede wurden in ND und LT entlang des Hippocampalaxis nachgewiesen ( $p < 0.05$ ); andererseits, unterschieden sich die AD nicht. Zudem wurden Referenzwerte für diese Parameter etabliert. Rasse und Alter hatten keinen Einfluss auf ND, AD oder LT. Die Studie beschreibt eine neue chirurgische Methode zur Behandlung von Katzen mit refraktärer TLE, welche eine Alternative zur bisherigen Behandlung von Katzen mit TLE darstellen. Die Evaluierung der Normalwerte der hippocampalen Zytoarchitektur könnte in der standardisierten histopathologischen Untersuchung resezierten Proben aus dem Hippocampus helfen.

## 9 List of Abbreviations

AD	Astrocytes Density
AED	Antiepileptic Drugs
BID	Bis In Die
BEL	Basic Epileptogenic Level
CA	Cornu Ammoni
CAH	Cortico-Amigdalohippocampectomy
CNS	Central Nervous System
CPS	Complex Partial Seizures
CT	Computed Tomography
DG	Dentate Gyrus
EEG	Electroencephalography
EUC	Epilepsy of Unknown Cause
FCD	Focal Cortical Dysplasia
FHN	Feline Hippocampal Necrosis
GC	Granule Cells
GCL	Granule Cell Layer
GTC	Generalized Tonic-Clonic seizures
HS	Hippocampal Sclerosis
IE	Idiopathic Epilepsy
ILAE	International League against Epilepsy
LS	Least-Squares
LT	Layer Thickness

mCT	micro-Computed Tomography
MRI	Magnetic Resonance Imaging
MTE	Mesial Temporal Epilepsy
MTLE	Mesial Temporal Lobe Epilepsy
ND	Neuronal Density
OI	Orofacial Involvement
PBS	Phosphate Buffered Saline
SAH	Selective Amygdalohippocampectomy
SPS	Simple Partial Seizures
TLE	Temporal Lobe Epilepsy
TSAH	Transcortical Selective Amygdalohippocampectomy
VGKC	Voltage-Gated Potassium Channel



## 10 List of figures

- Figure 1.** The human hippocampus was originally named after a sea horse due to its structural similarities with this animal (A). Indeed, hippocampus means in greek “sea horse”. On the other hand, in mammals, the hippocampus shows a rather linear and uniform morphology; indeed, no clear divisions are present between its three sections (head, body and tail). In animals, the two hippocampi are characterised by a typical elongated, dorso-caudally curved shape, on each side of the thalamus and resemble a pair of horns on the head of a ram, which is why it was also called Ammon’s horn (B), from the Egyptian god Ammon, who was always represented with an Aries head (Barone and Bortolami, 2006a)..... 7
- Figure 2.** Mesial temporal lobe and surrounding structures..... 8
- Figure 3.** Schema of the ammon’s horn layers’ structure (NeuN stained CA2 area from a feline hippocampus)..... 9
- Figure 4.** Hippocampal subdivisions..... 11
- Figure 5.** Magnetic resonance imaging of a cat with suspected HS. 5-year-old male castrated Domestic Shorthair cat, which was presented in the small animal hospital of the JLU in Giessen due to chronic, refractory epileptic seizures. In the magnetic resonance imaging of the head, the hippocampus (star) presented a mild to moderate atrophy, with multiple, irregular, hyperintens areas in the T2-weighted (A) and FLAIR (B) images. The atrophy is also evident in the 3D CISS sequence. No contrast enhancement was present (D). The findings were suggestive for HS, possibly secondary to the chronic epileptic activity. In the figure above, transverse T2-weighted (A), FLAIR (B) and T1-weghted SUB after application of gadolinium (D) images, and a dorsal section of a CISS sequence (C) are shown..... 25
- Figure 6.** Comparison of anterior temporal lobectomy and selective amygdalohippocampectomy (Spencer and Burchiel, 2012). On the left an anterior temporal lobectomy or cortico-amygdalohippocampectomy can be observed, while on the right the much less invasive selective amygdalohippocampectomy can be seen..... 28
- Figure 7.** Selective transcortical amygdalohippocampectomy through the second temporal gyrus (Spencer and Burchiel, 2012). Surgical approach (left) and coronal views of the brain, temporal lobe and nearby structures (centre and right). A retractor is placed along the white matter corridor in T2 after opening the lateral ventricle to fully expose the hippocampal formation. The first step in the SAH is to enter the lateral ventricular sulcus to empty the parahippocampus in a subpial fashion. Then, the hippocampus is separated from the fimbria (\*), tail and removed en-bloc. Lastly, the subpial emptying of the uncus and the resection of the amygdala are carried out. The mesial temporal structures that are removed in this technique are the hippocampal complex and parahippocampus. SF = Sylvian Fissure; T2 = middle temporal gyrus; PH = parahippocampal gyrus (T5)..... 32
- Figure 8.** Localization of the hippocampus within the brain. 3D models of the skull and brain of a domestic shorthair cat based on CT- and MRI-images. Model A shows the whole brain (red) within the skull. Model B gives an overview of the neocortical sulci and gyri of the same brain. The brain surface is transparent in model C that displays the hippocampus (yellow) within the brain. Most of the hippocampus (head, body and parts of the tail) is situated underneath the caudal ectosylvian sulcus. ob: olfactory bulb; cor: coronal sulcus; Ecs: ectosylvian sulcus; ecs: ectosylvian gyrus; syl: sylvian gyrus; psyl: pseudosylvian fissure; emg: ectomarginal gyrus; Ems: ectomarginal sulcus; cb: cerebellum; flo: flocculonodular lobe..... 48
- Figure 9.** Localization of the ectosylvian sulcus and the hippocampus from the skin surface and skull. 3D models of the head, skull, and brain of a mesocephalic Domestic Shorthair cat (A, B) and a brachycephalic Persian cat (C, D), in lateral (A, C) and a dorsal view and a dorsal view (B,

D). The graphical software combines MRI- and CT-images. The hippocampus can be localized within the brain and the position can be projected on the brain and skull surface. .... 49

**Figure 10. Pterional craniotomy: Bony anatomical landmarks.** The cat's head is turned 45° to the side in order to place the zygomatic arch at the highest point. Landmarks for skin incision are the frontal process of the zygomatic bone and the external occipital protuberance. A skin incision is made in the middle of an imaginary line connecting the two landmarks (A). After dissection and spreading of the temporalis muscle, the left parietal and temporal bone is exposed. The crossing of the coronal and squamous suture is visible (B). The same landmarks that can be used for the orientation on the skin surface can be used at the calvaria as well. The middle point of these imaginary line marks the position of the craniectomy site with the hippocampus body at the centre. .... 50

**Figure 11. Transcortical approach to the hippocampus (part 1).** Intraoperative photograph showing the view on the left sylvian and ectosylvian gyri and corresponding sulci after craniectomy and dural exposure (A). Tripartite dural incision (B). View of the brain surface after reflection of the dura (C). Magnified view on the incision in the dorsal ectosylvian gyrus (D). High magnification photograph of the transcortical access to temporal horn (E) and exposure of the hippocampal body (F). Ecs: ectosylvian sulcus; ecs: caudal ectosylvian gyrus; hip: hippocampus; lv: lateral ventricle syl: caudal sylvian gyrus. .... 51

**Figure 12. Transcortical approach to the hippocampus-hippocampal resection (part 2).** Intraoperative photograph showing the hippocampus after resection of the temporal neocortex (caudal ectosylvian gyrus). The hippocampus is cut off dorsally (B) and ventrally (C) with an 11-scalpel blade; then its mesial connections are carefully transected with the help of a nerve hook (D) and the hippocampus is pulled out and removed (E). After completing the resection, the medial geniculate body and the caudal cerebral artery become visible (F, enlarged view). ecs: caudal ectosylvian gyrus; syl: caudal sylvian gyrus; rcha: rostral choroidal artery; hip: hippocampus; lv: lateral ventricle; fi: fimbria; hcf: hippocampal fissure; phg: parahippocampal gyrus; mgb: medial geniculate body; cca: caudal cerebral artery; lha: longitudinal hippocampal artery. .... 53

**Figure 13. Illustration of the blood supply of the hippocampus.** Maximum intensity projection of the contrast-injected vascular supply of the hippocampus in a dorsal view reveals the major blood vessels of the hippocampus (A). The brain and other vessel images have been removed using a grey threshold. The histopathological section of the hippocampus shows the relevant arteries in the surgical field (B). .... 55

**Figure 14. MRI before (A) and after (B) surgery and histological sections of the resected hippocampus (C-E).** In the MRI post-resection, the left hippocampus (body) as well as the temporal neocortex are absent. Nevertheless, most of the hippocampal tail and the whole head are still in situ (B). Histological sections of the hippocampus after resection show that the specimen allow the examination of all CA-fields in most cases (C, D), but in some of them not all fields are preserved and can be examined (E). The completeness of the resected specimens is also related to the surgeon's learning curve. .... 56

**Figure 15. Standardized brain processing for obtaining head, body and tail sections from a hippocampus.** First, the brainstem was approached ventrally and a ventro-dorsal section at the level of the rostral cerebellar colliculi and pons was trimmed with a scalpel blade in order to separate the cerebellum and medulla oblongata from the region of interest (A). Then, a transverse cut at the level of the pituitary gland was obtained with a long blade (B). Subsequently, the right and left hemispheres were separated over the midline with the same blade (C). At this point, the left hippocampal body was dissected through a 90° cut directly underneath the mesocephalic aqueduct (D). Two further parallel sections, respectively 2-4 mm

under (E) and 2-4 mm over (F) the previous cut were made, in order to obtain a specimen from the head and one from the body of the hippocampus, respectively. Finally, from the residual dorsal part of the temporal lobe a section from the hippocampal tail was obtained: the cut line was set through the vertex of the occipitotemporal flexure with an inclination of 45° (G). Once done, a further cut parallel and dorsal to the previous one was performed, obtaining the dorsal hippocampal specimen (F)..... 65

**Figure 16. Hippocampal areas of the assessed sections. From each hippocampus two rectangular areas were selected from the regions CA1-4 and GCL for cell counting at NeuN (A) and GFAP (B) stained slides. CA2 alone was not assessed for GFAP. Evaluation of the LTs of the different areas at Nissl-stained sections (C). A 3D model of the skull of a Domestic Shorthair cat based on CT and MRI images showing the localization of the hippocampus and its divisions (tail, body and head) (D). .... 68**

**Figure 17. Estimated ND values (LS-means +/- standard error) (Least-Squares-means) from the variance analysis for repeated measurements comparing the hippocampal tail, body and head. The data are relative to all examined areas and show the presence of statistically significant differences. \* p < 0.05, \*\* p < 0.01, \*\*\* p < 0.001. .... 72**

**Figure 18. Estimated LT values (LS-means +/- standard error) from the variance analysis for repeated measurements comparing the hippocampal tail, body and head. The data are relative to all examined areas and show the presence of statistically significant differences. \* p < 0.05, \*\* p < 0.01, \*\*\* p < 0.001. .... 73**

**Figure 19. Neuronal morphology of the pyramidal cell layer areas and GCL in NeuN. All examined areas, including the four CA regions (CA1-4), the GCL and an example of the combination of CA2 and 3 can be seen. Significant morphological differences were present along the pyramidal cell layer. Both, cell form and distribution meaningfully changed along the transverse hippocampal axis. .... 75**

**Figure 20. Astroglial cell morphology of the different hippocampal pyramidal layers and GCL. All examined areas, including CA1, CA3 and CA4, the GCL and an example of the combination of CA2 and 3 can be seen. The distribution of astroglia was homogenous throughout the pyramidal cell layer. Nevertheless, in CA4, astrocytes were more abundant compared to the other CA areas. In the GCL, astroglial cells were mainly located at the border towards CA4. ... 76**

**Figure 21. Estimated ND, AD and LT values (LS-means +/- standard error) from the variance analysis for repeated measurements comparing the hippocampal tail, body and head with the fixed effect of breed. The data are relative to neuronal densities in CA1 (A), astrocyte density in CA2-3 (B), and in the GCL (C), and layer thickness in CA3 (D). The data were not statistically significant. .... 122**

**Figure 22. Estimated AD values (LS-means +/- standard error) from the variance analysis for repeated measurements comparing the hippocampal tail, body and head. The data are relative to all examined areas and show the presence of statistically significant differences. \*\* p < 0.01. .... 123**

## 11 List of tables

**Table 1. Signalment and cause of death of the study cats (surgical study). .... 43**

**Table 2. Hydration process. Before staining all slides undergo a hydration process as shown. ... 46**

**Table 3. Dehydration process (Nissl staining). After staining with cresyl violet, all sections undergo a differentiation process, which ends two passages in xylene 100%. During this process, part of the stain is washed away from the slides..... 47**

<b>Table 4. Signalment and cause of death of the study cats.....</b>	<b>70</b>
<b>Table 5. Mean values, standard deviation, and minimum and maximum values for NDs.....</b>	<b>120</b>
<b>Table 6. Mean values, standard deviation, and minimum and maximum values for ADs.....</b>	<b>120</b>
<b>Table 7. Mean values, standard deviation, and minimum and maximum values for LT.....</b>	<b>121</b>

## 12 References

1. Adada B. Selective amygdalohippocampectomy via the trans-sylvian approach. *Neurosurg Focus* 2008;25:E5.
2. Adamec RE, Stark-Adamec C. Partial kindling and emotional bias in the cat: lasting aftereffects of partial kindling of the ventral hippocampus. I. Behavioral changes. *Behav Neural Biol* 1983(a);38(2):205-222.
3. Adamec RE, Stark-Adamec C. Partial kindling and emotional bias in the cat: lasting aftereffects of partial kindling of the ventral hippocampus. II. Behavioral changes. *Behav Neural Biol* 1983(b);38(2):223-239.
4. Amaral DG. A Golgi study of cell types in the hilar region of the hippocampus in the rat. *J Comp Neurol* 1978;182(4):851-914.
5. Amaral DG, Insausti R, Cowan WM. The commissural connections of the monkey hippocampal formation. *J Comp Neurol* 1984;224(3):307-336.
6. Amaral DG, Ishizuka N, Claiborne B. Neurons, numbers and the hippocampal network. *Prog Brain Res* 1990;83:1-11.
7. Amaral DG, Scharfman HE, Lavenex P. The dentate gyrus: fundamental neuroanatomical organization (dentate gyrus for dummies). *Prog Brain Res* 2007;163:3-22.
8. Andy OJ, Peeler DF, Foshee DP. Avoidance and discrimination learning following hippocampal ablation in the cat. *J Comp Physiol Psych* 1967;64:516–519.
9. Arrol L, Penderis J, Garosi L, Cripps P, Gutierrez-Quintana R, Goncalves R. Aetiology and long-term outcome of juvenile epilepsy in 136 dogs. *Vet Rec* 2012;170(13):335.
10. Asadi-Pooya AA, Sharan AS, Nei M, Sperling MR. Corpus callosotomy. *Epilepsy Behav* 2008;13(2):271-278.
11. Bagley RS, Baszler TV, Harrington ML, Pluhar GE, Moore MP, Keegan RD, Greene SA. Clinical effects of longitudinal division of the corpus callosum in normal dogs. *Vet Surg* 1995;24:122–7.

12. Ball MJ. Neuronal Loss, Neurofibrillary Tangles and Granulovacuolar Degeneration in the Hippocampus with Ageing and Dementia. *Acta Neuropath* 1977;37:111-118.
13. Barone R, Bortolami R. Capitolo VIII, Rinencefalo. In: *Anatomia comparata dei mammiferi domestici*, Vol. 6 Neurologia, Sistema nervoso centrale. Bologna, 2006a;395-436.
14. Barone R, Bortolami R. Capitolo IX, Neopallio. In: *Anatomia comparata dei mammiferi domestici*, Vol. 6 Neurologia, Sistema nervoso centrale. Bologna, 2006b;437-446.
15. Barnes HL, Chrisman CL, Mariani CL, Sims M, Alleman AR. Clinical signs, underlying cause, and outcome in cats with seizures: 17 cases (1997-2002). *J Am Vet Med Assoc* 2004;225:1723-1726.
16. Bartesaghi R, Gessi T. Parallel activation of field CA2 and dentate gyrus by synaptically elicited perforant path volleys. *Hippocampus* 2004;14(8):948-963.
17. Bartsch T. *The Clinical Neurobiology of the Hippocampus: An integrative view*. Oxford University, 2012.
18. Bate H, Eldridge P, Varma T, Wiesmann UC. The seizure outcome after amygdalohippocampectomy and temporal lobectomy. *Eur J Neurol* 2007;14:90-94.
19. Benbadis SR, Heriaud L, Tatum WO, Vale FL. Epilepsy surgery, de-lays, and referral patterns. *Seizure* 2003;12:167-170.
20. Berendt M, Gredal H, Ersbøll AK, Alving J. Premature death, risk factors, and life patterns in dogs with epilepsy. *J Vet Int Med* 2007;21:754-759.
21. Berendt M, Gredal H, Pedersen LG, Alban L, Alving J. A cross-sectional study of epilepsy in Danish Labrador Retrievers: prevalence and selected risk factors. *J Vet Int Med* 2002;16:262-268.
22. Berendt M, Gullov CH, Christensen SLK, Gudmindsdottir H, Gredal HB, Fredholm M, Alban L. Prevalence and characteristics of epilepsy in the Belgian Shepherd variants Groenendael and Turvueren born in Denmark 1995-2004. *Acta Vet Scand* 2008;50:51.

23. Berendt M, Gullov CH, Fredholm M. Focal epilepsy in the Belgian Shepard: Evidence for simple Mendelian inheritance. *J Small Anim Pract* 2009;50:655-661.
24. Berendt M, Farquhar RG, Mandigers PJ, Pakozdy A, Bhatti SF, De Risio L, Fischer A, Long S, Matiasek K, Muñana K, Patterson EE, Penderis J, Platt S, Podell M, Potschka H, Pumarola MB, Rusbridge C, Stein VM, Tipold A, Volk HA. International veterinary epilepsy task force consensus report on epilepsy definition, classification and terminology in companion animals. *BMC Vet Res* 2015;11:182.
25. Bhatti SF, De Risio L, Muñana K, Penderis J, Stein VM, Tipold A, Berendt M, Farquhar RG, Fischer A, Long S, Löscher W, Mandigers PJ, Matiasek K, Pakozdy A, Patterson EE, Platt S, Podell M, Potschka H, Rusbridge C, Volk HA. International Veterinary Epilepsy Task Force consensus proposal: medical treatment of canine epilepsy in Europe. *BMC Vet Res* 2016;11:176.
26. Blackstad TW. Commissural connections of the hippocampal region in the rat, with special reference to their mode of termination. *J Comp Neurol* 1956;105(3):417-537.
27. Blümcke I, Coras R, Miyata H, Ozkara C. Defining clinico-neuropathological subtypes of mesial temporal lobe epilepsy with hippocampal sclerosis. *Brain Pathol* 2012;22:402-411.
28. Blümcke I, Spreafico R. Cause matters: a neuropathological challenge to human epilepsies. *Brain Pathol* 2012;22:347-349.
29. Blumcke I, Spreafico R, Haaker G, Coras R, Kobow K, Bien CG, Pfäfflin M, Elger C, Widman G, Schramm J, Becker A, Braun KP, Leijten F, Baayen JC, Aronica E, Chassoux F, Hamer H, Stefan H, Rössler K, Thom M, Walker MC, Sisodiya SM, Duncan JS, McEvoy AW, Pieper T, Holthausen H, Kudernatsch M, Meencke HJ, Kahane P, Schulze-Bonhage A, Zentner J, Heiland DH, Urbach H, Steinhoff BJ, Bast T, Tassi L, Lo Russo G, Özkara C, Oz B, Krsek P, Vogelgesang S, Runge U, Lerche H, Weber Y, Honavar M, Pimentel J, Arzimanoglou A, Ulate-Campos A, Noachtar S, Hartl E, Schijns O, Guerrini R, Barba C, Jacques TS, Cross JH, Feucht M, Mühlebner A, Grunwald T, Trinka E, Winkler PA, Gil-Nagel A, Toledano Delgado R, Mayer T, Lutz M, Zountsas B, Garganis K, Rosenow F, Hermsen A, von Oertzen TJ, Diepgen TL, Avanzini G; EEBB Consortium. Histopathological Findings in Brain Tissue Obtained during Epilepsy Surgery. *N Engl J Med* 2017;377(17):1648-1656.

30. Blümcke I, Thom M, Aronica E, Armstrong DD, Bartolomei F, Bernasconi A, Bernasconi N, Bien CG, Cendes F, Coras R, Cross JH, Jacques TS, Kahane P, Mathern GW, Miyata H, Moshé SL, Oz B, Özkara C, Perucca E, Sisodiya S, Wiebe S, Spreafico R. International consensus classification of hippocampal sclerosis in temporal lobe epilepsy: A task Force report from the ILAE Commission on Diagnostic Methods. *Epilepsia* 2013;54(7):1315-1329.
31. Bonelli SB, Powell RHW, Yogarajah M, Samson RS, Symms MR, Thompson PJ, Koepp MJ, Duncan JS. Imaging memory in temporal lobe epilepsy: predicting the effects of temporal lobe resection. *Brain* 2010;133:1186-1199.
32. Braak H. Architectonics of the human telencephalic cortex. In: Braitenberg V, Barlow HB, Bizzi E, Florey E, Grüsser OJ, Van der Loos H, editors. *Studies of brain function*, vol 4. New York, 1980;1–147.
33. Briellmann RS, Wellard RM, Jackson GD. Seizure-associated abnormalities in epilepsy: evidence from MR imaging. *Epilepsia* 2005;46:760-766.
34. Brini E, Gandini G, Crescio I, Fatzer R, Casalone C. Necrosis of hippocampus and piriform lobe: Clinical and neuropathological findings in two Italian cats. *J Feline Med Surg* 2004;6:377–381.
35. Brown TS, Kaufmann PG, Marco LA. The hippocampus and response perseveration in the cat. *Brain Research* 1969;12:86–98.
36. Buckmaster PS, Smith MO, Buckmaster CL, LeCouteur RA, Dudek FE. Absence of temporal lobe epilepsy pathology in dogs with medically intractable epilepsy. *Vet Int Med* 2002;16:95-99.
37. Bujarski KA, Hirashima F, Roberts DW, Jobst BC, Gilbert KL, Roth RM, Flashman LA, McDonald BC, Saykin Aj, Scott RC, Dinnerstein E, Preston J, Williamson PD, Thadani VM. Long-term seizure, cognitive, and psychiatric outcome following trans-middle temporal gyrus amygdalohippocampectomy and standard temporal lobectomy. *J Neurosurg* 2013;119:16–23.
38. Bush WW, Barr CS, Darrin EW, Shofer FS, Vite CH, Steinberg SA. Results of cerebrospinal fluid analysis, neurologic examination findings, and age at the onset of seizures as predictors for results of magnetic resonance imaging of the brain in dogs



- examined because of seizures: 115 cases (1992-2000). *J Am Vet Med Assoc* 2002;220(6):781-784.
39. Cantile C, Chianini F, Arispici M, Fatzer R. Necrotizing meningoencephalitis associated with cortical hippocampal hamartia in a Pekingese dog. *Vet Path* 2001;38:119-122.
40. Casal MI, Munuve RM, Janis MA, Werner P, Henthorn PS. Epilepsy in Irish Wolfhounds. *J Vet Intern Med* 2006;20:131-135.
41. Casey KM, Bollen AW, Winger KM, Vernau KM, Dickinson PJ, Sisó. Bilaterally Symmetric Focal Cortical Dysplasia in a Golden Retriever Dog. *J Comp Pathol* 2014;151(4):375-379.
42. Cenquizca LA, Swanson LW. Spatial organization of direct hippocampal field CA1 axonal projections to the rest of the cerebral cortex. *Brain Res Rev* 2007;56(1):1-26.
43. Cerbone A, Patacchioli FR, Sadile AG. A neurogenetic and morphogenetic approach to hippocampal functions based on individual differences and neurobehavioral covariations. *Behav Brain Res* 1993;55(1):1-16.
44. Cervera V, Mai W, Vite CH, Johnson V, Dayrell-Hart B, Seiler GS. Comparative magnetic resonance imaging findings between gliomas and presumed cerebrovascular accidents in dogs. *Vet Rad Ultr* 2011;52:33-40.
45. Chang Y, Mellor DJ, Anderson TJ. Idiopathic epilepsy in dogs: owner's perspectives on management with phenobarbitone and/or potassium bromide. *J Small Anim Pract* 2006;47:574-581.
46. Charalambous M, Pakozdy A, Bhatti SFM, Volk HA. Systematic review of antiepileptic drugs' safety and effectiveness in feline epilepsy. *BMC Vet Res* 2018;14(1):64.
47. Cheung L. An Animal Model for Maxillary Reconstruction Using a Temporalis Muscle Flap. *J Oral Maxillofac Surg* 1996;54:1439-1445.
48. Cheung MC, Chan AS, Lam JM, Chan YL. Pre- and postoperative fMRI and clinical memory performance in temporal lobe epilepsy. *J Neurol Neurosurg Psychiatry* 2009;80:1099-1106.

49. Chicurel ME, Harris KM. Three-dimensional analysis of the structure and composition of CA3 branched dendritic spines and their synaptic relationships with mossy fiber boutons in the rat hippocampus. *J Comp Neurol* 1992;325(2):169-182.
50. Claßen A, Kneissl S, Lang J, Tichy A, Pakozdy A. Magnetic resonance features of the feline hippocampus in epileptic and non-epileptic cats: a blinded, retrospective, multi-observer study. *BMC Vet Research* 2016;12:165.
51. Clusmann H, Schramm J, Kral T, Helmstaedter C, Ostertun B, Fimmers R, Haun D, Elger CE. Prognostic factors and outcome after different types of resection for temporal lobe epilepsy. *J Neurosurg* 2002;97:1131-1141.
52. Cole AJ. Status epilepticus and periictal imaging. *Epilepsia* 2004; 45(Suppl. 4):72-77.
53. Colombo M, Fernandez T, Nakamura K, Gross CG. Functional differentiation along the anterior-posterior axis of the hippocampus in monkeys. *J Neurophysiol* 1998;80(2):1002-1005.
54. Craige EH, Gibson WC. The world of Ramon y Cajal —With Selections from his Nonscientific Writings. Thomas CC, Springfield, Illinois; 1968.
55. Cuckiert A, Cuckiert C, Argenton M, Baise-Zung C, Forster CR, Mello VA, Burattini JA, Mariani PP. Outcome after corticoamygdalohippocampectomy in patients with refractory temporal lobe epilepsy and mesial temporal sclerosis without preoperative ictal recording. *Epilepsia* 2009;50(6):1371-1376.
56. Czerwik A, Plonek M, Podgórski P, Wrzosek M. Comparison of electroencephalographic findings with hippocampal magnetic resonance imaging volumetry in dogs with idiopathic epilepsy. *J Vet Int Med* 2018;32(6):2037-2044.
57. Dam AM. The density of neurons in the human hippocampus. *Neuropathol App Neurobiol* 1979;5(4):249-264.
58. Delgado JMR, Sevillano M. Evolution of repeated hippocampal seizures in the cat. *Electroenceph Clin Neurophys* 1961;13:722–733.
59. De Risio. Clinical and Diagnostic Investigation of the Seizure Patient. In: De Risio L, Platt S, editors. *Canine and Feline Epilepsy Diagnosis and Management*. Wallingford, 2014;274-324.

60. De Risio L, Bhatti S, Muñana K, Penderis J, Stein V, Tipold A, Berendt M, Farquhar R, Fischer A, Long S, Mandigers PJJ, Matiasek K, Packer RMA, Pakozdy A, Patterson N, Platt S, Podell M, Potschka H, Pumarola Batlle M, Rusbridge C, Volk HA. International veterinary epilepsy task force consensus proposal: diagnostic approach to epilepsy in dogs. *BMC Vet Res* 2015;11:148.
61. Devaney KO, Johnson HA. Changes in cell density within the human hippocampal formation as a function of age. *Gerontology* 1984;30(2):100-108.
62. Dong H-W, Swanson LW, Chen L, Fanselow MS, Toga AW. Genomic-anatomic evidence for distinct functional domains in hippocampal field CA1. *Proc Natl Acad Sci U S A* 2009;196(28):11794-17799.
63. Dupont S, Tanguy ML, Clemenceau S, Adam C, Hazemann P, Baulac M. Long-term prognosis and psychosocial outcomes after surgery for MTLE. *Epilepsia* 2006;47:2115-2124.
64. Ellenberger W, Baum H. *Handbuch der vergleichenden Anatomie der Haustiere*. 18th ed. Springer, Berlin, 1977.
65. Engel Jr J. Etiology as a risk factor for medically refractory epilepsy: a case for early surgical intervention. *Neurology* 1998;51:1243-1244.
66. Engel Jr J. A Greater Role for Surgical Treatment of Epilepsy: Why and When? *Epilepsy Curr* 2003;3(2):37-40.
67. Eriksson SH, Nordborg C, Rydenhag B, Malmgren K. Parenchymal lesions in pharmacoresistant temporal lobe epilepsy: dual and multiple pathology. *Acta Neurol Scand* 2005;112:151–156.
68. Estey CM, Dewey CW, Rishniw M, Lin DM, Bouma J, Sackman J, Burkland E. A Subset of Dogs with Presumptive Idiopathic Epilepsy Show Hippocampal Asymmetry: A Volumetric Comparison with Non-Epileptic Dogs Using MRI. *Front Vet Sci* 2017;4(183).
69. Fabricius K, Wörtwein G, Pakkenberg B. The impact of maternal separation on adult mouse behaviour and on the total neuron number in the mouse hippocampus. *Brain Struct Funct* 2008;212:403-416.

70. Famula TR, Oberbauer AM. Segregation analysis of epilepsy in the Belgian Tervueren dog. *Vet Rec* 2000;147:218-221.
71. Fanselow MS, Dong H-W. Are the dorsal and ventral hippocampus functionally distinct structures? *Neuron* 2010;65(1):7-19.
72. Farid N, Girard HM, Kemmotsu N, Smith ME, Magda SW, Lim WY, Lee RR, McDonald CR. Temporal lobe epilepsy: quantitative MR volumetry in detection of hippocampal atrophy. *Radiology* 2012;264(2):542-550.
73. Fatzer R, Gandini G, Jaggy A, Doherr M, Vandevelde M. Necrosis of hippocampus and piriform lobe in 38 domestic cats with seizures. A retrospective study on clinical and pathologic findings. *J Vet Intern Med* 2000;14:100–104.
74. Fauser S, Schulze-Bonhage A. Epileptogenicity of cortical dysplasia in temporal lobe dual pathology: an electrophysiological study with invasive recordings. *Brain* 2006;129:82-95.
75. Fors S, Van Meervenne S, Jeserevics J, Rakauskas M, Cizinauskas S. Feline hippocampal and piriform lobe necrosis as a consequence of severe cluster seizures in two cats in Finland. *Acta Vet Scand* 2015;57:41.
76. Forterre F, Jaggy A, Rohrbach H, Dickomeit M, Konar M. Modified temporal approach for a rostro-temporalbasal meningioma in a cat. *J Fel Med Surg* 2009;11:510–513.
77. Gaarskjaer FB. Organization of the mossy fiber system of the rat studied in extended hippocampi. II. Experimental analysis of fiber distribution with silver impregnation methods. *J Comp Neurol* 1978;178(1):73-88.
78. Gambarian LS, Gekht K, Sarkisov GT, Koval IN, Kazarian GM. Role of the hippocampus in conditioned reflex activity. *Zh Vyssh Nerv Deiat Im I P Pavlova* 1979;29:56–63.
79. Geisert Jr EE, Williams RW, Geisert GR, Fan L, Asbury AM, Maecker HT, Deng J, Levy S. Increased brain size and glial cell number in CD81-null mice. *J Comp Neurol* 2002;453(1):22-32.

80. Gelberg HB. Diagnostic exercise: sudden behaviour change in a cat. *Vet Path* 2013;50:1156-1157.
81. Gibbs FA, Gibbs El. The convulsion threshold of various parts of the cat's brain. *Arch Neurol Psychiatr (Chicago)* 1936;11:7-17.
82. Gillilan LA. Extra- and intra-cranial blood supply to brains of dog and cat. *Am J Anat* 1976;146:237– 253.
83. Glass EN, Kapatkin A, Vite C, Steinberg SA. A modified bilateral transfrontal sinus approach to the canine frontal lobe and olfactory bulb: surgical technique and five cases. *J Am Anim Hosp Assoc* 2000;36:43–50.
84. Gleissner U, Helmstaedter C, Schramm J, Elger CE. Memory outcome after selective amygdalohippocampectomy in patients with temporal lobe epilepsy: one-year follow-up. *Epilepsia* 2004;45:960-962.
85. Gloor P, Olivier A, Quesney LF, Andermann F, Horowitz S. The role of the limbic system in experimental phenomena of temporal lobe epilepsy. *Ann Neurol* 1982;12:129-144.
86. Goetzen B, Sztamska E. Comparative anatomy of the arterial vascularization of the hippocampus in man and in experimental animals (cat, rabbit and sheep). *Neuropatol Pol* 1992;30:173–184.
87. Grammaldo LG, Di Gennaro G, Giampà T, De Risi M, Meldolesi GN, Mascia A, Sparano A, Esposito V, Quarato PP, Picardi A. Memory outcome 2 years after anterior temporal lobectomy in patients with drug-resistant epilepsy. *Seizure* 2009;18:139-144.
88. Grattan-Smith JD, Harvey AS; Desmond PM, Chow CW. Hippocampal sclerosis in children with intractable temporal lobe epilepsy: detection with MR imaging. *Am J Roentgenol* 1993;161(5):1045-1048.
89. Graus F, Saiz A, Dalmau J. Antibodies and neuronal autoimmune disorders of the CNS. *J Neurol* 2010;257(4):509-517.
90. Gül G, Yandım Kuşcu D, Özerden M, Kandemir M, Eren F, Tuğcu B, Keskinilic C, Kayrak N, Kirbaş D. Cognitive outcome after surgery in patients with mesial temporal lobe epilepsy. *Noro Psikiyatrs Ars* 2017;54:43-48.

91. Gullov CH, Toft N, Baadsager MM, Berendt M. Epilepsy in the Petit Basset Griffon Vendeen: prevalence, semiology, and clinical phenotype. *J Vet Int Med* 2011;25:1372-1378.
92. Harker KT, Whishaw IQ. Impaired place navigation in place and matching-to-place swimming pool tasks follows both retrosplenial cortex lesions and cingulum bundle lesions in rats. *Hippocampus* 2004;14(2):224-231.
93. Hasegawa D. Diagnostic techniques to detect the epileptogenic zone: Pathophysiological and presurgical analysis of epilepsy in dogs and cats. *Vet J* 2016;215:64-75.
94. Hasegawa D, Asada R, Hamamoto Y, Yu Y, Kuwabara T, Mizoguchi S, Chambers JK, Uchida K. Focal Cortical Resection and Hippocampectomy in a Cat With Drug-Resistant Structural Epilepsy. *Front Vet Sci* 2021;8:719455.
95. Helmstaedter C, Petzold I, Bien CG. The cognitive consequence of resecting nonlesional tissues in epilepsy surgery-Results from MRI- and histopathology negative patients with temporal lobe epilepsy. *Epilepsia* 2011;52:1402-1408.
96. Helmstaedter C, van Roost D, Clusmann H, Urbach H, Elger CE, Schramm J. Collateral brain damage, a potential source of cognitive impairment after selective surgery for control of mesial temporal lobe epilepsy. *J Neurol Neurosurg Psychiatry* 2004;75:323-326.
97. Henke PG. Granule cell potentials in the dentate gyrus of the hippocampus: coping behavior and stress ulcers in rats. *Behav Brain Res* 1990;36(1-2):97-103.
98. Hertz-Pannier L, Chiron C, Jambaque I, Renaux-Kieffer V, Van de Moortele PF, Delalande O, Fohlen M, Brunelle F, Le Bihan D. Late plasticity for language in a child's non-dominant hemisphere: a pre- and post-surgery fMRI study. *Brain* 2002; 125(Pt 2):361-372.
99. Heynold Y, Faissler D, Steffen F, Jaggy A. Clinical, epidemiological and treatment results of idiopathic epilepsy in 54 Labrador Retrievers: a long-term study. *J Small Anim Pract* 1997;38:7-14.

100. Hori A, Kiwamu H, Kenjiro M, Tetsuya N. Porencephaly in dogs and cats: relationships between magnetic resonance imaging (MRI) features and hippocampal atrophy. *J Vet Med Sci* 2015;77(7):889-892.
101. Hori T, Tabuchi S, Kurosaki M, Kondo S, Tekenobu A, Watanabe T. Subtemporal amygdalohippocampectomy for treating medially intractable temporal lobe epilepsy. *Neurosurg* 1993;33(1):50-56.
102. Ho SS, Kuzniecky RI, Gilliam F, Faught E, Bebin M, Morawetz R. Congenital porencephaly: MR features and relationship to hippocampal sclerosis. *Am J Neuroradiol* 1998;19:135-141.
103. Hulsmeyer V, Zimmermann R, Brauer C, Sauter-Louis C, Fischer A. Epilepsy in Border Collies: Clinical manifestation, outcome and mode of inheritance. *J Vet Intern Med* 2010;24:171-178.
104. Hu W, Zhang C, Zhang K, Meng F, Chen N, Zhang J. Selective amygdalohippocampectomy versus anteriortemporal lobectomy in the management of mesial temporal lobe epilepsy: a meta-analysis of comparative studies. *J Neurosurg* 2013;119:1089–1097.
105. Jaggy A, Faissler D, Gaillard C, Srenk P, Graber H. Genetic aspects of idiopathic epilepsy in Labrador Retrievers. *J Small Anim Pract* 1998;39:275-280.
106. Jarrard LE. The hippocampus and motivation. *Psychol Bull* 1973;79(1):1-12.
107. Jinno S, Fleischer F, Eckel S, Schmidt V, Kosaka T. Spatial arrangement of microglia in the mouse hippocampus: a stereological study in comparison with astrocytes. *Glia* 2007;55(13):1334-1347.
108. Jinno S, Kosaka T. Stereological Estimation of Numerical Densities of Glutamatergic Principal Neurons in the Mouse Hippocampus. *Hippocampus* 2010; 20(7):829-40.
109. Jokinen TS, Metsähonkala L, Bergamasco L, Viitmaa R, Syrjä P, Lohi H, Snellman M, Jeserevics J, Cizinauskas S. Benign familial juvenile epilepsy in Lagotto Romagnolo dogs. *J Vet Intern Med* 2007;21(3):464–471.

110. Kathmann I, Jaggy A, Busato A, Bartschi M, Gaillard C. Clinical and genetic investigations of idiopathic epilepsy in the Bernese Mountain Dog. *J Small Anim Pract* 1999;40:319-325.
111. Kearsley-Fleet L, O'Neill DG, Volk HA, Church DB, Brodbelt DC. Prevalence and risk factors for canine epilepsy of unknown origin in the UK. *Vet Rec* 2013;172.
112. Keller D, Erö C, Markram H. Cell Densities in the Mouse Brain: A Systematic Review. *Front Neuroanat* 2018;12:83.
113. Kim DW, Lee SK, Nam H, Chu K, Chung CK, Lee S-Y, Choe G, Kim HK. Epilepsy with dual pathology: surgical treatment of cortical dysplasia accompanied by hippocampal sclerosis. *Epilepsia* 2010;51(8):1429-1435.
114. Kitamura T, Nakanishi K, Watanabe S, Endo Y, Fujita S. GFA-protein gene expression on the astroglia in cow and rat brains. *Brain Res* 1987;423:189–195.
115. Kitz S, Thalhammer JG, Glantschnigg U, Wrzosek M, Klang A, Halasz P, Shouse MN, Pakozdy A. Feline temporal lobe epilepsy: review of the experimental literature. *J Vet Intern Med* 2017;31:633–640.
116. Kjelstrup KG, Tuvnes FA, Steffenach HA, Murison R, Moser EI, Moser MB. Reduced fear expression after lesions of the ventral hippocampus. *Proc Natl Acad Sci USA* 2002;99:10825–10830.
117. Klang A, Leschnik M, Schmidt P, Pakozdy A. Bilateral hippocampal malformation and concurrent granulomatous meningoencephalitis in a dog with refractory epilepsy. *J Comp Path* 2014;150:424-428.
118. Kline KL. Epilepsy in cats. *Clin Tech Small Anim Pract* 1998;13:152-158.
119. Ko DY, Sahai-Srivastava S. Temporal Lobe Epilepsy Clinical Presentation. *Medscape* 2017. Bendadis SR editor.
120. Kowalska DM. Effects of hippocampal lesions on spatial delayed responses in dog. *Hippocampus* 1995;5:363-370.
121. Kowalska DM. Effects of the anterior temporal lobe lesions, separate or combined with hippocampal damage, on spatial delayed responses guided by auditory stimulus. *Acta Neurobiol Exp (Wars)* 1999;59:303–313.



122. Kowalska DM. Cognitive functions of the temporal lobe in the dog: A review. *Prog Neuropsychopharmacol Biol Psychiatry* 2000;24(5):855-880.
123. Kowalska DM, Kosmal A. The method of surgical hippocampal lesions in dogs. *Acta Neurobiol Exp* 1992;52:119.
124. Kurt MA, Kafa MI, Dierssen M, Davies DC. Deficits of neuronal density in CA1 and synaptic density in the dentate gyrus, CA3 and CA1, in a mouse model of Down syndrome. *Brain Res* 2004;1022(1-2):101-109.
125. Kwan P, Arzimanoglou A, Berg AT, Brodie MJ, Allen Hauser W, Mathern G, Moshé SL, Perucca E, Wiebe S, French J. Definition of drug resistant epilepsy: consensus proposal by the ad hoc Task Force of the ILAE Commission on Therapeutic Strategies. *Epilepsia* 2010;51:1069–1077.
126. Kwan P, Brodie MJ. Early identification of refractory epilepsy. *New Engl J Med* 2000;342:314-319.
127. Lee TM, Yip JT, Jones-Gotman M. Memory deficits after resection from left or right temporal lobe in humans: a meta-analytic review. *Epilepsia* 2002;43:283-291.
128. Licht BG, Lin S, Luo Y, Hyson LL, Licht MH, Harper KM, Sullivan SA, Fernandez SA, Johnston EV. Clinical characteristics of inheritance of familial focal seizures in Standard Poodles. *J Am Vet Med Assoc* 2007;231:1520-1528.
129. Ling EA, Leblond CP. Investigation of glial cells in semithin sections. II. Variation with age in the numbers of the various glial cell types in rat cortex and corpus callosum. *J Comp Neurol* 1973;149:73–81.
130. Loiselle M, Rouleau I, Nguyen D, Dubeau F, Macoir J, Whatmough C, Lepore F, Joubert S. Comprehension of concrete and abstract words in patients with selective anterior temporal lobe resection and in patients with selective amygdalo-hippocampectomy. *Neuropsychologia* 2012;50:630–639.
131. Long S, Frey S, Freestone DR, LeChevoir M, Stypulkowski P, Giftakis J, Cook M. Placement of Deep Brain Electrodes in the Dog Using the Brainsight Frameless Stereotactic System: A Pilot Feasibility Study. *J Vet Intern Med* 2014;28:189–197.

132. Lorente de N6. Studies on the structure of the cerebral cortex. II. Continuation of the study of the ammonic system. *Journal für Psychologie und Neurologie* 1934;46:113–177.
133. Löscher W, Potschka H. Role of multidrug transporters in pharmacoresistance to antiepileptic drugs. *J Pharm Exp Ther* 2002;301:7-14.
134. Löscher W, Potschka H, Rieck S, Tipold A, Rundfeldt C. Anticonvulsant efficacy of the low-affinity partial benzodiazepine receptor agonist ELB 138 in a dog seizure model and in epileptic dogs with spontaneously recurrent seizures. *Epilepsia* 2004;45:1228–1239.
135. Lüders HO, Turnbull J, Kaffashi F. Are the dichotomies generalized versus focal epilepsies and idiopathic versus symptomatic epilepsies still valid in modern epileptology? *Epilepsia* 2009;50:1336-1343.
136. Lutz MT, Clusmann H, Elger CE, Schramm J, Helmstaedter C. Neuropsychological outcome after selective amygdalohippocampectomy with transsylvian versus transcortical approach: A randomized prospective clinical trial of surgery for temporal lobe epilepsy. *Epilepsia* 2004;45(7):809-816.
137. Lynch G, Cotman CW. The Hippocampus as a Model for Studying Anatomical Plasticity in the Adult Brain. *Behav Brain Res* 1993;55(1):1-16.
138. Machado GF, Laranjeira MG, Schweigert A, Dias de Melo G. Porencephaly and cortical dysplasia as cause of seizures in a dog. *BMC Vet Res* 2012;8:246.
139. Manford M, Fish DR, Shorvon SD. An analysis of clinical seizure patterns and their localizing value in frontal and temporal lobe epilepsies. *Brain* 1996;119:17-40.
140. Marioni-Henry K, Monteiro R, Behr S. Complex partial orofacial seizures in English cats. *Vet Rec* 2012;170:471.
141. Martlé VA, Caemaert J, Tshamala M, Van Soens I, Bhatti SFM, Gielen I, Piron K, Chiers K, Tiemessen I, Van Ham LM. Surgical treatment of a canine intranasal meningoencephalocele. *Vet Surg* 2009;38(4):515-519.
142. Martlé VA, Van Ham L, Raedt R, Vonck K, Boon P, Bhatti S. Non-pharmacological treatment options for refractory epilepsy: an overview of human treatment modalities and their potential utility in dogs. *Vet J* 2014;199:332–339.

143. Mathern GW, Babb TL, Armstrong DL. Hippocampal sclerosis. In: Engel J Jr, Pedley TA, editors. *Epilepsy: a comprehensive textbook*. Philadelphia, 1997;133-155.
144. Matiasek K, Pumarola i Batlle M, Rosati M, Fernández-Flores F, Fischer A, Wagner E, Berendt M, Bhatti SFM, De Risio L, Farquhar RG, Long S, Muñana K, Patterson EE, Pakozdy A, Penderis J, Platt S, Podell M, Potschka H, Rusbridge C, Stein VM, Tipold A, Volk HA. International veterinary epilepsy task force recommendations for systematic sampling and processing of brains from epileptic dogs and cats. *BMC Vet Res* 2015;11:216.
145. Mayhew TM, Gundersen HJG. 'If you assume, you can make an ass out of u and me': A decade of the disector for stereological counting of particles in 3D space. *J Anat* 1996;188:1–15.
146. McCormick C, Quraan M, Cohn M, Valiante TA, McAndrews MP. Default mode network connectivity indicates episodic memory capacity in mesial temporal lobe epilepsy. *Epilepsia* 2013;54:809-818.
147. McIntosh AM, Kalnins RM, Mitchell LA, Fabinyi GC, Briellmann RS, Berkovic SF. Temporal lobectomy: long-term seizure outcome, late recurrence and risks for seizure recurrence. *Brain* 2004;127(Pt 9):2018-2030.
148. Meldrum BS, Brierley JB. Neuronal loss and gliosis in the hippocampus following repetitive epileptic seizures induced in adolescent baboons by allylglycine. *Brain Research* 1972;48:361-365.
149. Mellema LM, Koblik PD, Kortz GD, LeCouteur RA, Chechowicz MA, Dickinson PJ. Reversible magnetic resonance imaging abnormalities in dogs following seizures. *Vet Radiol Ultrasound* 1999;40(6):588-595.
150. Mestrinho L, Gawor J, Serrano A, Niza M. Superficial temporal myofascial flap application in temporomandibular joint arthroplasty in a cat. *J Fel Med Surg* 2015;1:(2).
151. Miller LA, McLachlan RS, Bouwer MS, Hudson LP, Munoz DG. Amygdalar sclerosis: preoperative indicators and outcome after temporal lobectomy. *J Neurol Neurosurg Psychiatry* 1994;57:1099–1105.

152. Moser E, Moser MB, Andersen P. Spatial learning impairment parallels the magnitude of dorsal hippocampal lesions, but is hardly present following ventral lesions. *J Neurosci* 1993;13:3916–3925.
153. Mueller SG, Laxer KD, Cashdollar N, Lopez RC, Weiner MW. Spectroscopic evidence of hippocampal abnormalities in neocortical epilepsy. *Eur J Neurol* 2006;13:256-260.
154. Muzumdar D, Patil M, Goel A, Ravat S, Sawant N, Shah U. Mesial temporal lobe epilepsy - An overview of surgical techniques. *Int J Surg* 2016;36(Pt B):411-419.
155. Najm IM, Sarnatt HB, Blümcke I. Review: The international consensus classification of Focal Cortical Dysplasia-a critical update 2018. *Neuropathol Appl Neurobiol* 2018;44(1):18-31.
156. Nascimento F, Gatto L, Silvado C, Mäder-Joaquim M, Moro M, Araujo J. Anterior temporal lobectomy versus selective amygdalohippocampectomy in patients with mesial temporal lobe epilepsy. *Arq Neuropsiquiatr* 2016;74:35–43.
157. Nayel MH, Awad IA, Luders H. Extent of mesiobasal resections determines outcome after temporal lobectomy for intractable complex partial seizures. *Neurosurgery* 1991;29:55-61.
158. Neddens J, Buonanno A. Selective populations of hippocampal interneurons express ErbB4 and their number and distribution is altered in ErbB4 knockout mice. *Hippocampus* 2010;20(6):724-744.
159. Nickel E. *Lehrbuch der Anatomie der Hautiere Band IV: Nervensystem, Sinnesorgane, Endokrine Drüsen*. Parey editor, Berlin, Hamburg;2004.
160. Niemeyer P. The transventricular amygdalo-hippocampectomy in temporal lobe epilepsy. In: Baldwin M, Bailey P, editors. *Temporal Lobe Epilepsy: A Colloquium Sponsored by the National Institute of Neurological Diseases and Blindness, National Institutes of Health, Bethesda, Maryland, in Cooperation with the International League Against Epilepsy*; Springfield, 1958;461-482.
161. Niemeyer P, Bello H. Amygdalo-hippocampectomy in temporal lobe epilepsy. *Microsurgical technique*. *Excerpta Medica* 1973;293:20 (abst. n°48).

162. Nieuwenhuys R, ten Donkelaar HJ, Nicholson C. The central nervous system of vertebrates, Vol. 3. Springer, Heidelberg, Berlin;1998.
163. Nilges RG. The arteries of the mammalian cornu ammonis. *JCN* 1944;80(2):177-190.
164. Oberbauer AM, Belanger JM, Grossman DI, Regan KR, Famula TR. Genome-wide linkage scan for loci associated with epilepsy in Belgian shepherd dogs. *BMC Genet.* 2010;11:35.
165. Oddo S, Solis P, Consalvo D, Seoane E, Giagante B, D'Alessio L, Kochen S. Postoperative neuropsychological outcome in patients with mesial temporal lobe epilepsy in Argentina. *Epilepsy Res Treat* 2012;2012:370351.
166. Ogata K, Kosaka T. Structural and quantitative analysis of astrocytes in the mouse hippocampus. *Neuroscience* 2002;113(1):221-233.
167. Oliver, JEJ. Surgical relief of epileptiform seizures in the dog. *Vet Med Anim Clin* 1965;60:367-8.
168. Olivier A, Cukiert A, Palomino-Torres X, Andermann F. Transcortical selective amygdalo-hippocampectomy: microsurgical technique and results. *Proc Am Epilepsy Assoc.* Seattle;1992.
169. Olivier A, Bolding WW, Tanriverdi T. Techniques in epilepsy surgery, the MNI approach. Cambridge, UK;2012.
170. Olivier A, Warren WB, Taner T. Surgery of temporal lobe epilepsy. Cortico-amygdalohippocampectomy. In: Olivier A, Bolding WW, Tanriverdi T, editors. Techniques in epilepsy surgery, The MNI approach. Cambridge, UK, 2012a;97-114.
171. Olivier A, Warren WB, Taner T: Surgery of temporal lobe epilepsy. Transcortical selective amygdalohippocampectomy. In: Olivier A, Bolding WW, Tanriverdi T, editors. Techniques in epilepsy surgery, The MNI approach. Cambridge, UK, 2012b;115-131.
172. Paglioli E, Palmini A, Portuguese M, Paglioli E, Azambuja E, Costa da Costa J, da Silva Filho HF, Martinez JV, Hoeffel JR. Seizure and memory outcome following temporal lobe surgery: selective compared with nonselective approaches for hippocampal sclerosis. *J Neurosurg* 2004;104:70-78.

173. Pakozdy A, Angerer C, Klang A, König EH, Probst A. Gyration of the Feline Brain: Localization, Terminology and Variability. *Anat Histol Embryol* 2015;44:422–427.
174. Pakozdy A, Glantschnigg U, Leschnik M, Hechinger H, Moloney T, Lang B, Halasz P, Vincent A. EEG-confirmed epileptic activity in a cat with VGKC-complex/LGI1 antibody-associated limbic encephalitis. *Epileptic Disord* 2014; 16(1):116-120.
175. Pakozdy A, Gruber A, Kneissl S, Leschnik M, Halasz P, Thalhammer JG. Complex partial cluster seizures in cats with orofacial involvement. *J Feline Med Surg* 2011;13:687-693.
176. Pakozdy A, Halasz P, Klang A, Bauer J, Leschnik M, Tichy A, Thalhammer JG, Lang B, Vincent A. Suspected limbic encephalitis and seizure in cats associated with voltage-gated potassium channel (VGKC) complex antibody. *J Vet Intern Med* 2013a;27(1):212-214.
177. Pakozdy A, Klang A, Kneissl S, Halasz P. Naturally Occurring Temporal Lobe Epilepsy in Cats. In: Pitkänen A, Buckmaster PS, Galanopoulou AS, Moshé SL, editors. *Models of Seizures and Epilepsy*, 2<sup>nd</sup> ed. London, UK, 2017;399–4.
178. Pakozdy A, Sarchahi AA, Leschnik M, Tichy AG, Thalhammer, JG. Clinical comparison of primary versus secondary epilepsy in 125 cats. *J Fel Med Surg* 2010;12:910–916.
179. Pakozdy A, Thaller D, Gumpenberger M, Leschnik M, Galler A, Shiby S, Klang A. Concurrent bilateral temporal lobe pathology and unilateral oligodendroglioma in a dog with status epilepticus. *J Small Anim Pract* 2013b;54(2):112-113.
180. Parent JM, Quesnel AD. Seizures in cats. *Vet Clin North Am Small Anim Pract* 1996;26:811-825.
181. Parker AJ, Cunningham JG. Successful surgical removal of an epileptogenic focus in a dog. *J Small Anim Pract* 1971;12:513–21.
182. Park TS, Bourgeois BF, Silbergeld DL, Dodson WE. Subtemporal transparahippocampal amygdalohippocampectomy for surgical treatment of mesial temporal lobe epilepsy. *J Neurosurg* 1996;86(6):1172-1176.

183. Parmar H, Lim SH, Tan NC, Lim CC. Acute symptomatic seizures and hippocampus damage: DWI and MRS findings. *Neurology* 2006;66:1732-1735.
184. Parrent AG, Blume WT. Stereotactic amygdalohippocampectomy for the treatment of medial temporal lobe epilepsy. *Epilepsia* 1999;40(10):1408-1416.
185. Patterson EE, Mickelson JR, Da Y, Roberts MC, McVey AS, O'Brien DP, Johnson GS, Armstrong PJ. Clinical characteristics and inheritance of idiopathic epilepsy in Vizslas. *J Vet Intern Med* 2003;17:319-325.
186. Patterson EE, Munana KR, Kirk CA, Lowry S, Amstrong P. Results of a ketogenic food trial for dogs with idiopathic epilepsy. *J Vet Intern Med* 2005;19:421.
187. Picot MC, Baldy-Moulinier M, Daures JP, Dujols P, Crespel A. The prevalence of epilepsy and pharmaco-resistant epilepsy in adults: a population-based study in a Western European country. *Epilepsia* 2008;49:1230–1238.
188. Podell M, Fenner WR. Bromide therapy in refractory canine idiopathic epilepsy. *J Vet Int Med* 1993;7:318–327.
189. Poncelet L, Poma R. Electrophysiology. In: Platt S, Olby N, editors. *BSAVA Manual of Canine and Feline Neurology*, 4<sup>th</sup> ed. Gloucester, UK, 2013;72-76.
190. Ramon Y Cajal SR. Estructura del asta de Ammon. *Annals Soc Esp Hist Nat Madrid* 1893;22:53-114.
191. Ramon Y Cajal SR. *Histologie Du Système Nerveux De L'homme Et Des Vertébrés*. Paris: Maloine A, 1911.
192. Rasmussen T, Branch C. Temporal lobe epilepsy. Indications for and results of surgical therapy. *Postgraduate Med J* 1962;31:9-14.
193. Reale RA, Imig TJ. Tonotopic organization in auditory cortex of the cat. *J Comp Neurol* 1980;192(2):265–291.
194. Regesta G, Tanganelli P. Clinical aspects and biological bases of drug-resistant epilepsies. *Epil Res* 1999;34:109-122.
195. Rieck S, Rundfeldt C, Tipold A. Anticonvulsant activity and tolerance of ELB138 in dogs with epilepsy: a clinical pilot study. *Vet J* 2006;172:86–95.

196. Rickmann M, Wolff JR. S100 immunoreactivity in a subpopulation of oligodendrocytes and Ranvier's nodes of adult rat brain. *Neurosci Lett* 1995;186(1):13-16.
197. Rundfeldt C, Löscher W. The pharmacology of imepitoin: the first partial benzodiazepine receptor agonist developed for the treatment of epilepsy. *CNS Drugs* 2014;28(1):29–43.
198. Rusbridge C. Diagnosis and control of epilepsy in the cat. In *Practice* 2005;27:208-214.
199. Salanova V, Markand O, Worth R. Temporal lobe epilepsy surgery: outcome, complications, and late mortality rate in 215 patients. *Epilepsia* 2002;43:170-174.
200. Santana MT, Jackowski AP, da Silva HH, Caboclo LO, Centeno RS, Bressan RA, Carrete H Jr, Yacubian EM. Auras and clinical features in temporal lobe epilepsy: a new approach on the basis of voxel-based morphometry. *Epilepsy Res* 2010;89(2-3):327-338.
201. Sato M. Hippocampal Seizure and Secondary Epileptogenesis in the “Kindled” Cat Preparations. *Psychiatry Clin Neurosci* 1975;29(3):239-250.
202. Sato M, Racine RJ, McIntyre DC. Kindling basic mechanism and clinical validity. *Electroenceph Clin Neurophysiol* 1990;76:459-472.
203. Savchenko VL, McKanna JA, Nikonenko IR, Skibo GG. Microglia and astrocytes in the adult rat brain: comparative immunocytochemical analysis demonstrates the efficacy of lipocortin 1 immunoreactivity. *Neuroscience* 2000;96:195–203.
204. Schmidt MJ, Kampschulte M, Enderlein S, Gorgas D, Lang J, Ludewig E, Fischer A, Meyer-Lindenberg A, Schaubmar A, Failing K, Ondreka N. The relationship between brachycephalic head features in modern Persian cats and dysmorphologies of the skull and internal hydrocephalus. *J Vet Intern Med* 2017;31: 1487–1501.
205. Schmied O, Scharf G, Hilbe M, Michal U, Tomsa K, Steffen K. Magnetic resonance imaging of feline hippocampal necrosis. *Vet Rad Ultrasound* 2008;49(4):343-349.



206. Schober W, Brauer K. Makromorphologie des Zentralnervensystems. In: Helmcke JG, Starck D, Wermuth H, editors. Handbuch der Zoologie, Vol. 8. Berlin, 1974;1–296.
207. Schramm J. Temporal lobe epilepsy surgery and the quest for optimal extent of resection: a review. *Epilepsia* 2008;49:1296-1307.
208. Schriefl S, Steinberg TA, Matiasek K, Ossig A, Fenske N, Fischer A. Etiologic classification of seizures, signalment, clinical signs, and outcome in cats with seizure disorders: 91 cases (2000-2004). *J Am Vet Med Assoc* 2008;233:1591–1597.
209. Schultz C, Engelhardt M. Anatomy of the hippocampal formation. *Front Neurol Neurosci* 2014;34:6-17.
210. Schwartz-Porsche D, Löscher W, Frey HH. Therapeutic efficacy of phenobarbital and primidone in canine epilepsy: a comparison. *J Vet Pharmacol Ther* 1985;8(2):113-119.
211. Schwerdtfeger WK. Structure and fiber connections of the hippocampus. A comparative study. *Adv Anat Embryol Cell Biol* 1984;83:1-74.
212. Semah F, Picot MC, Adam C, Broglin D, Arzimanoglou A, Bazin B, Cavalcanti D, Baulac M. Is the underlying cause of epilepsy a major prognostic factor for recurrence? *Neurology* 1998;51:1256-1262.
213. Seppala EH, Jokinen TS, Fukata M, Fukata Y, Webster MT, Karlsson EK, Kilpinen SK, Steffen F, Dietschi E, Leeb T, Eklund R, Zhao X, Rilstone JJ, Lindblad-Toh K, Minassian BA, Lohi H. LGI2 truncation causes a remitting focal epilepsy in dogs. *PLoS Genet* 2011;7(7):e1002194.
214. Seppala EH, Koskinen LLE, Gulløv CH, Jokinen P, Karlskov-Mortensen P, Bergamasco L, Baranowska Körberg I, Cizinauskas S, Oberbauer AM, Berendt M, Fredholm M, Lohi H. Identification of a novel idiopathic epilepsy locus in Belgian Shepherd dogs. *PLoS One* 2012;7(3):e33549.
215. Shefer VF. Hippocampal pathology as a possible factor in the pathogenesis of senile dementias. *Neurosci Behav Physiol* 1977;8:236-239.
216. Sherman SM, Guillery RW. Distinct functions for direct and transthalamic corticocortical connections. *J Neurophysiol* 2011;106(3):1068-1077.

217. Shihab N, Bowen J, Volk HA. Behavioural changes in dogs associated with the development of idiopathic epilepsy. *Epilepsy and Behaviour* 2011;21:160-167.
218. Shihab N, Summers BA, Benigni L, McEvoy AW, Volk HA. Novel approach to temporal lobectomy for removal of a cavernous hemangioma in a dog. *Vet Surg* 2014;43:877-881.
219. Shimada M, Akagi N, Goto H, Watanabe H, Nakanishi M, Hirose Y, Watanabe M. Microvessel and astroglial cell densities in the mouse hippocampus. *J Anat* 1992;180(Pt 1):89-95.
220. Shores A, Brisson BA. *Current techniques in canine and feline neurosurgery*. Hoboken, New Jersey;2017.
221. Shorvon S. The concept of symptomatic epilepsy and the complexities of assigning cause in epilepsy. *Epilepsy Behav* 2014;32C:1-8.
222. Shouse MN, Scordato JC, Farber PR. Ontogeny of feline temporal lobe epilepsy in amygdala-kindled kittens: an update. *Brain Res* 2004;1027:126–143.
223. Simons JS, Spiers HJ. Prefrontal and medial temporal lobe interactions in long-term memory. *Nat Rev Neurosci* 2003;4:637-648.
224. Sloviter RS. Hippocampal epileptogenesis in animal models of mesial temporal lobe epilepsy with hippocampal sclerosis: the importance of the “latent period” and other concepts. *Epilepsia* 2008;49:85– 92.
225. Sloviter RS, Kudrimoti HS, Laxer HD, Barbaro NM, Chan S, Hirsch LJ, Goodman RR, Pedley PA. “Tectonic” hippocampal malformations in patients with temporal lobe epilepsy. *Epil Res* 2004;59:123-153.
226. Small SA, Nava AS, Perera GM, De La Paz R, Mayeux R, Stern Y. Circuit mechanisms underlying memory encoding and retrieval in the long axis of the hippocampal formation. *Nat Neurosci* 2001;4:442–449.
227. Snider RS, Niemer WT. *Stereotaxic atlas of the cat brain*. Chicago, USA: The University of Chicago Press;1961.

228. So N, Gloor P, Quesney LF, Jones-Gotman M, Olivier A, Andermann F. Depth electrode investigations in patients with bitemporal epileptiform abnormalities. *Ann Neurol* 1989;25:423-431.
229. Spencer D, Burchiel K. Selective amygdalohippocampectomy. *Epilepsy Res Treat* 2012;2012:382095.
230. Spencer DD, Spencer SS, Mattson RH, Williamson PD, Novelly RA. Access to the posterior medial temporal lobe structures in the surgical treatment of temporal lobe epilepsy. *Neurosurgery* 1984;15:667-671.
231. Stanciu G, Packer RMA, Pakozdy A, Solcan G, Volk HA. Clinical reasoning in feline epilepsy: Which combination of clinical information is useful? *Vet J* 2017;225:9-12.
232. Stassen W, van Steenbeek F, van Rhijn N, Tenwolde R, Leegwater P. Identification of a novel epilepsy gene in Boerboel dogs. *J Vet Intern Med* 2013;27:30.
233. Stephan H. *Handbuch der mikroskopischen Anatomie des Menschen*. Allocortex. Oksche A, Vollrath L, Bargmann W editors, 1975.
234. Swanson LW, Cowan WM. An autoradiographic study of the organization of the efferent connections of the hippocampal formation in the rat. *J Comp Neurol* 1977;172(1):49-84.
235. Tanaka T, Tanaka S, Yonemasu Y. Experimental limbic seizure status epilepticus and focus resection in cats. *No To Shinkei* 1989;41:1239–1244.
236. Tanriverdi T, Ajlan A, Poulin N, Olivier A. Morbidity in epilepsy surgery: an experience based on 2449 epilepsy surgery procedures from a single institution. *J Neurosurg* 2009;110:1111-1123.
237. Tanriverdi T, Dudley RW, Hasan A, Al Jishi A, Al Hinai Q, Poulin N, Colnat-Coulbois, Olivier A. Memory outcome after temporal lobe epilepsy surgery: corticoamygdalohippocampectomy versus selective amygdalohippocampectomy. *J Neurosurg* 2010;113:1164-1175.
238. Tanriverdi T, Olivier A. Cognitive changes after unilateral cortico-amigdalohippocampectomy unilateral selective amygdalohippocampectomy mesial temporal lobe epilepsy. *Turk Neurosurg* 2007;17:91-99.

239. Tartygin NA. The Influence of ablation of the dorsal section of the hippocampus on alimentary conditioned reflexes in cats. *Soviet Psychology* 1996;5:38–42.
240. Taupin P, Gage FH. Adult neurogenesis and neural stem cells of the central nervous system in mammals. *J Neurosci Res* 2002;69(6):745-749.
241. Teitelbaum H. A comparison of effects of orbitofrontal and hippocampal lesions upon discrimination learning and reversal in the cat. *Experimental Neurology* 1964;9:452–462.
242. Thomas WB, Dewey CW. Seizures and narcolepsy. In: Dewey CW, da Costa R, editors. *Practical guide to canine and feline neurology*. 3<sup>rd</sup> edn. Ames, Iowa, 2016;9:249-267.
243. Thompson CL, Pathak SD, Jeromin A, Ng LL, MacPherson CR, Mortrud MT, Cusick A, Riley ZL, Sunkin SM, Bernard A, Puchalski RB, Gage FH, Jones AR, Bajic VB, Hawrylycz MJ, Lein ES. Genomic anatomy of the hippocampus. *Neuron* 2008;60(6):1010-1021.
244. Tipold A, Keefe TJ, Löscher W, Rundfeldt C, de Vries F. Clinical efficacy and safety of imepitoin in comparison with phenobarbital for the control of idiopathic epilepsy in dogs. *J Vet Pharmacol Ther* 2015;38:160–168.
245. Trepanier LA, Van Schoick A, Schwark WS, Carillo J. Therapeutic serum drug concentrations in epileptic dogs treated with potassium bromide alone or in combination with other anticonvulsants: 122 cases (1992-1996). *J Am Vet Med Assoc* 1998;213(10):1449-1453.
246. Vanhaesebrouck A, Posch B, Baker S, Plessas I, Palmer A, Costantino-Casas F. Temporal lobe epilepsy in a cat with pyriform lobe oligodendroglioma and hippocampal necrosis. *J Fel Med Surg* 2012;14(12):932-937.
247. van Praag H, Schinder AF, Christie BR, Toni N, Palmer TD, Gage FH. Functional neurogenesis in the adult hippocampus. *Nature* 2002;415(6875):1030-1034.
248. Vincent A, Buckley C, Schott JM, Baker I, Dewar B, Detert N, Clover L, Parkinson A, Bien CG, Omer S, Lang B, Rossor MN, Palace J. Potassium channel

antibody-associated encephalopathy: a potentially immunotherapy-responsive form of limbic encephalitis. *Brain* 2004;127(Pt 3):701-712.

249. Vincent A, Crino PB. Systemic and neurologic autoimmune disorders associated with seizures or epilepsy. *Epilepsia* 2011;52(Suppl 3):12-17.
250. Vogt HA, Rodan I, Brown M, Brown S, Buffington CA, Larue Forman MJ, Neilson J, Sparkes A. AAFP-AAHA: feline life stage guidelines. *J Feline Med Surg* 2010;12(1):43-54.
251. Vojtěch Z, Krámská L, Malíkova H, Seltenreichová K, Procházka T, Kalina M, Liščák R. Cognitive outcome after stereotactic amygdalohippocampectomy. *Seizure* 2012;21:327-333.
252. Volk H. Pathophysiology of pharmaco-resistant epilepsy. In: De Risio L, Platt S, editors. *Canine and feline epilepsy, diagnosis and management*. Wallingford, 2014;2:28-38.
253. von Rhein B, Nelles M, Urbach H, Lehe M, Schramm J, Helmstaedter C. Neuropsychological outcome after selective amygdalohippocampectomy: subtemporal versus transsylvian approach. *J Neurol Neurosurg Psychiatry* 2012;83:887-893.
254. Wagner E, Rosati M, Molin J, Foitzik U, Wahle AM, Fischer A, Matiask LA, Reese S, Flegel T, Matiasek K. Hippocampal sclerosis in feline epilepsy. *Brain Pathol* 2014;24(6):607-19.
255. Wahle A, Brühshwein A, Matiasek K, Putschbach K, Wagner E, Müller RS, Fischer A. Clinical Characterization of Epilepsy of Unknown Cause in Cats. *J Vet Intern Med* 2014;28:182-188.
256. Walz W, Lang MK. Immunocytochemical evidence for a distinct GFAP-negative subpopulation of astrocytes in the adult rat hippocampus. *Neurosci Lett* 1998;257(3):127-130.
257. Wendling A, Hirsch E, Wisniewski I, Davanture C, Ofer I, Zentner J, Bilic S, Scholly J, Staack AM, Valenti M, Schulze-Bonhage A, Kehrli P, Steinhoff BJ. Selective amygdalohippocampectomy versus standard temporal lobectomy in patients

- with mesial temporal lobe epilepsy and unilateral hippocampal sclerosis. *Epilepsy Res* 2013;104:94–104.
258. Wessmann A, Volk HA, Parkin T, Ortega M, Anderson TJ. Living with canine idiopathic epilepsy: A questionnaire-based evaluation of quality of life. *J Vet Int Med* 2012;26:1.
259. West MJ. Regionally Specific Loss of Neurons in the Aging Human Hippocampus. *Neurobiol Aging* 1993;14(4):287-293.
260. West MJ. Stereological methods for estimating the total number of neurons and synapses: Issues of precision and bias. *Trends Neurosci* 1999;22:51–61.
261. Wieser HG, Ortega M, Friedman A, Yonekawa Y. Long-term seizure outcomes following amygdalohippocampectomy. *J Neurosurg* 2003;98:751-763.
262. Wieser HG. Mesial temporal lobe epilepsy with hippocampal sclerosis. *Epilepsia* 2004;45:695-714.
263. Wininger F. Neuronavigation in Small Animals: Development, Techniques, and Applications. *Vet Clin North Am Small Anim Pract* 2014;44(6):1235-1248.
264. Wolff CA, Holmes SP, Young BD, Chen AV, Kent M, Platt SR, Savage MY, Schatzberg SJ, Fosgate GT, Levine JM. Magnetic resonance imaging for the differentiation of neoplastic, inflammatory, and cerebrovascular brain disease in dogs. *J Vet Int Med* 2012;52(2):589-597.
265. Wouters EGH, Beukers M, Theyse LFH. Surgical treatment of a cerebral brain abscess in a cat. *Vet Comp Orthop Traumatol* 2010;24:72–75.
266. Wu Y, Zhang AQ, Yew DT. Age related changes of various markers of astrocytes in senescence-accelerated mice hippocampus. *Neurochem Int* 2005;46:565–574.
267. Yam D, Nicolle D, Steven DA, Lee D, Hess T, Burneo JG. Visual field deficits following anterior temporal lobectomy: long-term follow-up and prognostic implications. *Epilepsia* 2010;51:1018-1023.

268. Yasargil MG, Teddy PJ, Roth P. Selective amygdalo-hippocampectomy: operative anatomy and surgical technique. *Adv Tech Stand Neurosurg* 1985;12:93-123.
269. Yasargil MG, Türe U, Yasargil DCH. Impact of temporal lobe surgery. *J Neurosurg* 2004;101(5):725-738.
270. Yasargil MG, Wieser HG, Valvanis A, von Ammon K, Roth P. Surgery and results of selective amygdalo-hippocampectomy in one hundred patients with nonlesional limbic epilepsy. *Neurosurg Clin N Am* 1993;4:243-261.
271. Yu Y, Hasegawa D, Hamamoto Y, Mizoguchi S, Kuwabara T, Fujiwara-Igarashi A, Tsuboi M, Chambers JK, Fujita M, Uchida K. Neuropathologic features of the hippocampus and amygdala in cats with familial spontaneous epilepsy. *Am J Vet Res* 2018;79:324–332.
272. Zilli J, Kressin M, Schänzer A, Kampschulte M, Schmidt MJ. Partial cortico-hippocampectomy in cats, as therapy for refractory temporal epilepsy: A descriptive cadaveric study. *Plos One* 2021;16(1):e0244892.

## 13 Appendix

**Table 5. Mean values, standard deviation, and minimum and maximum values for NDs.**

	<b>Hippocampal part</b>	<b>Numerical density (cells/mm<sup>2</sup>)</b>	<b>Maximum (cells/mm<sup>2</sup>)</b>	<b>Minimum (cells/mm<sup>2</sup>)</b>
	Tail	412.063 ± 84.315	616.395	283.32
<b>CA1</b>	Body	424.45 ± 84.45	552.595	231.575
	Head	443.934 ± 101.327	601.9	239.63
	Tail	535.915 ± 149.32	800.675	281.2
<b>CA2</b>	Body	398.263 ± 110.218	564.36	210.775
	Head	468.855 ± 162.733	740.335	216.19
	Tail	506.645 ± 141.282	754.95	313.21
<b>CA2-3</b>	Body	351.408 ± 84.922	472.52	191.145
	Head	349.127 ± 77.754	482.45	249.85
	Tail	446.513 ± 180.898	806.41	209.89
<b>CA3</b>	Body	307.249 ± 81.906	470.535	189.89
	Head	315.499 ± 97.041	480.955	142.08
	Tail	48.938 ± 18.178	76.74	7.225
<b>CA4</b>	Body	52.377 ± 18.625	84.88	14.12
	Head	74.435 ± 29.667	144.265	22.405
	Tail	4607.87 ± 975.97	6456.09	3053.81
<b>GCL</b>	Body	3851.26 ± 639.91	4978.56	2851.16
	Head	3339.40 ± 523.27	4395.30	2391.16

**Table 6. Mean values, standard deviation, and minimum and maximum values for ADs.**



	<b>Hippocampal part</b>	<b>Numerical density (cells/mm<sup>2</sup>)</b>	<b>Maximum (cells/mm<sup>2</sup>)</b>	<b>Minimum (cells/mm<sup>2</sup>)</b>
	Tail	143.497 ± 44.836	219.183	64.932
<b>CA1</b>	Body	166.691 ± 61.582	283.739	68.189
	Head	211.511 ± 69.282	324.696	98.421
	Tail	181.222 ± 70.51	293.408	88.173
<b>CA2-3</b>	Body	167.334 ± 62.989	279.977	45.295
	Head	160.372 ± 59.044	301.743	90.268
	Tail	232.54 ± 70.708	361.24	117.255
<b>CA3</b>	Body	224.644 ± 59.227	330.153	112.167
	Head	207.268 ± 65.739	399.164	113.612
	Tail	276.645 ± 64.096	368.236	125.291
<b>CA4</b>	Body	258.18 ± 52.31	346.269	176.853
	Head	254.963 ± 58.29	370.259	154.576
	Tail	220.544 ± 114.609	504.189	63.209
<b>GCL</b>	Body	296.108 ± 107.069	488.89	170.81
	Head	318.379 ± 130.745	554.902	95.553

**Table 7. Mean values, standard deviation, and minimum and maximum values for LT.**

	<b>Hippocampal part</b>	<b>Numerical density (µm)</b>	<b>Maximum (µm)</b>	<b>Minimum (µm)</b>
	Tail	332.791 ± 46.388	412.575	254.73
<b>CA1</b>	Body	267.93 ± 33.121	315.81	211.135
	Head	256.658 ± 38.004	344.42	209.585
	Tail	117.123 ± 32.387	202.385	72.97

<b>CA2</b>	Body	159.817 ± 29.938	210.54	113.21
	Head	161.558 ± 42.139	236.595	105.075
	Tail	157.414 ± 20.983	188.015	115.965
<b>CA2-3</b>	Body	177.084 ± 30.2	238.75	139.84
	Head	224.334 ± 48.062	348.77	156.44
	Tail	188.458 ± 34.344	258.795	119.715
<b>CA3</b>	Body	217.284 ± 32.616	266.58	159.13
	Head	257.283 ± 41.512	320.12	183.71
	Tail	98.686 ± 17.879	129.505	68.04
<b>GCL</b>	Body	88.169 ± 12.139	108.725	65.965
	Head	84.978 ± 9.736	96.355	64.155

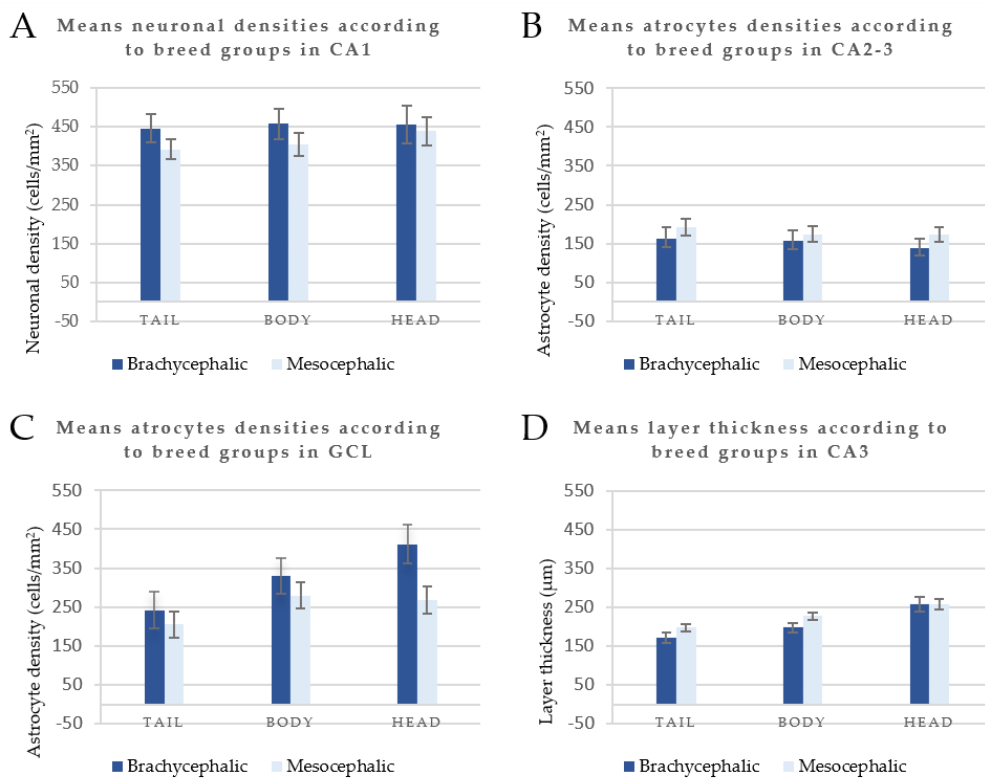


**Figure 21. Estimated ND, AD and LT values (LS-means +/- standard error) from the variance analysis for repeated measurements comparing the hippocampal tail, body and head with the fixed effect of breed. The data are relative to neuronal densities in CA1 (A),**

astrocyte density in CA2-3 (B), and in the GCL (C), and layer thickness in CA3 (D). The data were not statistically significant.

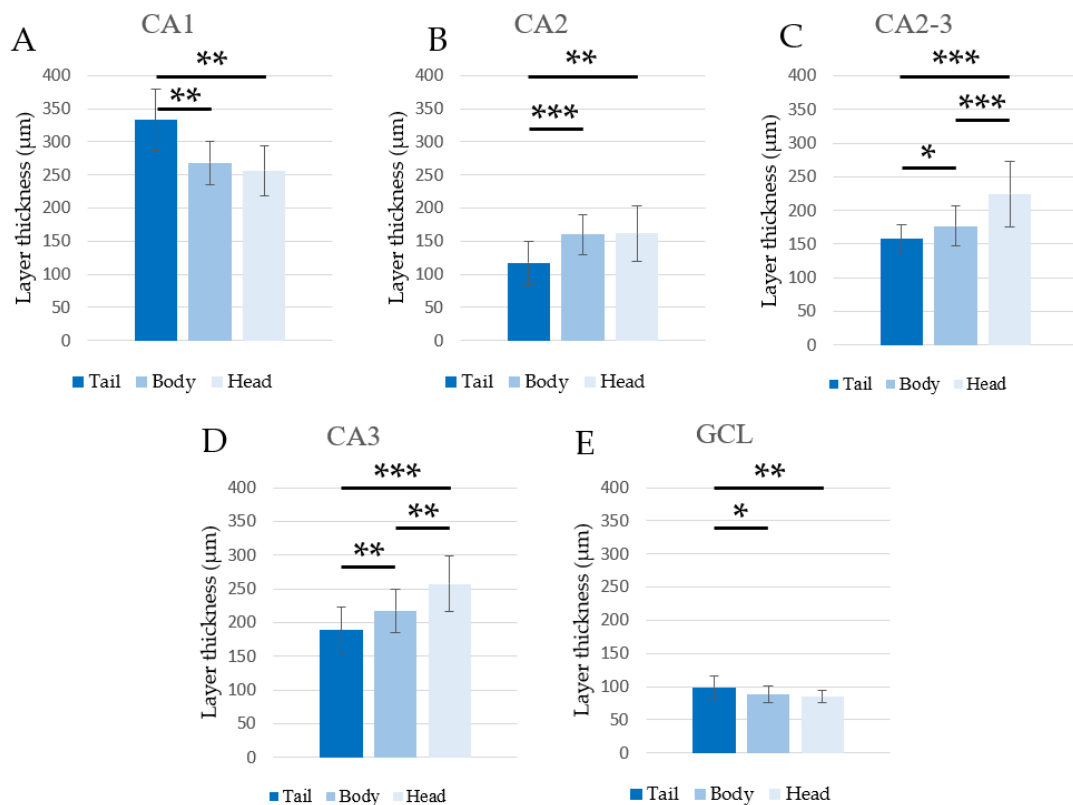


**Figure 22. Estimated AD values (LS-means +/- standard error) from the variance analysis for repeated measurements comparing the hippocampal tail, body and head. The data are relative to all examined areas and show the presence of statistically significant differences. \*\* p < 0.01.**

## **14 List of publications**

1. Zilli J, Kressin M, Schänzer A, Kampschulte M, Schmidt MJ. Partial cortico-hippocampectomy in cats, as therapy for refractory temporal epilepsy: A descriptive cadaveric study. *PLoS One* 2021;16(1):e0244892.
2. Zilli J, Schänzer A, Büttner K, Kressin M, Schmidt MJ. Quantitative and qualitative evaluation of the hippocampal cytoarchitecture in adult cats with regard to the pathological diagnosis of hippocampal sclerosis. *Plos One* 2022;17(5):e0268010.

## **15 Declaration/Erklärung**

„I declare that I have prepared the submitted thesis independently without unauthorized assistance. Any help that I received I have indicated in the thesis. All cited literature has been taken from published sources and any statements based on verbal or communicated information are identified as such. I have adhered to the principles of good scientific practice as laid down in the ‘Statute of the Justus-Liebig University Giessen for the assurance of good scientific practice’ when undertaking the research presented. “

„Ich erkläre: Ich habe die vorliegende Dissertation selbstständig und ohne unerlaubte fremde Hilfe und nur mit den Hilfen angefertigt, die ich in der Dissertation angegeben habe. Alle Textstellen, die wörtlich oder sinngemäß aus veröffentlichten oder nicht veröffentlichten Schriften entnommen sind, und alle Angaben, die auf mündlichen Auskünften beruhen, sind als solche kenntlich gemacht. Bei den von mir durchgeführten und in der Dissertation erwähnten Untersuchungen habe ich die Grundsätze guter wissenschaftlicher Praxis, wie sie in der „Satzung der Justus-Liebig-Universität Gießen zur Sicherung guter wissenschaftlicher Praxis“ niedergelegt sind, eingehalten.“

## 16 Acknowledgements

I would kindly like to thank my supervisors, Prof. Dr. Martin Schmidt and PD Dr. Anne Schänzer, for their immense support and guidance, as well as for the opportunity to undertake a PhD program at the Justus Liebig University. Martin was a great teacher to me; his door was always open and thanks to him I could overcome all the difficulties of this “journey”.

Furthermore, I cannot forget to mention my first clinical supervisor, Dr. Christine Pepler and Prof. Dr. Martin Kramer who made it possible for me to start my carrier here and looked after me above all in my first years at the Small Animal Hospital of the JLU. As I arrived in Giessen, I was not much more than a student, and over the past six years I have grown up and become a scientist and an experienced clinician thanks to them and to my team and team leaders, Daniela and Agnieszka, who were always present and became an important part of my life.

I would also like to thank Prof. Dr. Monika Kressin and her laboratory technician Sigi (Ms Sigrid Kettner), who provided me assistance while performing the histological studies, as well as the laboratory technicians from the Human Neuropathology team of the Justus Liebig University, Ms Kerstin Leib, Ms Annika May and Ms Angela Roth, who helped me with the immunohistochemical stainings. Above all with Sigi, I spent a lot of time and I will keep many good memories of the work together. Moreover, I would like to acknowledge Prof. Dr. Ingmar Blümcke for allowing me to have an insight into the world of human mesial temporal epilepsy histopathology, which was a priceless experience to me.

A special thanks must go to my boyfriend, who always supported me, helped me and cheered me up in the good and bad moments. I am very lucky to have him in my life. Least but not last, I would like to thank my parents, family, friends and colleagues who were always at my side and accompanied me during my doctoral studies. Among these, I owe a special appreciation to my mom, who always believed in me and in her own way never stopped encouraging me, despite the distance.

## **17 Curriculum Vitae**

Der Lebenslauf wurde aus der elektronischen Version der Arbeit entfernt.  
The curriculum vitae was removed from the electronic version of the paper.